Titre: Title:	Behaviour of Double and Triple Vertical Rows of Bolts Shear Tab Connections and Weld Retrofits
Auteur: Author:	Marco D'Aronco
Date:	2013
Type:	Mémoire ou thèse / Dissertation or Thesis
Référence: Citation:	D'Aronco, M. (2013). Behaviour of Double and Triple Vertical Rows of Bolts Shear Tab Connections and Weld Retrofits [Mémoire de maîtrise, École Polytechnique de Montréal]. PolyPublie. https://publications.polymtl.ca/1341/

UNIVERSITÉ DE MONTRÉAL

BEHAVIOUR OF DOUBLE AND TRIPLE VERTICAL ROWS OF BOLTS SHEAR TAB CONNECTIONS AND WELD RETROFITS

MARCO D'ARONCO

DÉPARTEMENT DES GÉNIES CIVIL, GÉOLOGIQUE ET DES MINES

ÉCOLE POLYTECHNIQUE DE MONTRÉAL

MÉMOIRE PRÉSENTÉ EN VUE DE L'OBTENTION

DU DIPLÔME DE MAÎTRISE ÈS SCIENCES APPLIQUÉES

(GÉNIE CIVIL)

DÉCEMBRE 2013

UNIVERSITÉ DE MONTRÉAL

ÉCOLE POLYTECHNIQUE DE MONTRÉAL

Ce mémoire intitulé:

BEHAVIOUR OF DOUBLE AND TRIPLE VERTICAL ROWS OF BOLTS SHEAR TAB CONNECTIONS AND WELD RETROFITS

présenté par: D'ARONCO Marco

en vue de l'obtention du diplôme de : Maîtrise ès sciences appliquées

a été dûment accepté par le jury d'examen constitué de :

M. MASSICOTTE Bruno, Ph.D., président

M. TREMBLAY Robert, Ph.D., membre et directeur de recherche

M. ROGERS Colin, Ph.D., membre et codirecteur de recherche

M. FRAPPIER Martin, M.Sc.A., membre

ACKNOWLEDGMENTS

Thanks to the industrial partners which have made this Project possible, especially the ADF Group Inc. and D'Aronco Pineau Hébert Varin Inc. as well as the National Science and Engineering Research Council of Canada.

Thanks to anyone else who has made this research possible, they will recognize themselves.

RÉSUMÉ

Les assemblages par plaque de cisaillement sont une solution simple et efficace et économique de réaliser les assemblages de poutre-à-poutre et de poutre-à-colonne. La méthode de conception actuelle pour ce type d'assemblages présente dans le Manuel de la construction en acier de l'ICCA 2010 est basée sur des recherches qui ont été conduites il y a de nombreuses années et qui s'avèrent dépassées. D'ailleurs, cette méthode de conception n'est pas applicable pour les assemblages à plaque de cisaillement comportant plus d'une rangée verticale de boulons. Dans cette optique, une méthode de conception permettant des assemblages d'une géométrique ayant jusqu'à trois rangées verticales de boulons est suggérée pour l'utilisation au Canada.

Une série de dix essais pleine grandeur a été réalisée afin d'approfondir les connaissances sur le comportement des assemblages avec plaques de cisaillement comportant deux ou trois rangées verticales de boulons ainsi que les réparations par soudure de chantier. Huit de ces essais étaient des connexions avec deux ou trois rangées verticales de boulons, quatre de chaque type, desquels deux ont été réalisés avec une condition de support rigide et six avec une condition de support flexible. Les deux essais restants étaient des reproductions de réparation d'assemblages par soudure au chantier, ces essais étant réalisés pour analyser le comportement et la ductilité offerte par ce type d'assemblage fréquemment utilisés sur en chantier.

Les essais réalisés sur les assemblages par réparation au chantier ont démontré que ce type de connexion possède une ductilité suffisant pour accommoder la demande en rotation et en déformation de l'assemblage en plus de résister à un effort tranchant similaire à leurs équivalents boulonnés.

Les essais boulonnés ont révélé que les assemblages par plaque de cisaillement se comporte de façon similaire n'importe le type de support avec lesquels ils sont combinés. Dans chacun des cas, les assemblages ont résisté à un effort tranchant supérieur à l'effort prédit indépendamment du type de support. Il a été observé qu'un moment fléchissant est induit dans les colonnes et il est possible de prédire ce moment avec justesse lors de la conception des colonnes. Il s'avère que l'utilisation d'une troisième rangée verticale de boulons n'influence que très légèrement la capacité de l'assemblage lorsque les autres paramètres de la plaque de cisaillement demeurent constants.

ABSTRACT

Shear tab connections are one of the most cost efficient and time saving connection methods used throughout the steel industry. The current design procedure for single-plate shear connections of the 2010 CISC Handbook of Steel Construction is based on research conducted decades ago and is found to be outdated. This method is also not applicable to shear tab connection configurations of multiple vertical rows of bolts. Thus, an updated design method applicable to connections up to three vertical rows of bolts is proposed for use in Canada.

A series of ten full-scale experiments were conducted in order to deepen the knowledge and knowhow of the behavior of shear tab connections detailed with double and triple vertical lines of bolts and their welded retrofit counterparts. Eight of these full-scale experiments were double or triple vertical rows of bolt connections, four of each, of which two were carried out on rigid supports and six on flexible supports. The remaining two tests were full-scale weld retrofit shear tab connection specimens without bolts carried out on rigid supports. These tests were performed to examine the ductility of this type of connection and their shear resistance since these are often performed on construction sites.

The tests performed on weld retrofit connections allowed to determine that these connections possessed sufficient ductility to accommodate the rotational demand of the connection and reach at least the same loads as their corresponding bolted counterparts.

The tests on bolted connections revealed that shear tab connections behave in similar fashion regardless of the support condition they are combined with. In all cases, the shear tab connections reached and surpassed the targeted rotations and the predicted connection strengths regardless of the support condition. It was found that a significant bending moment is generated in the support column and that this flexural moment can be efficiently predicted at the column design stage. The use of an additional vertical line of bolts, from double vertical rows to triple vertical rows of bolts, has very little influence on the connection capacity when the remaining shear tab parameters are kept constant.

TABLE OF CONTENTS

LIST OF TABLES

LIST OF FIGURES

LIST OF ABBREVIATIONS

AISC	American Institute of Steel Construction
CISC	Canadian Institute of Steel Construction
E	Elastic Modulus of steel
Fy	Specified yield stress
Fu	Specified tensile strength
I	Moment of inertia
Lu	Unbraced Length
M	Bending moment in a member
Xu	Ultimate strength as rated by the welding electrode classification member

LIST OF APPENDICES

CHAPTER 1: INTRODUCTION

1.1 Overview

Structural steel fabricators and structural consulting engineers have the responsibility to conceive connections such that the erection of steel structures is simple and safe. For that matter, single plate shear tabs are one of the most frequently adopted type of assembly when designing beam to beam or beam to column connections. This type of connection, known under several names such as cleat plates, fin plates, single plates and shear tabs, relies on a simple design approach and is very cost effective for the erector and steel fabricator. This type of assembly, which will be referred to as a shear tab in this thesis, is commonly fillet welded to the supporting member in the fabrication shop and field bolted into the web of the supported member.

The supporting member can be classified in two separate categories: a rigid support or a flexible support. This classification is based on the capability of the connection to follow the rotation of the supported framing member. A rigid support defines a situation where the connection is restrained from following the rotation of the supported member; this condition is mostly observed in beam to column flange connections or beam to concrete embedded plate assemblies as illustrated in Figure 1-1.

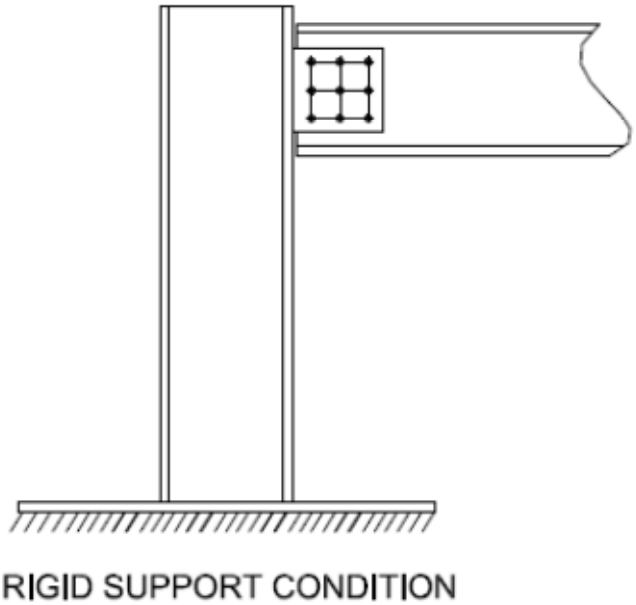

Figure 1-1 - Beam to Column Flange Shear Tab Connection

On the other hand, a flexible support will still provide some stiffness to the connection but will allow an increased rotation of the connection in comparison to the rigid support. Column weak axes and girders, as shown in Figure 1-2, are commonly considered as flexible supports.

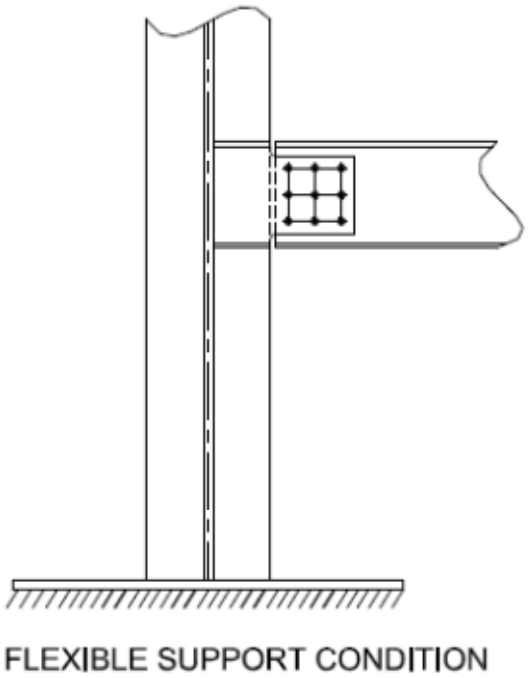

Figure 1-2 - Beam to Column Web Connection

Although this type of connection is simple, mistakes can still be made in the fabrication plant and those will be detected only on the construction site during the erection of frame members. One such type of mistake is the misalignment of the bolt holes in the shear tab with those in the beam web, as depicted in Figure 1-3. This issue can occur if detailing errors have been made, if the shear tab has been installed up-side-down on the column or girder or if it has been installed at the wrong elevation. Even though these mistakes can create concerns on the job site, the correction works may create a connection capable of developing the same resistance as the originally designed connection.

Figure 1-3 - Hole Misalignment in Shear Tab and Supported Beam Web (Photo: DPHV)

A possible practical and cost effective retrofit is to field weld the shear tab on one side to the supported beam web. This approach avoids the substantial costs of replacing the shear tab on site or reaming of the bolt holes. Figure 1-4 illustrates the type of field welding required in these situations.

Figure 1-4 - Retrofit Weld on Shear Tab Connection (Photo: DPHV)

The use of the shear tab connections throughout the years has been mostly restricted to configurations with a single vertical row of bolts. This configuration has been evaluated by means of various full scale laboratory test programs which have led to the current design procedures of the 10th Edition of the Handbook of Steel Construction of the Canadian Institute of

Steel Construction (CISC) (CISC, 2010) and the Steel Construction Handbook of the American Institute of Steel Construction (AISC) 14th Edition (AISC, 2011). Conversely, configurations with multiple vertical rows of bolts have been frequently utilized in construction in recent years due to increased shear loads in beams and to the possibility of axial loading, again in the beams, due to column stability restraint forces in beam to column connections and lateral force transfer to bracing bents, among other reasons. Currently, the design procedure provided by the CISC for shear tab connections is limited to configurations having a single vertical row of two to seven bolts based on research by Astaneh et al. (1989). The CISC design method does not contain any guidance on the design of shear tab connections for multiple bolt column configurations and does not address the resistance of shear tab connections to axial loads. Alternatively, the AISC Steel Construction Manual does offer a design procedure for extended shear tab connections, such as shown in Figure 2-2, these having configurations with multiple vertical rows of bolts and without any limitation on the number of fasteners in the connection. However, only limited full-scale shear tab laboratory tests were available to verify this design method in addition to finite element models. These existing CISC and AISC shear tab design procedures will be described in Chapter 2.

1.2 Objectives

The goal of the research presented in this thesis is to recommend a design approach for shear tab connections with configurations of multiple vertical rows of bolts making it a modified approach to the current AISC design procedure. The predicted connection capacities obtained with this modified approach will be compared with the current design methods of the AISC (2011) and CISC (2010) combined with experimental results. To verify the efficiency of this proposed method, full scale experimental tests will be undertaken on a series of single plate connections welded to rigid and flexible supports in order to determine the input of various support conditions on the beam end rotation allowed by the connection as well as the amount of rotation allowed retrofit field welded shear tab connections. Additionally, the research aims to determine the effect of the support on the connection capacity and the effect of a shear tab connection to a flexible support seeking to develop guidelines for column design allowing for shear tab connections.

1.3 Scope of research

A total of ten full scale laboratory tests were conducted. Parameters in this series of tests included varying beam sizes, number of bolts and vertical rows of bolts, shear plate thicknesses and column support conditions. In fact, a total of four connection tests were conducted with a rigid support condition of which two contained three vertical rows of bolts and two were retrofit field welded connections. In addition, six more tests were performed on W310 and W610 beams with two or three vertical rows of three and six bolts framing into a 4 meter long column web acting as a flexible support. Loads were applied at the connection by a main actuator and rotations were imposed to the supported beams by an end actuator. These beams were laterally supported to prevent lateral-torsional buckling. Numerous instruments allowed for the measurement of parameters such as strains, deflections, displacements, strength of the connection and observed rotation at the assembly. With this data, comparisons between the predicted results and collected values were made, leading to conclusions and a recommendation of an updated design procedure.

1.4 Outline of thesis

This thesis covers the following topics:

Chapter 2 provides a summary of previous research findings on the single plate shear connections but is mainly focused on current design procedures applicable in North America.

Chapter 3 contains a detailed explanation of the two test setups erected in the laboratory and a description of each test connection. In addition, this chapter contains the instrumentation and procedures applied for the complete series of tests.

Chapter 4 is the core of this thesis and examines the data collected throughout the research program. A comparison is provided of the resistance obtained experimentally with the predicted values based on current CISC and AISC design methods.

Chapter 5 presents findings on the effect of the shear tab connections on flexible column supports with the use of finite element analysis.

Chapter 6 concludes on the findings of the research and recommends modifications to the current design approach and provides suggestions for future studies in structural steel shear connections.

CHAPTER 2: LITTERATURE REVIEW

2.1 Overview

This chapter contains a review of previous research and publications on the single plate shear connection topic as well as the current design procedures applicable in the North American industry, developed by the CISC and the AISC. Retrofit welding procedures used in the industry will also be described in the following.

2.2 Research on Bolted Connections

The first series of shear tab tests reviewed were performed by Lipson (1968) at the University of British Columbia and aimed to determine if this type of connection could sustain a constant factor of safety, find the maximum rotational capacities, evaluate the behavior of the connections under working loads and find out if they could be considered as flexible connections. The connections, varying from a single vertical row of two to six ¾''A325 bolts with a single plate of ¼'' thick A36 steel, were subjected to two test procedures which were pure-moment tests and moment-shear tests. The pure-moment tests were simulated by a splice in the center of a beam at the point of zero shear, whereas the moment-shear tests comprised a beam connected to a rigid column and loaded with a combination of shear and moment. Various failure modes were observed which included edge distance failure at the top and bottom holes and weld rupture. Lipson has found that the centre of rotation of the connection was near the centroid of the bolt group. Lipson came to the conclusion that this type of welded-bolted connection is feasible.

Richard et al. (1980) conducted research with the goal of determining the moments generated in the shear tab connections. Basing their research on the hypothesis that single plates do not act as perfect pins, the authors assumed that the magnitude of the eccentricity mainly depends on the number, size and configuration of the bolt pattern as well as the plate thickness selected for the connection and the beam span to beam depth ratio. For the purpose of the research, experiments were used to validate finite element models which were developed to determine the end moments in combination with the beam-line method. The beam-line is superimposed on a moment-rotation curve where the beam line crosses the y axis at the beam's fixed end moment and the x axis at the beam's simple span end rotation, see Figure 2-1.

Completing a total of 126 single shear load-deformation tests on ASTM A325 and A490 bolts in addition to finite element modeling Richard et al. were able to produce a calculation procedure to determine bolt group eccentricities. Finite element models were verified with seven single row tests of three, five and seven bolts. The procedure includes the span to depth ratio L/d and section modulus of the supported beam and the number and size of the fasteners used in the connection.

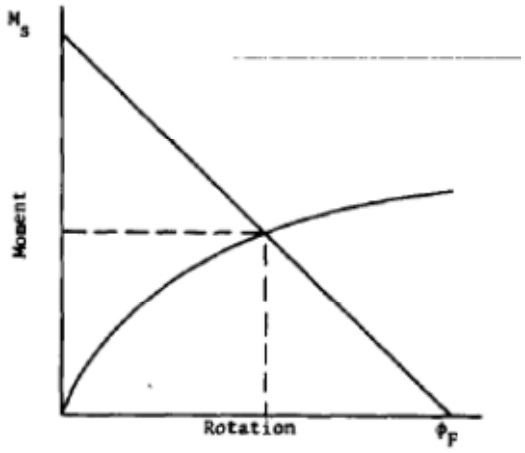

Figure 2-1 - Moment-Rotation Relationship (Richard et al. 1980)

Ricles (1980) later conducted a series of eight tests on double vertical rows of bolts shear connections combined with finite element models. The goal of his research was to determine the effects of edge and end distances as well as hole sizes, standard or short slotted, in bolted shear connections. The results of both finite element models and laboratory tests show that the block shear failure of these coped beam web controls the capacity of the connections and not the end nor the edge distances as predicted by the design method recommended in the 1978 AISC Manual of Steel Construction (1978). Ricles demonstrated that the equation used to predict block shear failure in the AISC Manual was not accurate for shear connections with two vertical rows of bolts. The author suggested a more accurate equation based on a triangular distribution of the load along the horizontal tension edge of the block shear failure path adding that shear fracture does not occur along the vertical edge of the failure path. This triangular stress distribution of the tensile load was based on the assumption that stress concentrations are higher in the region of the bolt located closest to the beam web's edge. In addition, since shear fracture was not observed, shear yielding should be considered instead of shear fracture and the von Mises criterion ($0.6F_y$)

should be applied for the shear yielding of the web. The proposed equation predicted block shear failure resistance with accuracy.

Astaneh-Asl (1989) investigated the demand and supply of ductility in steel shear connections. Astaneh-Asl evaluated the interaction of the shear force, bending moment and beam end rotations in flexible connections. He indicated that appropriate rotation must be applied in addition to a shear load in order to evaluate the realistic shear strength of the connections. Moment-rotation curves of these flexible connections should be obtained under the same conditions stated above. A modified beam-line curve was therefore proposed allowing the prediction of more realistic end moments and end rotations of single span beams. In addition, Astaneh-Asl suggested updated shear-rotation curves based on plastic design that simple shear connections should be able to attain.

Astaneh-Asl and his collaborators at the University of California, Berkeley, see Astaneh-Asl et al. (1989), later proposed a design method for single plate connections of a single of row of bolts. Based on previous research on demand for ductility (Astaneh-Asl 1989), a tri-segment curve for shear-rotation loading was proposed in order to provide a more realistic loading path for the shear connections to be tested, Figure 2-2. The first segment, ab, of the curve represents the elastic behavior of the beam. As yielding occurs, after midspan flexural yielding at point b, the beam gets softer and the second segment therefore correspond to the inelastic behavior of the beam. The yield moment M_y, expected at 0.02 radians, is obtained by dividing the plastic moment M_p by the shape factor Z_x/S_x, where Z_x and S_x are respectively the plastic and elastic sections moduli of the beam. The plastic moment is reached at point c and targeted at 0.03 radians. The last segment of the curve accounts for strain-hardening of the material and also explains the decrease in the curve slope.

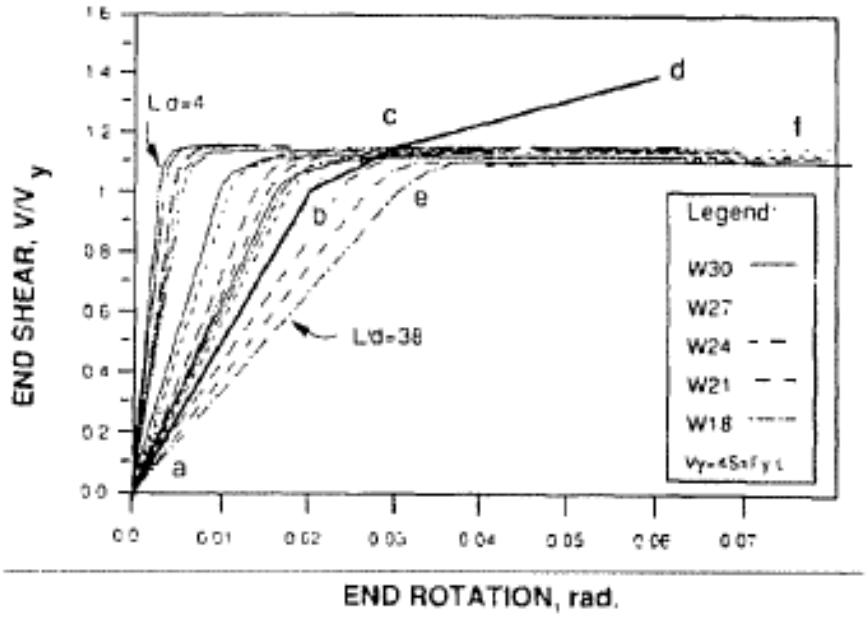

Figure 2-2 - Shear-Rotation Relationship Loading Curve (Astaneh-Asl et al. 1989)

A series of five full-scale experiments on shear tabs comprised of a single column of three, five or seven bolts was conducted following the load path presented in Figure 2-2. It was found that an increase in the number of bolts in the connection directly leads to a decrease in ductility of the assembly. The design procedure proposed by Astaneh-Asl et al. (1989) resulting from these experiments makes recommendations on material grades, plate thicknesses, bolt spacing and edge distances as well as aspect ratio of the shear plates.

The experiments also led to a series of equations allowing the calculation of the eccentricities of both the bolt line and the weld line to the shear load. Equations 2.1 to 2.4 reflect the findings of the authors in terms of eccentricity for design for both rigid and flexible supports. In these equations, n represents the number of bolts in the vertical row and a is the distance between the bolt line and the weld line. These eccentricities are reflected in the moment diagram of Figure 2-3.

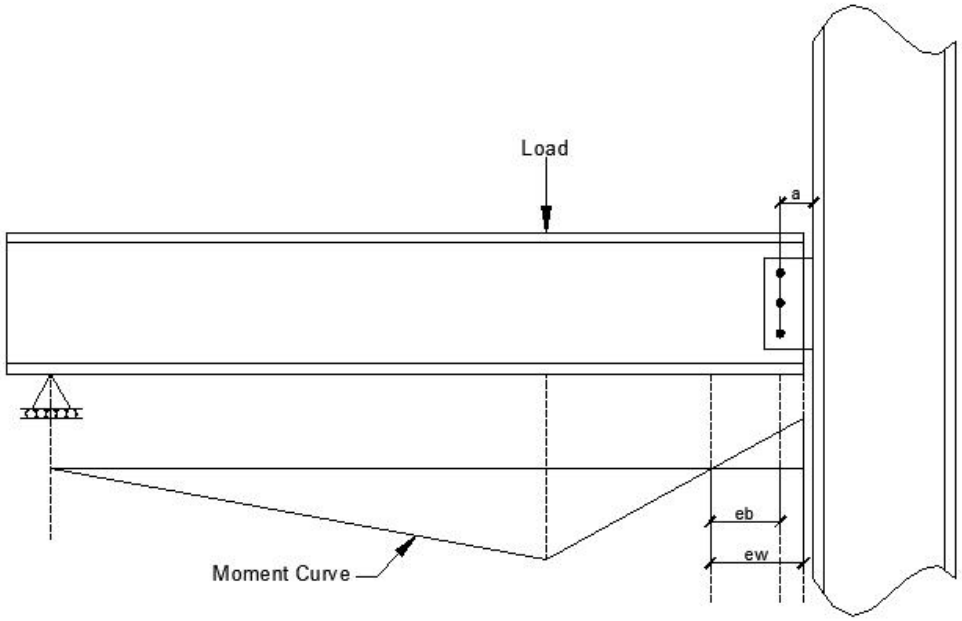

Figure 2-3 - Eccentricity in Shear Tab Connections

For the bolt line to the inflection point,

At rigid supports: $e_b = (n\text{-}1)\text{-}a,\ in.$ (Eq 2.1)

At flexible supports: $e_b = (n\text{-}1)\text{-}a \geq a,\ in.$ (Eq 2.2)

For the weld line to the inflection point,

At rigid supports: $e_w = (n\text{-}1),\ in.$ (Eq 2.3)

At flexible supports: $e_w = (n\text{-}1) \geq a,\ in.$ (Eq 2.4)

Astaneh-Asl et al. (1993) later proposed an updated design procedure after conducting eight tests of shear tabs with a single vertical row of three, five, seven or nine bolts. This procedure accounts for six limit states of strength of the connection. In the described procedure, these limit states should be ranked such that failure modes involving yielding shall occur before brittle failure modes which involve material fracture. The limit states concerned are plate yielding, bearing failure of bolt holes, fracture of plate along net section, edge distance fracture and bolt and weld fracture.

In addition, in a report by Astaneh-Asl et al. (1993), they insist that the previous equations developed in 1989 to calculate the proper eccentricity between the weld line and the bolt line to the inflection point should be modified to add absolute value operators in order to obtain better approximations. The modified equations are as follows:

For the bolt line to the inflection point,

At rigid supports: $e_b = |n\text{-}1\text{-}a|, in.$ (Eq 2.5)

At flexible supports: $e_b = |n\text{-}1\text{-}a| \geq a, in.$ (Eq 2.6)

For the weld line to the inflection point,

At rigid supports: $e_w = (n\text{-}1), in.$ (Eq 2.7)

At flexible supports: $e_w = n, in.$ (Eq 2.8)

Sherman and Ghorbanpoor (2002) went on to conduct laboratory testing research on the behavior of 31 full-scale extended shear tab connections. Extended shear tab connections are economical for the fabricator since they eliminate the need for coping supported beam flanges. This study investigated both stiffened and unstiffened extended shear tab connections which consisted of single vertical rows of three and five bolts where all bolt holes where slotted holes and shear tabs welded to a column or girder web. The authors presented new equations to evaluate eccentricities in the assemblies which were adopted by the AISC 13th Edition Manual (2005) as a design alternative to evaluate connection eccentricities. This shear tab design method described in the AISC (2005) manual was modified according to the design procedure proposed by Sherman and Ghorbanpoor (2002).

Ashakul (2004) investigated single plate shear connections using finite element models built in the software ABAQUS. The analyses were realized to investigate parameters such as the effect of the distance between the bolt line and the weld line, the plate thickness and material grade as well as the position of the connection relative to the beam's neutral axis. He also modeled single plate connections with two vertical rows of bolts. In bolted connections with a single vertical row of bolts, the results indicated that the a-distance, the distance between weld line and bolt line, does not affect the bolt shear rupture strength of the connections. On the other hand, it was found that plate parameters which do not allow sufficient ductility generate

significant horizontal forces at the bolts resulting in a reduction of the bolt group shear strength and creating a moment.

In double row connections, using A325 bolts, Ashakul (2004) found that a redistribution of the load occurs among the bolt rows. It was also observed that this redistribution does not occur when Grade 50ksi plates thicker than ½'' were used which resulted in the bolts of the outer column to fracture and the inner row of fasteners to resist much less loading. The results showed that the stress distribution in the plate is not constant throughout the cross section at the stage of strain hardening. Therefore, Ashakul proposed a relationship for the calculation of the plate shear yielding strength.

Creech (2005) went on to research single plate framing connections with rigid and flexible supports through the testing of 10 full-scale shear tabs with a single vertical row of fasteners. In addition, he performed an extensive review of past and present design methods aiming to improve the AISC LRFD 3rd Edition Manual (2003) design method for this type of shear connection. Various parameters of both connection components, plate and bolts, were investigated but particular attention was addressed to flexural yielding of the plate and bolt group shear strength. The connections were subjected to both shear and imposed rotation up to maximum beam end rotation of 0.03 radians at ultimate.

The rotational behavior of the connection was also considered in this research. It is known that the rotational neutral axis of single plate connections can significantly affect the connection capacity and behavior. Findings point out that the centroid of the bolt group does not always coincide with the point of rotation of the connection and depends of the support conditions.

Regarding bolt eccentricities, the eccentricity in the connection drifts significantly during the loading protocol. Creech concluded that the eccentricity equations in the AISC LRFD Manual (2003) under predict the bolt group eccentricities and that for tests with rigid support conditions with more than three bolts in a single row, eccentric shear considerations are unnecessary. Eccentricity calculations should be performed for connections with two or three fasteners in a single row only.

Creech (2005) also suggested that the hierarchy of the limit states should be maintained and that ductile failure modes are desired prior to brittle failure modes. In order to facilitate the ductility in the connection, lower grades of steel should be used for single plates. He

recommended that additional research on flexible support connections with more than three bolts should be conducted.

Baldwin Metzger (2006) went on to conduct eight full scale single plate shear connection tests with rigid support condition, four conventional configuration and four extended configurations, and compared results with predicted values according to the AISC 13th Edition Manual (2005) design procedure. Once again, the test procedure applied shear and rotation to the connection and the targeted rotation of the beam end at the plastic moment capacity of the beam was set to 0.03 radians. It was found that excluding the bolt group action factor of 0.8 would predict bolt shear strength more accurately. The author also found that the connection eccentricity should be taken as the distance between the bolt and weld lines. Baldwin Metzger recommended that further research be performed on the effects of 50ksi plate material on the rotational ductility of the connection.

Muir's and Thornton's (2011) research on shear tabs forms the basis of the revised design procedure for conventional and extended configurations of shear tab connections. The result of their work appears in the AISC Manual of Steel Construction 14th Edition (2011). The increase of the nominal bolt shear resistance created the need for a revised design procedure for shear tab connections. The procedure provided in the Manual 13th Edition (AISC 2005) relied on the 20% reserve in bolt shear strength to justify neglecting eccentricity in the bolt groups for most configurations. This reserve was obtained by applying the 0.8 factor for bolt group action in the design procedure from the Manual 13th Edition (AISC 2005). Muir and Thornton have shown that with updated bolt shear values neglecting the eccentricity is no longer appropriate and proposed an updated design procedure for both conventional and extended configurations of shear tab connections.

Muir and Thornton also explain that with the use of shear tab connections, negative bending moments are developed at the face of the columns and the inflexion point in the supported beam shifts away from the column face. This implies that the eccentricity of the connection can be on the span side of the bolt group, as it is pictured in Figure 2-3, which would result in an eccentricity higher than the distance of the bolt group to the weld group. With data based on past research results where bolt shear failure was observed, they have determined an effective eccentricity resulting in the same ultimate capacity for the bolt group as measured in the past research results.

Marosi (2011) conducted a series of sixteen full-scale tests on single and double row shear tab connections including bolted and retrofit field welded tests without bolts. The connection resistances were predicted using two design methods; the AISC Steel Construction Manual 13th Edition (2005) and the CISC Handbook of Steel Construction (2010). It was shown that the use of 50ksi (345MPa) steel for the shear tabs provided enough ductility such that rotational demand was met in all types of connections whether they had single or double rows of bolts, exceeding rotational goals at ultimate for each test. Noticeable deformations could be seen around bolt holes.

It was also found that the connections which could be predicted using the CISC (2010) design method displayed the most conservative results, except for connections with single or double vertical rows of 10 bolts which cannot be designed with the CISC method. This design method was considered as outdated since various clauses from the current CSA S16 Steel Design Standard (2009) and resistance factors were omitted or not up to date. On the contrary, the AISC (2005) design method was found to be the most accurate in predicting connection resistances except for bolt group resistance to shear fracture.

Based on these findings, Marosi proposed an updated design method for single and double vertical row of bolts shear tab connections. This procedure is mostly based on design checks from the AISC (2005) design procedure except that it uses higher shear strength values when determining the bolt group capacity. The adoption of this proposed method would result in a decrease in the number of bolts required in the connection and higher connection capacities. The details of this modified method will be presented in Section 3.3.

2.2.1 Research on Weld Retrofits

When field problems result in shear tabs not fitting properly with the supported beam, a practical solution is to retrofit the connection using welds. Field welding the shear tab to the supported beam web with various weld patterns such as a single vertical weld or even partial C-shape or L-shape weld have been used in construction. The weld group capacity can be determined by using the tabulated values given in the CISC Handbook (2010) or the AISC Manual (2011). These values are defined by the instantaneous center of rotation method and depend on the orientation and dimensions of the weld group as well as the eccentricity of the loading.

Marosi (2011) has found that the retrofit weld groups possessed sufficient ductility to meet the rotational demand at the supported beams end. The retrofit welds were designed using the tables for eccentric weld groups from the CISC Handbook (2010). These weld groups were designed to resist the same loads as their bolted counterparts and were found to be able to resist the same loads and, in some cases, these connections resisted even greater shear loads. For retrofit welds of single vertical row of bolts shear tabs, the typical failure modes observed were edge distance failure for partial L-shape welds and shear fracture through the net area of the plate for C-shape welds. In the case of double vertical rows of fasteners shear tabs, the typical failure mode observed was shear fracture through the net are of the shear plate.

2.3 Current Design Procedures

2.3.1 CISC Design Procedure

The current design procedure for shear tabs in the CISC Handbook of Steel construction 10th Edition (2010) is based on the findings by Astaneh-Asl (1989) and is limited to a shear plate with a single vertical line of bolts which is welded to the supporting member as illustrated in Figure 2-4. The Handbook provides a design table (Table 3-41 (CISC2010)) containing factored values of single plate connections with one row of two to seven bolts. These factored resistances are based on a series of assumptions:

- Weld to bolt line distance limited to 75mm
- Distance between bolts is 80mm
- 35mm horizontal and vertical edge distances
- A325 or A325M Grade bolts only with intercepted threads
- E490 Weld Material
- Shear tab Grade 300W steel
- Punched holes (Bolt diameter + 4mm)

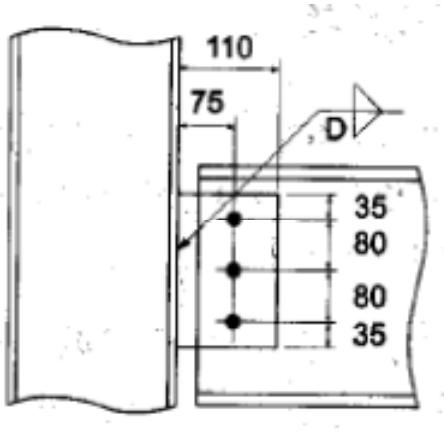

Figure 2-4 - Shear Tab Beam Connections (CISC 2010)

Astaneh-Asl's (1989) research on eccentricity in shear tab connections (described earlier) forms the basis of the design method. The distance between the weld line and the bolt line is calculated, this length is defined as the eccentricity of the bolt group. Using Table 3-14: *Eccentric Loads on Bolt Groups* (CISC 2010) the bolt group coefficient (*C*) can be calculated. The bolt group capacity can be determined by multiplying the coefficient *C* by the bolt capacity (V_{rbolt}). The bolt capacity can be found in Table 3-4: *Factored Shear and Tensile Resistances* (CISC 2010). It is important to note that the tabulated values use $\phi_b = 0.67$ in the bolt shear resistance, this value has been revised to $\phi_b = 0.8$ in the CSA S16 Standard (2009) which results in tabulated values being conservative. Also, in earlier versions of the S16, the resistance factor of ϕ=0.9 was multiplied by a factor of 0.85 in the equation for tension rupture of members in their net section. The current S16 (2009) standard replace this calculation with a new ϕ_u=0.75 factor which is slightly lower than the previous 0.85ϕ.

Since the connection geometry is now determined, the required shear tab thickness can be determined by calculating the shear and bearing capacity of the plate. The following equations are to be used

$$t_p \geq V_{r\,bolt} / (3\,\phi_{br} d F_u) \quad \text{(Eq. 2.9)}$$

$$t_p \geq V_f / (0.5\,\phi\, L_{vn} F_u) \quad \text{(Eq. 2.10)}$$

$$t_p \geq 6mm \quad \text{(Eq. 2.11)}$$

$$t_p \geq (d/2) + 2mm \quad \text{(Eq. 2.12)}$$

$$T_r = \phi_u [U_t A_{nt} F_u + 0.6 A_{gv} (F_y + F_u)/2] \quad \text{(Eq. 2.13)}$$

where t_p is the shear tab thickness, L_{vn} refers to the net shear length of the plate, A_{gv} is the gross shear area of the block shear fracture pattern of the shear tab, A_{nt} is the net tension area of the block shear fracture pattern of the shear tab, U_t is a reduction coefficient based on the tensile stress distribution equal to 1.0 in this case, F_u refers the ultimate tensile strength of the shear tab material, ϕ_{br} is the bolt bearing resistance factor set to 0.67, ϕ is the structural steel resistance factor set to 0.9, ϕ_u is the steel resistance factor for ultimate limit states and d is the bolt diameter. The different possible failure planes of the shear tab are depicted in Figure 2-5.

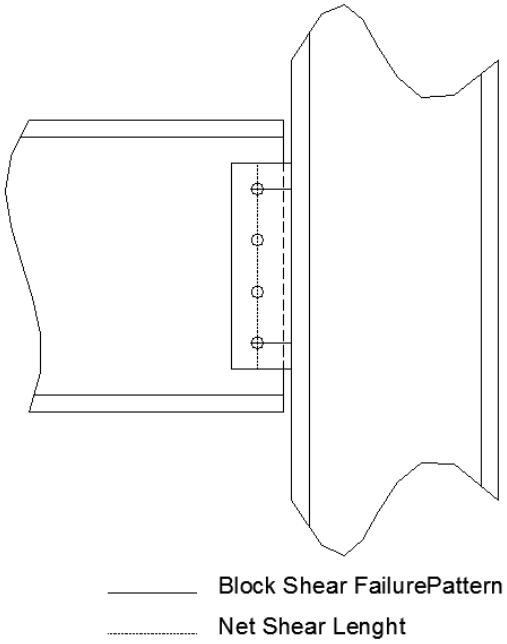

Figure 2-5 Shear Tab Failure Planes

Equation 2.9 defines the shear tab bearing capacity and, as mentioned earlier, the bearing resistance factor ϕ_{br} has been revised to 0.8 and is not included in the tabulated values. Equation 2.10 was part of Cl. 13.4.4 of the S16-1994 Standard (CSA 1994) and has since been removed from the latest edition of the Standard and replaced by Equation 2.13, but is still present in the tabulated values. This equation defined the factored net shear resistance of the plate. It was found to be overly conservative with regards to the block shear failure mode. Equation 2.11 describes the minimum plate thickness to be used. Equation 2.12 is a recommendation which can be found in the research by Astaneh-Asl (1989). These last two equations are present to insure the connection provides enough rotation, ductility and flexibility to the supported member by allowing small bolt hole deformations. Equation 2.13 defines the block shear rupture where A_{nt} is

the net cross-sectional area in tension, A_{gv} is the gross cross-sectional area in shear, F_y is the yield strength of the plate material, U_t is an efficiency factor relative to the geometry of the failure path and ϕ_u=0.75. This equation and the related efficiency factor can be found in Cl. 13.11 of the CSA S16-09 Standard (CSA 2009).

The size of the weld of the shear tab to the supporting member in the table is based on the research by Astaneh-Asl (1989) and should be equal to ¾ of the thickness of the shear tab.

The procedure described above is limited to single columns of two to seven bolts. For connections requiring more than seven bolts, bolt group capacities can be found in Tables 3-14 through 3-20 of the CISC Handbook of Steel Construction (2010) for up to four vertical rows of twelve bolts, but no design procedure for the shear tab connection is provided. In those cases, most professionals refer to the AISC design procedure (Section 2.3.2) for situations where different configurations are required.

2.3.2 American Design Procedure

The AISC Steel Construction Manual 14th Edition (2011) presents a design method for the conventional configuration of shear tab connections and another for the extended configurations.

2.3.2.1 Conventional Configuration

The method described in this section is only applicable if the dimensional limitations listed below (illustrated in Figure 2-6) are met.

- There is a single vertical row of bolts.
- There are between 2 and 12 bolts in the connection.
- The distance from the bolt line to the weld line is limited to 3½".
- Standard holes or horizontal short-slotted holes.
- The vertical edge distance, L_{ev}, should meet the AISC *Specification* Table J3.4 (AISC 2011).
- The horizontal edge distance, L_{eh}, should be greater or equal to two times the bolt diameter.

- Either the plate or beam web thickness must not exceed half the bolt diameter + 1/16".

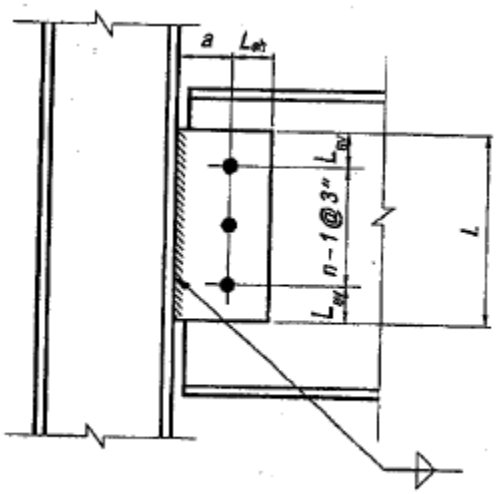

Figure 2-6 - Conventional Configuration Single-Plate Connection (AISC 2011)

If all these dimensional limitations are met, the connection bolts and plate must then be checked for the vertical shear reaction of the supported member. Potential failure modes are bolt bearing, bolt group failure, block shear rupture, shear rupture of the plate and weld failure.

Recent analysis performed by Muir and Thornton (Muir and Thornton 2011) show that neglecting the eccentricity is no longer appropriate considering the increased bolt strengths. Therefore, as opposed to the procedure in the AISC Manual 13th Edition (AISC 2005), the eccentricities must be taken as shown in Table 10-9 of the AISC Manual (AISC 2011) and flexural and shear rupture through the net section of the shear tab must be verified. It is unnecessary to verify the shear tab compression capacity since in the conventional configuration the shear plate buckling does not govern the design.

Bolt bearing resistance of the plate or beam web should be determined as follows:

$$\phi R = 2.4\phi F_u t d_b \qquad \text{(Eq. 2.14)}$$

where t is the thickness of the beam web or the shear tab, d_b is the bolt diameter, F_u is the ultimate tensile strength of the plate or beam and ϕ =0.75.

The shear yielding, shear rupture and block shear rupture of the plate are given in the following equations in order:

$$\phi R = 0.6\phi F_y A_{gv} \qquad (\phi = 1.00) \qquad \text{(Eq. 2.15)}$$

$$\phi R = 0.6\phi F_u A_{nv} \qquad (\phi = 0.75) \qquad \text{(Eq. 2.16)}$$

$$\phi R = 0.6\phi F_y A_{gv} + U_{bs}\phi F_u A_{nt} \; (\phi = 0.75) \qquad \text{(Eq. 2.17)}$$

where F_y and F_u are respectively the yield and ultimate tensile strength of the plate material, A_{gv} and A_{nv} are the gross and net shear areas of the plate and U_{bs} is a reduction coefficient based on the tensile stress distribution.

Tabulated values in the AISC Manual of Steel Construction (AISC 2011) provide nominal strengths for bolt groups and welds for both Grade 36 ksi and 50 ksi plates and both A325 and A490 grade bolts, refer to tables 10-9a and 10-9b. Otherwise, the designer may calculate these values himself and determine the required welds and bolt groups. The weld size shall be of 5/8 times the shear tab thickness.

2.3.2.2 Extended Configuration

When dimensional limitations of the conventional configuration cannot be met, the extended configuration design procedure must be applied. In the extended configuration design method:

- The number of bolt vertical rows and bolts per row, *n*, is not limited.
- The distance from the weld line to the bolt line closest to the support, *a*, is not limited.
- The use of holes must meet the AISC *Specification* Section J3.2 requirements.
- The edge distances, horizontal and vertical, must meet AISC *Specification* Section J3.4 requirements.

Figure 2-7 illustrates the various dimensional and geometrical abbreviations and terms which will be referred to in the following paragraphs.

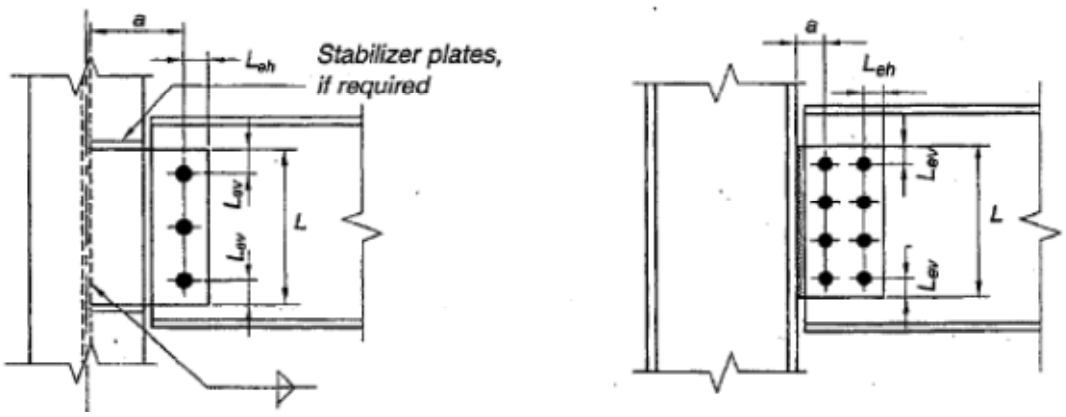

Figure 2-7 - Extended Configuration Single-Plate Connection (AISC 2011)

The eccentricity of the bolt group, *e*, is defined as the distance from the support to the centerline of the bolt group. The maximum plate thickness of the assembly must then be determined using the following equations:

$$t_{max} = 6M_{max} / (F_y d^2) \quad \text{(Eq. 2.18)}$$

$$M_{max} = F_v / 0.90(A_b C') \quad \text{(Eq. 2.19)}$$

where F_v is the shear strength of an individual bolt divided by a factor of 0.90 to remove the reduction for end loaded bolt groups, A_b is the area of an individual bolt, C' is a coefficient from Part 7 of the bolt group, F_y is the specified yield stress of the plate and d is the depth of the plate. This check is performed to ensure the ductility of the connection explaining why it is made at the nominal strength and not the ultimate strength of the plate. This calculation can be omitted if either the beam web or the plate thickness satisfies both the following:

For a single vertical row of bolts,

$$t \leq d_b/2 + 1/16" \quad \text{(Eq. 2.20)}$$

$$L_{eh} \geq 2d_b \quad \text{(Eq. 2.21)}$$

For two vertical rows of bolts,

$$t \leq d_b/2 + 1/16" \quad \text{(Eq. 2.20)}$$

$$L_{eh} \geq 2d_b \quad \text{(Eq. 2.21)}$$

Again, the shear tab shall be checked for shear yielding, shear rupture and block shear rupture as described in Equations 2.15 to 2.17. In addition, the plate shall be checked for shear yielding and shear buckling as follows:

$$(V_r/V_c)^2 + (M_r/M_c)^2 \leq 1.0 \quad \text{(Eq. 2.22)}$$

$$V_r = V_u \quad \text{(Eq. 2.23)}$$

$$V_c = 0.6F_yA_{gv}\phi_v \ (\phi_v=1.0) \quad \text{(Eq. 2.24)}$$

$$M_r = V_re \quad \text{(Eq. 2.25)}$$

$$M_c = \phi_bF_yZ_{pl} \ (\phi_b=0.90) \quad \text{(Eq. 2.26)}$$

where Z_{pl} is the plastic section modulus of the shear plate and e is the distance from the support to the centroid of the bolt group.

These equations have replaced the von-Mises shear reduction criterion which was present in the AISC 13th Edition Manual (AISC 2005). The flexural yielding strength of the shear tab is determined based on research by Mohr and Murray (2008) who found that the most accurate approximation of the plate's flexural capacity is Equation 2.26.

The last check to be performed by the designer consists of verifying the shear tab for the limit state of buckling with the procedure described in Equations 2.22 to 2.34, which accounts for the capacity of a coped beam:

$$M_n \geq M_u \quad \text{(Eq. 2.27)}$$

$$M_u = V_ue \quad \text{(Eq. 2.28)}$$

$$M_n = F_{cr}S_{net} \quad \text{(Eq. 2.29)}$$

$$F_{cr} = QF_y \quad \text{(Eq. 2.30)}$$

where Q is a reduction factor based on the slenderness of the shear tab acting as a compression element. This factor is based on the yield strength and the dimensions of the shear plate making the flexural local buckling stress smaller as the plate gets slenderer. Slenderness of the plate in the following equations is accounted for by the λ factor.

$$\lambda = (h_o/(F_y)^{1/2})/[10t_w/(475+280(h_o/c)^2)^{1/2}] \quad \text{(Eq. 2.31)}$$

$$Q = 1 \qquad \text{when } \lambda \leq 0.7 \quad \text{(Eq. 2.32)}$$

$Q = (1.34\text{-}0.486\,\lambda)$ when $0.7 < \lambda \leq 1.41$ (Eq. 2.33)

$Q = 1.30/\lambda^2$ when $\lambda \geq 1.41$ (Eq. 2.34)

where h_o is the shear plate depth and c is the dimension of the plate parallel to the compressive stress, t_w is the shear tab thickness and F_y is the yield stress of the plate material.

The eccentricity of the bolt group can be reduced when the shear tab is connected to a column web. In those cases, the support is considered as flexible, as depicted in Figure 2-8, and the eccentricity can be reduced by a percentage of the column's weak axis flexural strength, say 5%, considering that the column shaft has been designed accounting for this additional flexure. In rigid support cases, the moment to be resisted by the bolt group is equal to the shear load multiplied by the distance between the face of the column flange to the centerline of the bolt group. In the case of flexible supports, this moment is calculated from the centerline of the supporting column and can be reduced by 5% of the column flexural capacity and, taking the shear load as a constant, this has the effect of reducing the eccentricity.

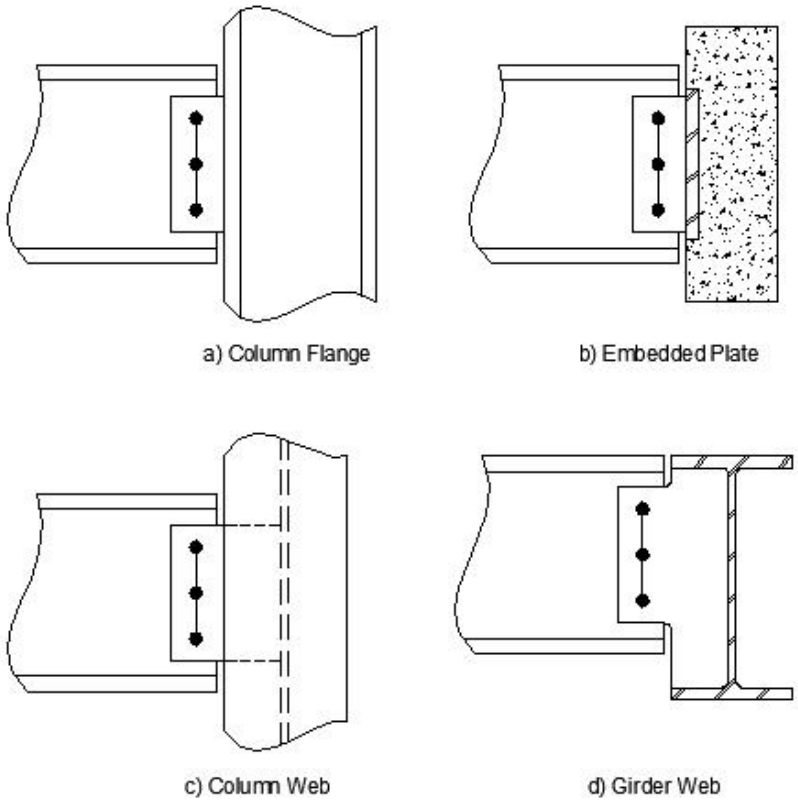

Figure 2-8 - Rigid Supports a) and b); Flexible Supports c) and d)

CHAPTER 3: TEST PROGRAM

3.1 Test Setup

3.1.1 Overview

The following chapter will describe the connection design and the setup necessary for the accomplishment of the laboratory testing. The specimens which have undergone testing will be presented under the form of a summary table aiming to outline the number, size and type of bolts used in each connection as well as grade, thickness and size of the plates and beams in addition to the grade and size of the welds tested. The instruments which were used to record test data will be explained in detail as to the position in which they were placed and to their exact functions. The complete test procedures will then be presented and will include exact loading patterns and targeted beam rotations during the testing. A thorough explanation of both test setups, for rigid and flexible supports, will be presented and will compose both the major sections of this chapter.

3.1.2 Rigid Support Setup

The first phase of the laboratory testing was realized with the typical shear tab detail where the single plates were welded to a rigid support, in this case a stub column's flange. There were three main sections to the rigid support test setup in addition to the test beam; the stub column, the end frame and the lateral bracing system. These three main sections are depicted in Figure 3-1.

The stub column, acting as the rigid support, is shown in Figure 3-2. The shear tabs are welded to the column's flange transferring the shear load from the beam into the column. In order to minimize column rotations, single L127x127x19 angles were bolted on each side of the stub and bolted down on a floor beam. These diagonals acted as vertical bracing restraints to the column. The W310x196 floor beam was pre-tensioned into the strong floor using four anchor rods. Once again this step was performed to limit anchor deformations and prevent column rotations. The floor beam was positioned to match the strong floor anchor layout. The strong floor anchor layout defined the entire geometry of the setup along with the position of 12MN hydraulic actuator used to perform the tests. Figures 3-2 and 3-3 outline plan views and elevation views of the layout of the anchor pattern of the strong floor, the position of the main

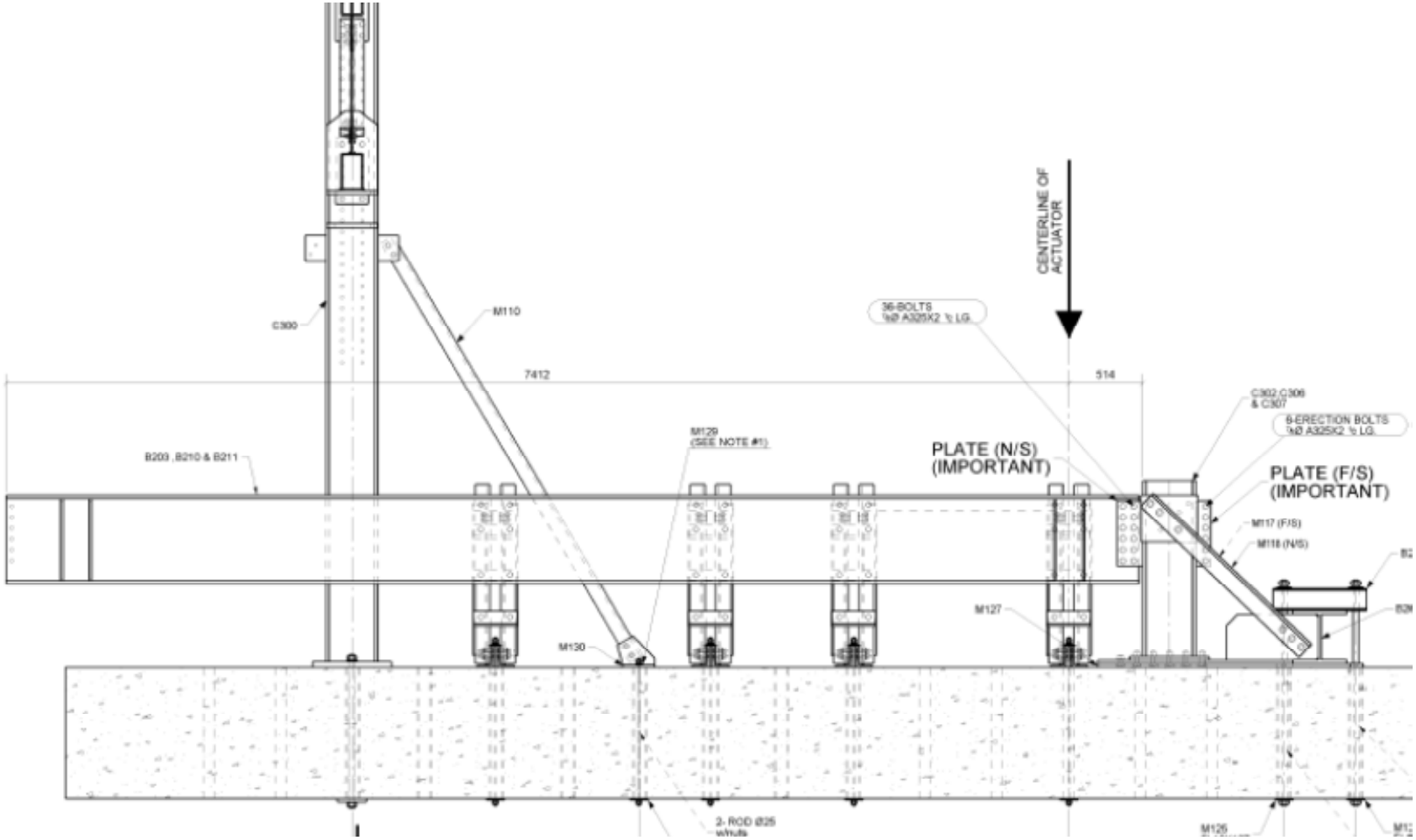

Figure 3-1 - Typical Elevation View of Test Setup

hydraulic actuator and of the stub column. Each stub column could be used twice since shear tabs were shop welded on each column flange.

Figure 3-2 - Stub column, restraining vertical braces and floor beam

The lateral bracing system was crucial to exclude possibilities of lateral-torsional buckling of the beam over its entire length. Since full-span beams were tested, lateral braces were positioned at spacings below the minimum un-braced length, L_u, before the flexural resistance of the beams decrease to account for lateral stability issues. The lateral bracing system was composed of plates clamped on to the top and bottom flanges of the supported beam; bottom flange lateral bracing was used at beam end only. These plates had a single high strength bolt welded upside down on top of them to which was tied a top plate free to rotate about the axis of this fastener. This top plate, positioned parallel to the axis of the test beam, had a high strength bolt welded to each of its ends. These bolts were chosen to fit exactly into an end-rod ball and socket joint which was attached to a threaded rod tied to the lateral bracing framing at their other end. This framing was tensioned to the strong floor using threaded rods. This entire system allowed the test beam to rotate and displace along the vertical plane but prevented any lateral displacements which could have led to stability issues. Figure 3-4 shows an enlarged view of the ball and sockets joints tied to the restrained test beams.

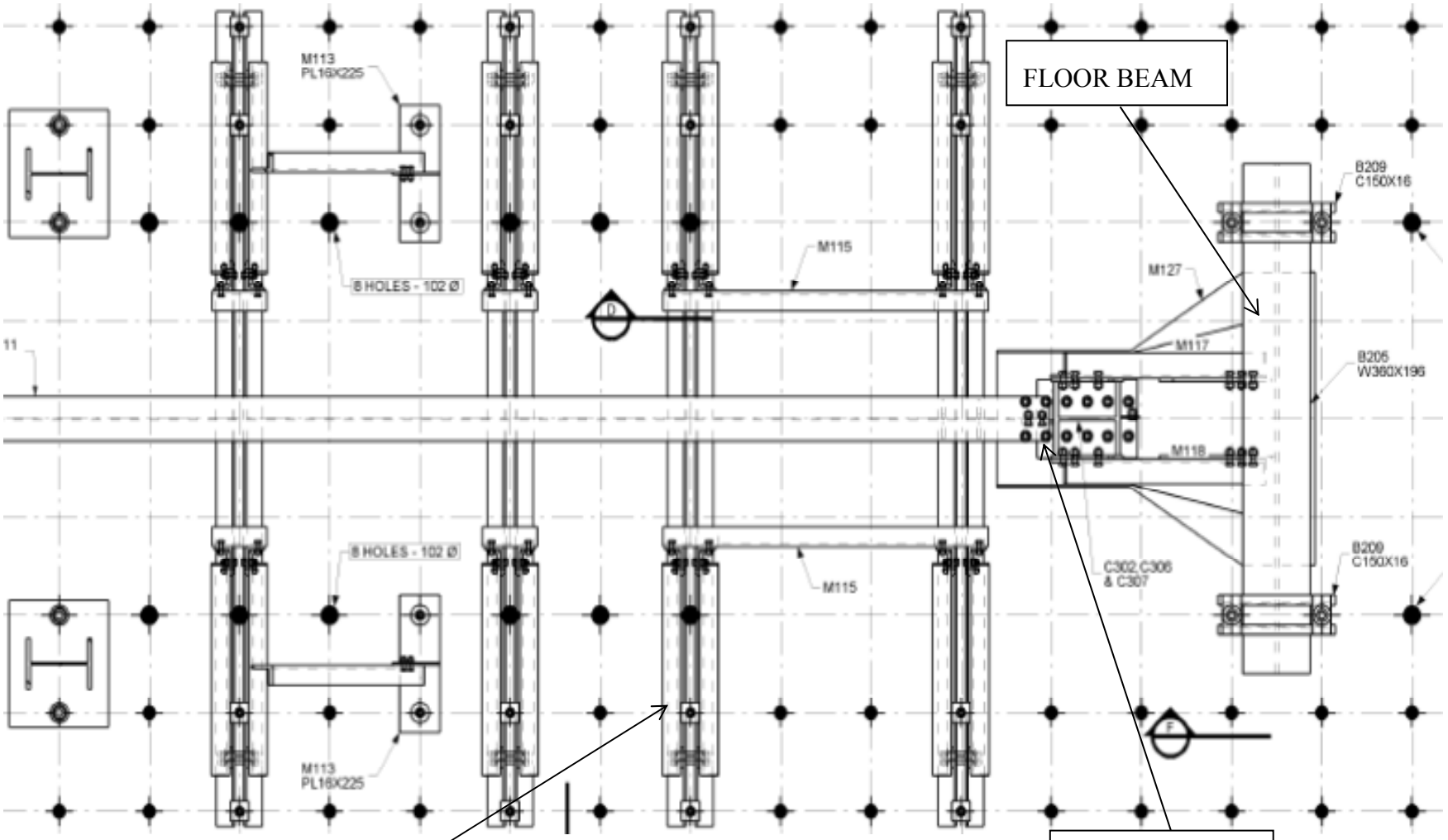

Figure 3-3 - Typical Plan View of Test Setup

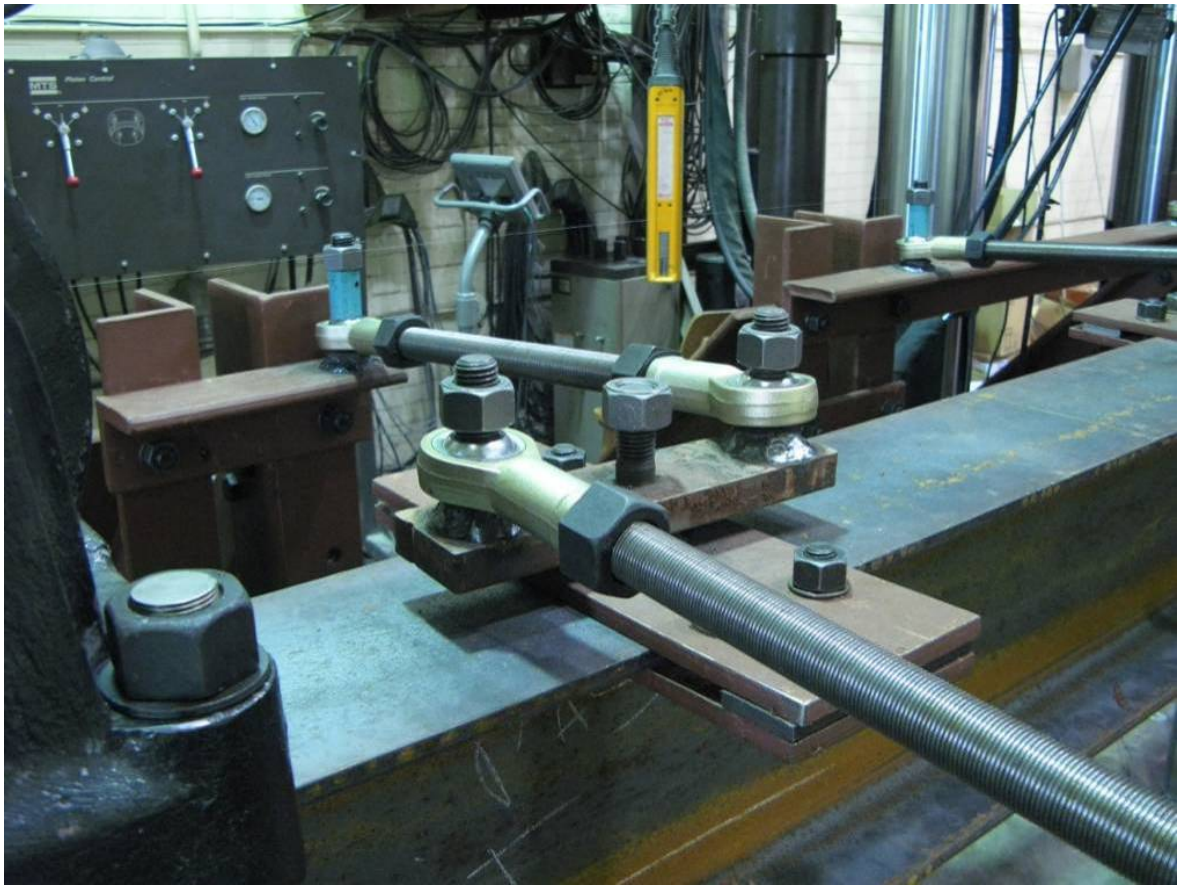

Figure 3-4 - Lateral Bracing Threaded Rods and Ball and Socket Joints

The end frame is composed of a chevron type braced frame with an HSS as the main beam and double angle diagonals. The supporting columns were drilled at various elevations to accommodate different test beam depths allowing the supporting braced frame to be displaced in elevation. The end frame was designed to support the 269 kN tension load imposed by the end actuator which provided an end vertical reaction to the supported beam in addition to a vertical displacement. Both columns of the end frame were braced and tensioned to the strong floor with threaded rods. Figure 3-5 depicts the layout of the entire end frame.

Figure 3-5 - End Frame and End Actuator for Flexible Support Setup

3.1.3 Flexible Support Setup

The second phase of the shear tab research was performed on shear plates welded into webs of full length columns, recreating a flexible support condition. The lateral bracing system and the end frame were the two main items from the rigid support setup reused for this flexible support setup. On the other hand, the entire column support frame was to be redesigned.

In order to simulate flexible supports with the best exactitude, full scale 3.7m long columns were used. End restraints of the test columns needed to simulate pins and allow movement in plane. Therefore, the slender column shafts needed to be stabilized during and

between tests. The bottom end of the columns sat on rollers, allowing displacement in plane, and was blocked from out of plane displacements, as depicted in Figure 3-6.

Figure 3-6 - Test Column End Restraints

In a similar fashion, the top end of the test columns were blocked from rocking out of plane using a cap plate onto which were welded heavy angles. Teflon pads were placed between the column flange and the angle legs to allow easy movement in plane. This cap plate was bolted on top of a back-up HSS column. This back-up column was meant to support the torque generated on the cap plate by a possible out of plane movement of the test column. To this back-up column were added vertical braces preventing torsion and displacement of the HSS. The HSS was bolted down to the strong floor with the base plate assembly used for the rigid stub columns

of the first phase. Figure 3-7 illustrates the layout of the elements described for the flexible support setup.

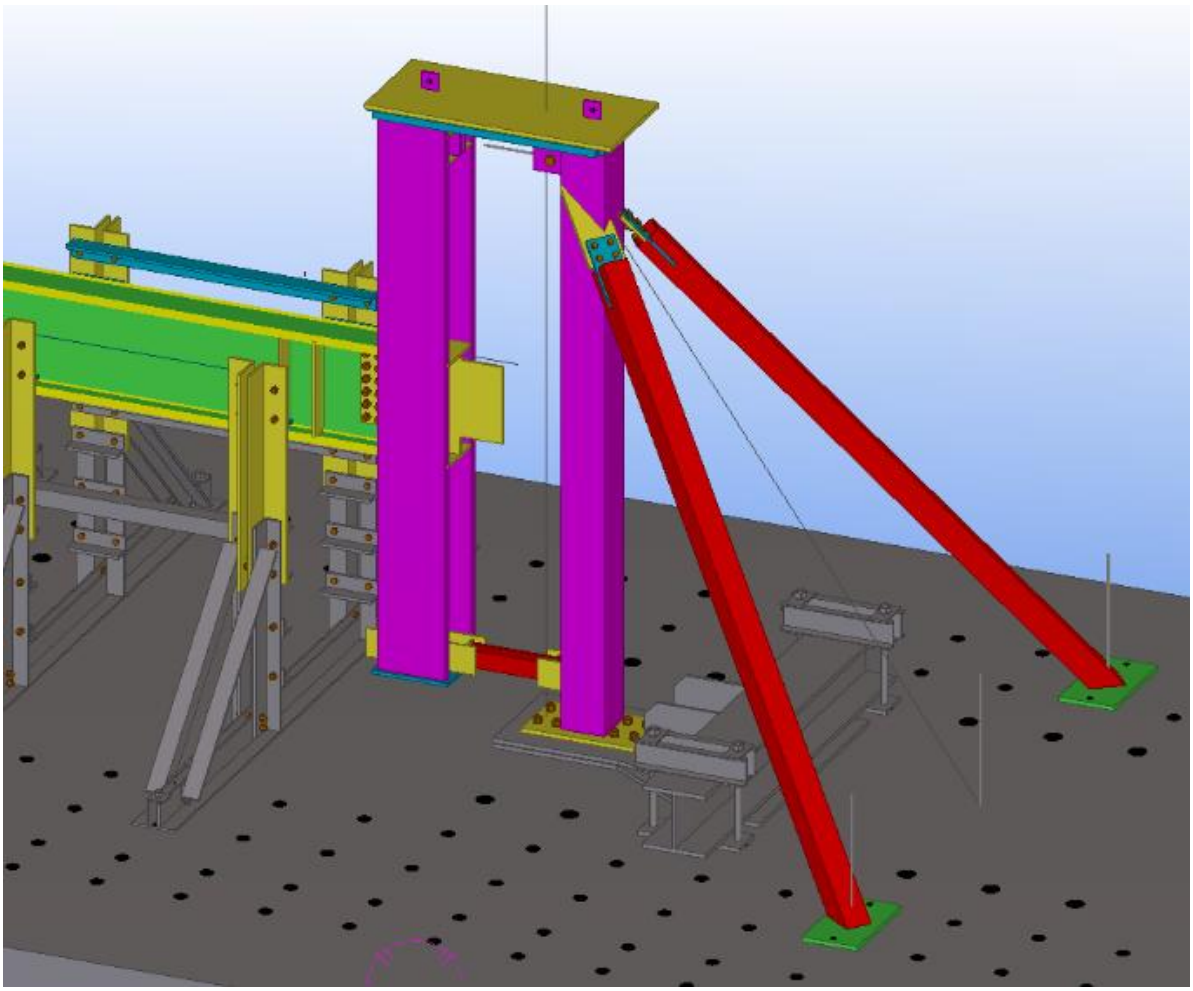

Figure 3-7 - Flexible Support Setup Layout

In a schematic illustration, Figure 3-8 shows the various components described for the flexible support condition setup.

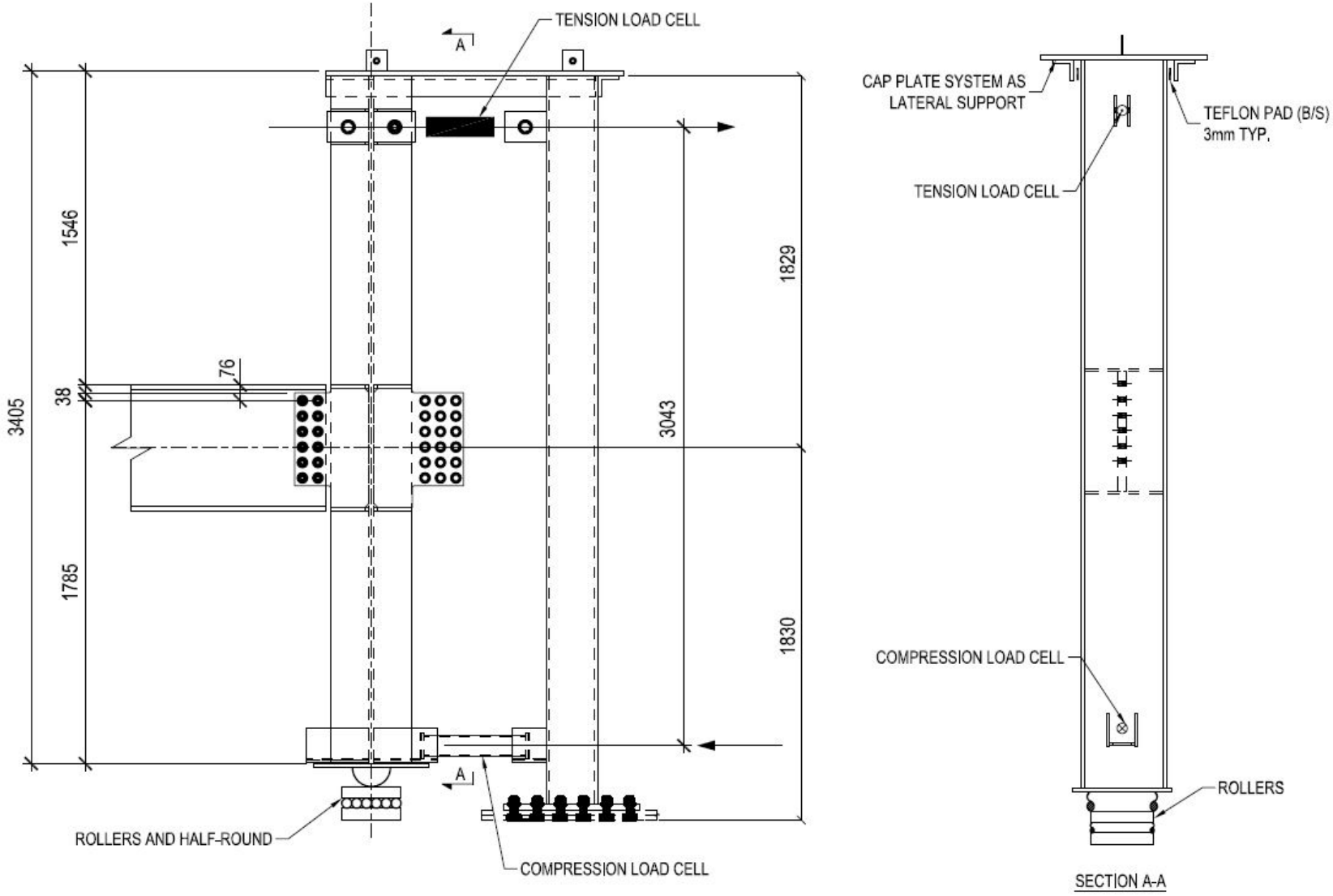

Figure 3-8 - Flexible Support Components Schematics

3.2 Test Specimens

This section will present the configuration and elements employed for each connection of the ten full-scale tests which were conducted in the structures laboratory. Table 3-1 presents the complete data for each laboratory test.

The shear tabs were shop welded in a flat position using a semi-automatic flux-core arc welding wire feeding process (FCAW). This dual-shielding welding procedure, performed in a controlled environment, is widespread in the heavy structural steel industry because of its efficiency and consistent and reliable results. This is the reason why this welding process was selected for this research project. It is a prequalified procedure upon the requirements of the American Welding Society (AWS) and Canadian Welding Bureau (CWB).

The welding procedure described in this section has been applied for the shop welds of the shear tabs. The field welds required for the retrofit connections were performed in the laboratory using shield metal arc welding (SMAW) standard procedures and were performed by a certified welder. Figure 3-9 illustrates the two retrofit weld patterns adopted for the test specimens. Both weld patterns are partial “C” shape welds which are done along the vertical length of the shear tab and extended to the center of the plate at its horizontal top and bottom edges where the shear tab makes contact with the beam web.

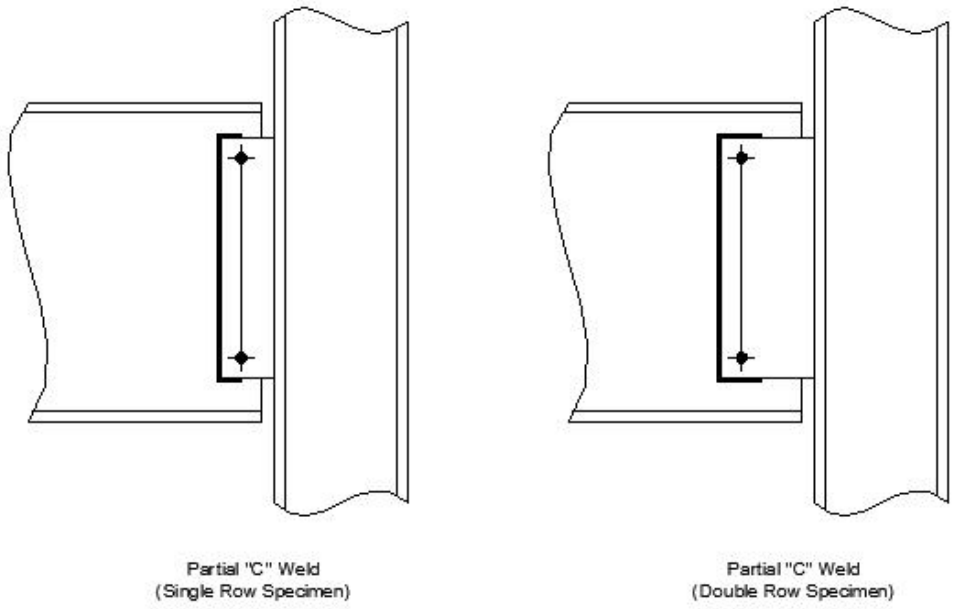

Figure 3-9 - Weld Retrofits

The shear tab connections included in the scope of this research are not covered by the design procedure suggested in the CISC Handbook of Steel Construction (2010) but are still frequently used in the North American steel construction industry. Therefore, the test results could not be compared to the CISC design procedure. Double and triple vertical rows of fasteners shear tab connections were considered in this research. The results obtained from this series of tests will be used to propose further recommendations on an updated design procedure for the Handbook (CISC 2010).

The steel grade selected for the shear tabs is ASTM A572-GR50 (50 ksi). This steel grade was chosen in order to determine the ductility and rotation that can be allowed to the connection by this type of steel in comparison with ASTM-A36 (36 ksi) which has been the steel grade mainly used in previous research programs. The test beams were selected to be able to withstand the shear loads predicted for the test shear tab connections. Also, indirectly to withstand the flexural moment generated by the eccentric shear loading. The beams being able to carry the shear load was essential since this research is focused on studying the behavior of the shear tab itself. Design sketches of each setup are provided in Appendix A along with the instrumentation related to each test.

Table 3-1 - Shear Tab Test Specimens

Test ID	Type	Support Condition	Column Size	Test Beam	Vertical Rows of Holes	Bolts per Vertical Row	Bolt Size	Shear Tab Thickness	Weld Retrofit	Retrofit Weld Size	Shear Tab to Column Weld Size
1	Bolted	Rigid	W360x196	W310x74	3	3	3/4"A325X	13 mm	N/A	N/A	8 mm
2	Bolted	Rigid	W360x196	W610x140	3	6	7/8"A325X	16 mm	N/A	N/A	11 mm
3	Welded	Rigid	W360x196	W610x140	1	N/A	N/A	8 mm	Partial "C"	6 mm	6 mm
4	Welded	Rigid	W360x196	W610x140	2	N/A	N/A	16 mm	Partial "C"	11 mm	11 mm
5	Bolted	Flexible	W360x122	W310x60	2	3	3/4"A325X	10 mm	N/A	N/A	6 mm
6	Bolted	Flexible	W360x122	W610x140	2	6	7/8"A325X	16 mm	N/A	N/A	11 mm
7	Bolted	Flexible	W360x314	W310x60	2	3	3/4"A325X	10 mm	N/A	N/A	6 mm
8	Bolted	Flexible	W360x314	W310x74	3	3	3/4"A325X	13 mm	N/A	N/A	8 mm
9	Bolted	Flexible	W360x314	W610x140	2	6	7/8"A325X	16 mm	N/A	N/A	11 mm
10	Bolted	Flexible	W360x314	W610x140	3	6	7/8"A325X	16 mm	N/A	N/A	11 mm

Notes:
- Test beams Grade A992-GR50
- Test shear tabs Grade A572-GR50
- Bolt threads excluded from shear plane (X-Type bolts)
- Grade E70XX electrodes for welding
- Vertical and horizontal edge distances set to 1.5"
- Bolt spacing and gage set to 3"
- First bolt hole at 3" from top of the beam
- Standard holes were used
- Refer to Appendix A for design sketches including shear tab dimensions and weld retrofit dimensions

3.3 Design of Test Specimens

3.3.1 Welded Connections

The shear tab connections simulating retrofit welds were designed using partial "C" shape welds. This type of weld retrofit pattern was chosen according to the results obtained in the research performed by Marosi (2011). These retrofit welds were designed using the tables available in the AISC Steel Construction Manual (2011), Table 8.8, and the CISC Handbook of Steel Construction (2010), Table 3-28, which provide the capacity of weld groups subjected to eccentric loads. The values given in these tables are based on the instantaneous centre of rotation method which depends on the eccentricity of the loading.

All the shear tabs used to simulate weld retrofits had only two holes drilled; the top and bottom bolt holes of the further vertical row from the support. These specimens intend to simulate a situation on the construction site where the shear tab was placed in the wrong position and needs to be replaced. Therefore, since the new plate would be field welded there would be no need to drill all the initial holes. The two drilled holes are required for erection and their purpose is to hold the beam in the right position with the shear tab while the field welding is performed.

With the configuration of the weld groups being dictated by the geometry of the shear plates, the size of the fillet welds was determined to resist the same shear loads as the connection capacity calculated using the probable material resistances. Once the required fillet weld sizes were determined, no additional checks were performed on the shear tab, assuming that its resistance would surpass the bolted shear tab resistance since fewer holes were drilled.

As in current standard practice, the capacity of the retrofit connection is only based on the weld capacity not accounting for the bolts left in place. This decision was taken to simulate a shear plate having to be replaced on site and on which the complete bolt group would not be entirely drilled since the shear tab would be field welded.

3.3.2 Bolted Connections

The bolted shear tab connections in the scope of this research were designed according to the procedure defined in the AISC Manual (2011). The CISC Handbook (2010) design method

could not be used because none of the bolted connections met the geometrical limitations imposed by the CISC Handbook method.

For all bolted connections, the extended configuration design method of the Manual (AISC 2011) described in Chapter 2 was used. Since the coupon tests could not be carried out before the shear tabs tests, over strength values of 10% were considered in design calculations for yield strength F_y and ultimate strength F_u. Later on, once the coupon tests were carried out as described in Section 4.4, the predicted connection strengths were adjusted to reflect the actual yield and ultimate strengths of the beam and shear tab material as depicted in Table 3-2.

In addition to the extended configuration design method of the AISC Manual (2011), a modified design method developed by Marosi (2011) has also been used to evaluate shear tab capacity. This method is based on the AISC 14th Edition Manual (2011) with the exception that it modifies the unit shear strength of one bolt therefore increasing the capacity of the bolt group. While the Manual (2011) defines the unit shear strength of an A325 bolt as 0.583 of the ultimate tensile strength of the bolt, using a reduction factor to account for uneven stress distribution in the bolt group in extended connections, research by Kulak et al. (1987) demonstrated that bolt shear resistance was most likely 62% of the ultimate tensile strength of the fastener. Based on that research, the modified AISC design method used this shear strength value for A325 fasteners to determine the bolt group resistance.

The main objective of the research program being to compare identical shear tabs whether the support condition was rigid or flexible, design assumptions had to be taken when designing the flexible support shear tab connections. In the case of flexible support conditions, the design methods used herein suggest that the connection eccentricity be taken as the distance between the centerline of the bolt group to the centerline of the column. In order to maintain the same connection resistances, this would have had the effect of increasing the plate and weld sizes and possibly the number of bolts in the connections. Therefore, the connection eccentricity has been taken from the centerline of the bolt group to the tip of the column flange making it the same distance as a rigid support connection. The remaining eccentricity of the node was transferred as a couple in the top and bottom column stiffener plates.

Table 3-2 illustrates the predicted connection resistances by the two methods that were used; the AISC 14th Edition Manual extended configuration and the modified AISC design

method as well as the failure mode expected by each method. Calculations leading to these predictions are presented in Appendix B for the modified method.

Table 3-2 - Predicted Connection Resistances

Test -	Method -	Unfactored Predicted Resistance Based on Probable Material Properties kN	Predicted Failure Mode -	Unfactored Predicted Resistance Based on Measured Material Properties kN	Predicted Failure Mode -
1	AISC Extended	583	PFY	597	BG
	Modified Method	583	PFY	605	PFY
2	AISC Extended	1455	BLS	1534	BLS
	Modified Method	1455	BLS	1534	BLS
5	AISC Extended	363	PFY	440	PFY
	Modified Method	363	PFY	440	PFY
6	AISC Extended	1455	BLS	1676	BLS
	Modified Method	1455	BLS	1676	BLS
7	AISC Extended	363	PFY	440	PFY
	Modified Method	363	PFY	440	PFY
8	AISC Extended	583	PFY	597	BG
	Modified Method	583	PFY	605	PFY
9	AISC Extended	1455	BLS	1676	BLS
	Modified Method	1455	BLS	1676	BLS
10	AISC Extended	1455	BLS	1534	BLS
	Modified Method	1455	BLS	1534	BLS

Failure Modes

BLS= Block Shear Rupture
BG= Bolt Group Shear Failure
SR= Shear Rupture through Plate Net Area
PFY= Plate Flexural Yielding

3.4 Specimen Installation and Instrumentation

3.4.1 Welded Connections

The retrofit weld connections were tested on rigid supports only and therefore only one installation procedure for the stub column and beam was required.

The first of all steps, which needed to be performed only once, was to tie down the floor beam onto the strong floor and to pre-tension the anchors rods. Once this assembly was positioned and secured to the strong floor, the stub column was installed on its base plate and nuts were tightened. At that time, the vertical bracing system required to add rigidity to the stub column was installed. The test beam was then positioned with the use of an overhead crane and both the erection bolts were inserted through the shear tab and beam web. These two erection bolts were snug-tightened to secure the test beam. Subsequently, the test beam was levelled and lined-up with the centerline of the two hydraulic actuators. To keep the beam in-line with its axis, the lateral bracing system, which also acts as a lateral-torsional buckling prevention system, was then installed. It is only once that all these steps were completed that the retrofit welds were performed by the certified welder.

The weld procedure adopted for the retrofit welds was shielded metal arc welding (SMAW) in order to replicate typical field welds performed in the steel erection industry. This procedure uses a consumable electrode stick coated in flux. When electric current is provided an arc is created between the electrode and the metal to be welded releasing a smoke created by the flux which protects the welding area from contaminants. The electrodes used for the retrofit welds in the laboratory were 1/8” E7018-1 MR Performance Plus electrodes Grade E70. Once the retrofit welds were completed, the erection bolts were removed from the connection and the instrumentation installed. Figure 3-10 shows the certified welder performing the retrofit weld on one of the test specimens.

Figure 3-10 - Retrofit Weld Performed by Certified Welder

The typical instruments required for the rigid support setup are shown in Figure 3-11 for one of the W610x140 test beams. Both actuators were equipped with linear variable differential transducers (LVDTs) which gave vertical displacements at both locations. These actuators were also equipped with load cells measuring the axial forces they induced to the system. For the 268kN end actuator, in addition to its inner load cell, string potentiometers were used to measure its vertical and horizontal displacements. The 12MN actuator did not have any additional instruments added to its inner components.

Linear displacements, vertical and horizontal, were measured with LVDTs of two different strokes, +/- 15mm and +/-25mm, depending on the required displacement allowance. A set of +/- 15mm stroke LVDTs were placed on the top and bottom flanges of the test beam and

measured horizontal displacements of the flanges against the face of the stub column. These displacements were required to calculate the relative rotation of the beam compared to the stub column. One +/-25mm stroke LVDT was placed under the test beam to measure its vertical displacement under the shear loading relative to the ground. Another pair of +/-25mm stroke LVDTs was placed perpendicular to the top and bottom flanges of the test beam and was used to determine if the test beam was twisting under the loading. These were purposed to monitor the lateral movement in real-time of the beam in case of unexpected stability issues. One last pair of separate +/-25mm stroke LVDTs were placed at the top and bottom edges of the shear tab to measure to rotation of the shear tab relative to the beam rotation and another +/-15mm stroke LVDT was placed vertically on the edge of the shear tab to measure the vertical displacement of the shear tab relative to the beam.

Inclinometers were placed on the top and bottom flanges of the test beam. The instrument on the bottom flange of the beam was aligned with the centerline of the 12MN actuator and the inclinometer on the top flange was placed at 165mm away from the face of the stub column. These inclinometers were used to determine the absolute rotation of the test beam.

Strain gauges were positioned on the shear tabs as depicted in Figure 3-11. Gauges closer to the face of the support were placed at a 45° angle required to measure the shear strain.

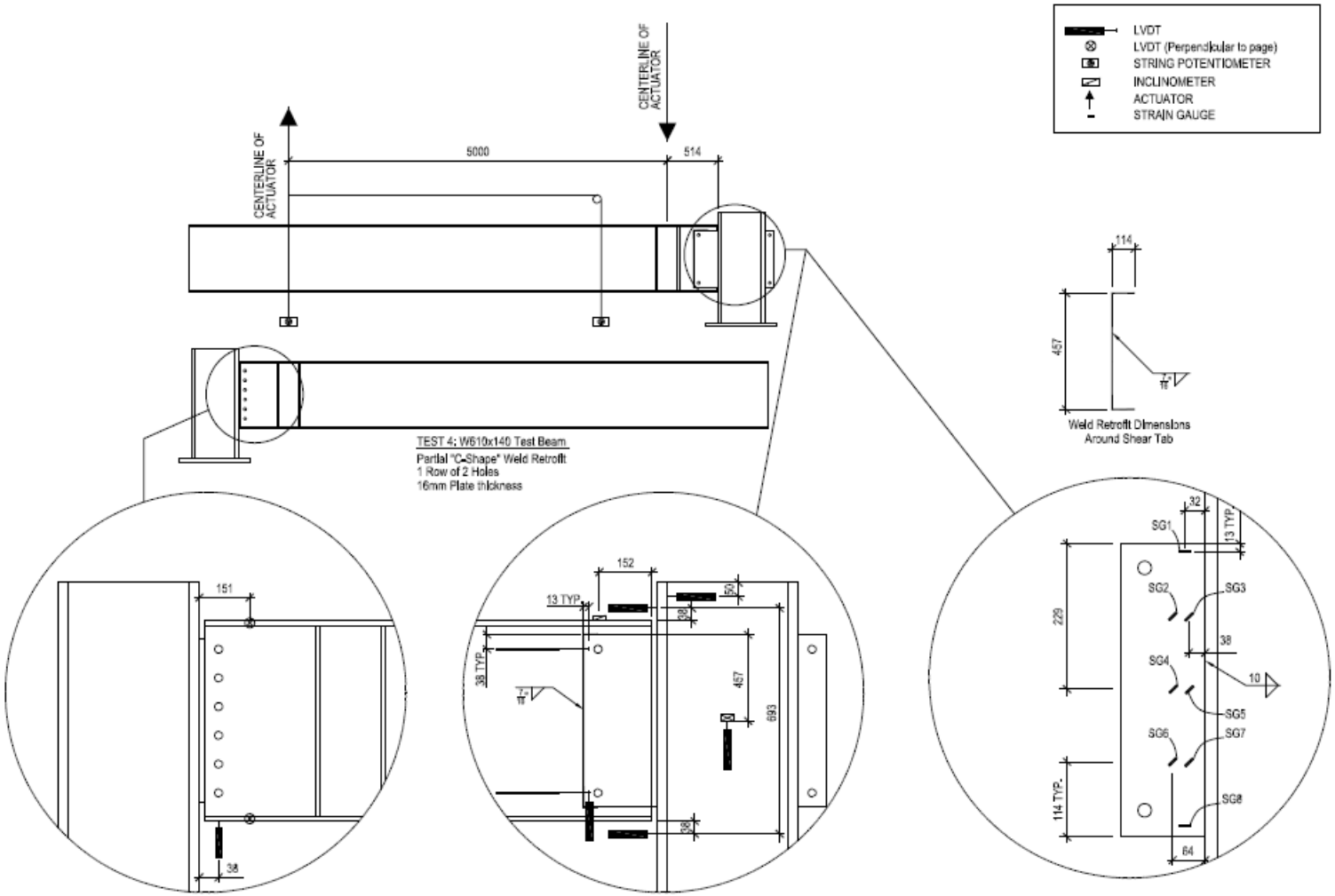

Figure 3-11 - Typical Setup Instrumentation for Welded Setup for a W610 Beam – Test 4

For each test, a set of rollers and a half round rocker were placed directly under the 12MN main actuator in order to accommodate the rotation of the test beam where the load was applied. These devices are shown in Figure 3-12.

Figure 3-12 - Roller Set and Half Round Rocker

In order to observe the yielding patterns as well as beam and plate deformations, both sides of the beam web and the shear tab were covered in a lime/water whitewash solution. Whitewash painting solution can be observed in Figure 3-13.

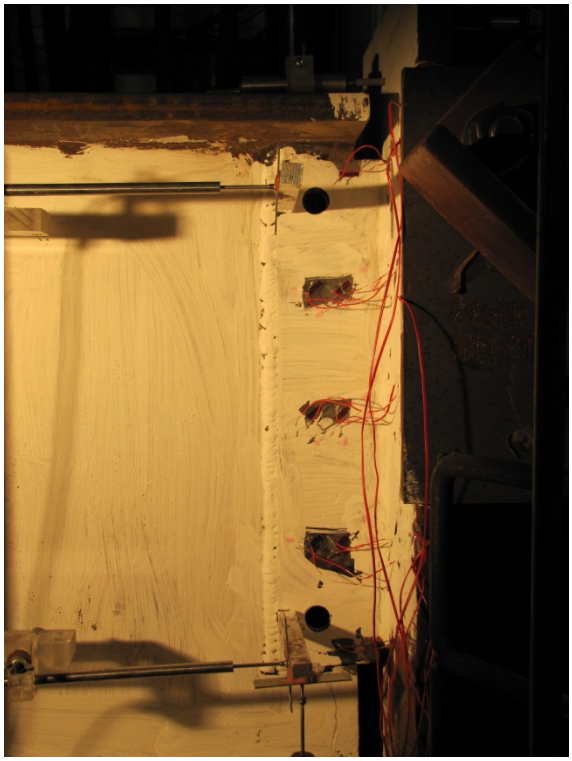

Figure 3-13 - Instrumentation on Welded Shear Tab Test 3 (Shear Tab Side and Back Side)

3.4.2 Bolted Connections

3.4.2.1 Rigid Support Condition

The setup for the bolted shear tab connection tests to rigid supports was identical to the retrofit weld shear tab connections except that all the bolts were inserted in the bolt holes after the beam has been centered and levelled.

In addition, another pair of +/-15mm stroke linear variable differential transducers (LVDTs) is added to the setup in order to measure the vertical and horizontal displacements at the centerline of the top and bottom bolts at the exterior row of bolts.

Figure 3-14 illustrates typical instrumentation required for a bolted test.

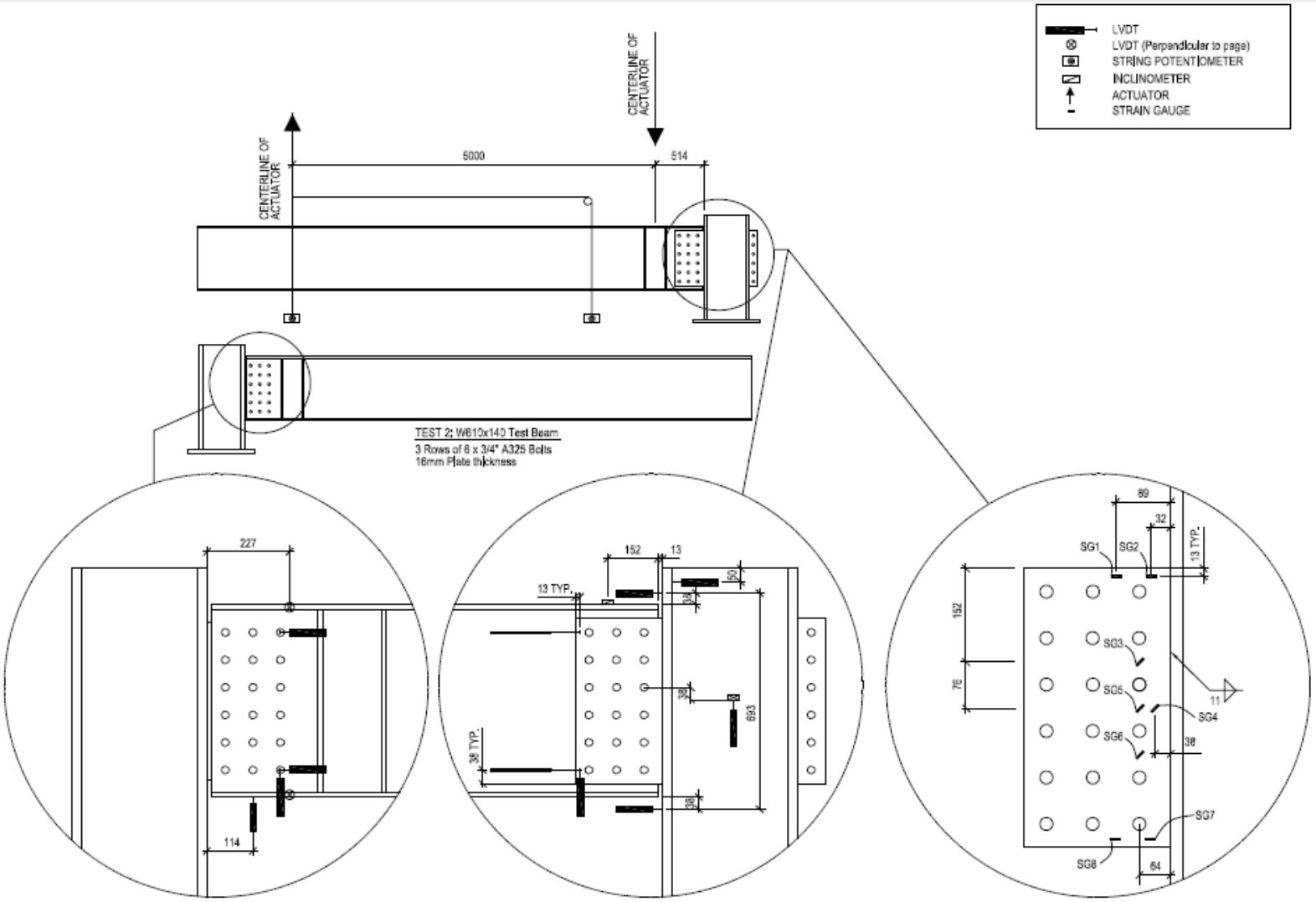

Figure 3-14 - Typical Setup Instrumentation for Bolted Setup for a W610 Beam – Test 2

3.4.2.2 Flexible Support Condition

On the other hand, the setup for the bolted shear tab connection tests to flexible supports is different from the rigid support setup.

As for the rigid support condition setup, the support beam and base plate were tensioned to the strong floor to receive the back-up column. Once this support was secured to the strong floor, the back-up column was erected and bolted down on its base plate. These two operations needed to be performed only once.

The test column was then erected and needed to be stabilized temporarily until the top cap plate was placed in position and the beam was erected. This was achieved by using a single angle bolted to the back-up column and bolted to the shear tab of the test column. Once the column was stabilized, the top plate was placed in position and bolted onto the top of the back-up column.

The next step was to bring the beam in position with the use of the overhead crane. Two bolts were inserted through the shear tab and the beam web and were snug-tightened. As for the rigid support condition, the beam was then centered and levelled, the remaining bolts were inserted and lateral bracing supports were installed.

Regarding the instrumentation, the same LVDTs and strain gauges were used as in the rigid support configuration. In addition, strain gauges were added to the top and bottom edges of the shear tab directly under the stiffeners welded in the column.

To determine the moment generated in the test column's weak axis, load cells were attached to the top and bottom ends of the test column and provided the horizontal tension and compression reactions of the column. Since these load cells are separated by a fixed distance, the axial loads they carried could be used to determine the moment induced in the column by the shear tab connection by using a simple span beam moment diagram. Figure 3-8 presented in Section 3.1 illustrates the positioning of the tension and compression load cells on the test column. This concept will be exposed in Chapter 5.

Figure 3-15 illustrates the positioning and support of the load cell at the base plate of the column. The red HSS stub is a tie between the back-up column and the test column since the load cell at the base of the test column carries only compression loads.

Figure 3-15 - Load Cell at Column Base

3.5 Test Procedure

3.5.1 Bolted Connections

Both the actuators were set in displacement control for all the tests. For the rigid support condition setup, the beam rotation targets relative to the stub column were set to 0.02 radians for the W310 beams and to 0.015 radians for the W610 beams at predicted ultimate connection capacity, which was consistent with that used by Marosi (2011). For the flexible support condition, these target rotations at predicted ultimate connection capacity were set to 0.02 radians for both the beam sizes since the connection layout and flexible column allowed for greater rotations. These targets were to be reached at the calculated probable ultimate resistance of the shear tab using a 10% increase for both the yield and ultimate strengths, F_y and F_u, of the shear plate material, since at the time the material properties were not known.

Once the targeted rotations were reached at the calculated probable ultimate resistance of the connections, the speed of displacement imposed to the connection was increased while keeping a constant ratio of main actuator displacement over tip actuator displacement.

For all tests, except Test 5, the beam end rotation relative to the column face used to control the test was calculated using the top and bottom LVDTs placed on the test beam. For Test 5, the relative rotation used to control the test was calculated using the inclinometers installed on the beam top flange and on the test column. As given by the inclinometers placed on the beam, the absolute rotation at the end of the test beam was slightly larger than the relative rotation

observed at the connection since minimal horizontal displacement of the stub column occurred during the loading.

For both support conditions, the rotations targeted at ultimate were based on the smallest predicted connection resistance value obtained with the two design methods used. The loading method proposed by Astaneh-Asl et al. (1989) was not considered in this test procedure since the shear tab material used in this project was of higher yield strengths and the loading method no longer was appropriate.

Table 3-3 summarizes the loading process for Test 7, which represents a typical loading process for a bolted connection with flexible support.

Table 3-3 - Typical Loading Process for Flexible Support Test

Interval	Main Actuator Speed	Tip Actuator Speed	Connection Load Range
-	mm/min	mm/min	kN
1	0.1125	0.1125	0-10
2	0.1125	0.225	10-15
3	0.1125	0.35	15-40
4	0.1125	0.3	40-50
5	0.1125	0.25	50-165
6	0.1125	0.3	165-185
7	0.1125	0.35	185-215
8	0.1125	0.4	215-370
9	0.1125	0.3	370-390
10	0.1125	0.25	390-420
11	0.225	0.5	420-470
12	0.45	1	470-614

This rotation, relative to the column face, was measured in real-time with the use of the LVDTs located at the top and bottom of the test beam. Since the distance between the LVDTs was measured before the tests were initiated, the relative rotations of the beam to column joint were calculated continuously during the experiment. The vertical displacement imposed by the end actuator needed to be slowed down as the testing progressed since as yielding occurs the shear tabs softens and greater displacements can be obtained in the same amount of time and load applied. Pauses had to be made throughout the procedure to adjust the displacement rates of both

the actuators in order to reach the targeted rotations. Generally, the initial rate of the main 12 MN actuator was set to 0.08 mm/min for the rigid support condition tests and set to 0.1125 mm/min for the flexible support condition tests and the rate of the end actuator was adjusted to reach the targeted rotation ratio.

Table 3-4 depicts the predicted ultimate loads calculated using the modified method at the targeted rotations based on probable yield and ultimate strengths of $1.1F_y$ and $1.1F_u$.

Table 3-4 - Predicted Ultimate Loads at Target Rotation for Bolted Connections

Test Beam	Support Condition	Vertical Rows of Bolt Holes	Predicted Unfactored Connection Strength (kN)*
W310x74	Rigid	3 x 3 Rows	583
W610x140	Rigid	3 x 6 Rows	1455
W310x60	Flexible	2 x 3 Rows	363
W610x140	Flexible	2 x 6 Rows	1455
W310x60	Flexible	2 x 3 Rows	363
W310x74	Flexible	3 x 3 Rows	583
W610x140	Flexible	2 x 6 Rows	1455
W610x140	Flexible	3 x 6 Rows	1455

* Based on probable yield and ultimate strenghts of shear tab material set to 1.1 F_y and 1.1 F_u

3.5.2 Welded Connections

The loading procedure for the welded tests was identical as for the bolted tests since their resistance was set to match their bolted counterparts. The W610 beam rotation relative to the stub column was targeted to 0.015 radians for the single row retrofit weld test and was set to 0.015 radians for the double row partial C-shape retrofit weld test. Table 3-54 depicts the factored strengths for which the weld groups were designed to resist based on the bolt group resistance of their bolted counterparts as a typical weld retrofit would be designed for.

Table 3-5 - Factored Strengths for Weld Groups

Test Beam	Vertical Rows of Bolt Holes *	Factored Weld Group Strength (kN)
W610x140	1 x 6 Rows	503
W610x140	2 x 6 Rows	504

* Bolt holes were drilled for the top and bottom holes of the vertical row only

CHAPTER 4: TEST RESULTS AND ANALYSIS

4.1 Overview

This chapter will present the results of the ten full-scale shear tab experiments in addition to the coupon tests performed to determine the material properties of the W-shapes and plates used in these experiments. The effect of the beam size, column size, number of bolts and vertical rows of bolts, the type of support and the type of connection, whether it is bolted or welded, will be described. The measured connection resistances will be compared with the predicted values obtained using the different design methods. A comparison of predicted and observed behaviors and failure modes will be developed. Finally, further recommendations will be made to improve the shear tab connection design method of the CISC Handbook of Steel Construction (2010).

4.2 Test Results and Observations

The results provided in this section will include a summary of the maximum connection shear force attained in each test, the maximum calculated beam rotation values relative to the column face are provided as well as the maximum beam deflection relative to the supporting column. These results are depicted in summary Table 4-1 for all tests. In each of the ten connections, the measured shear resistance exceeded the predicted unfactored capacity of the connections using the measured material properties with either the AISC (2011) extended configuration or the proposed modified method. The amount of beam rotation and deflection observed will be discussed in the following Sections 4.2.1 to 4.2.6. The discussion of the test results compared to predicted results will be presented in Section 4.3. Also, Appendix C contains complementary material such as additional photographs and graphs for each test.

The results obtained for the double and triple vertical rows of bolts shear tab connections are presented respectively in Tables 4-2 and Table 4-3. These experimental values are compared to the predicted resistances given previously in Table 3-2 which were obtained with both design methods applicable, as previously presented and detailed in Sections 2.3 and 3.3. When referring to probable properties, this indicates that the values provided are the results obtained with the various design methods without the application of the resistance factors and using $1.1*F_y$ and $1.1*F_u$ as probable strengths. When referring to measured material properties, this indicates that

the values given are based on actual material properties determined through coupon testing procedures.

Table 4-1 - Shear Tab Connection Tests - Summary of Results

Test	Support Condition	Failure Mode	Maximum Connection Shear (kN)	Maximum Beam End Rotation Relative to Column Face (rads)	Maximum Vertical Deflection of Beam End Relative to Column (mm)
Double Row - W310 Test Beam					
Test 5	Flexible	SR	501	0.0581	37.49
Test 7	Flexible	SR	508	0.0382	38.18
Triple Row - W310 Test Beam					
Test 1	Rigid	SR	652	0.0492	33.53
Test 8	Flexible	SR	614	0.0371	35.84
Double Row - W610 Test Beam					
Test 6	Flexible	SR	1910	0.0153	46.91
Test 9	Flexible	SR	1970	0.0285	47.23
Triple Row - W610 Test Beam					
Test 2	Rigid	SR	1834	0.0338	26.03
Test 10	Flexible	SR	1954	0.0289	29.61
Welded - W610 Test Beam					
Test 3	Rigid	SY	1166	0.0184	30.09
Test 4	Rigid	SY	2283	0.0361	33.22

Failure Modes:

SR = Shear Rupture through Plate Net Area
SY = Shear Yielding of Plate / Shear Deformation

Table 4-2 - Bolted Tests with Two Vertical Rows of Bolts Experimental Results Compared to Predicted Values

Test -	Measured Resistance kN	Observed Failure Mode -	Design Method -	Unfactored Predicted Resistance Based on Probable Material Properties kN	Predicted Failure Mode -	Measured/ Predicted Ratio -	Unfactored Predicted Resistance Based on Measured Material Properties kN	Predicted Failure Mode -	Measured/ Predicted Ratio -
5	501	SR	AISC Extended	363	PFY	1.38	440	PFY	1.14
			Modified Method	363	PFY	1.38	440	PFY	1.14
6	1910	SR	AISC Extended	1455	BLS	1.31	1676	BLS	1.14
			Modified Method	1455	BLS	1.31	1676	BLS	1.14
7	508	SR	AISC Extended	363	PFY	1.40	440	PFY	1.15
			Modified Method	363	PFY	1.40	440	PFY	1.15
9	1970	SR	AISC Extended	1455	BLS	1.35	1676	PFY	1.18
			Modified Method	1455	BLS	1.35	1676	BLS	1.18

Failure Modes:

BLS= Block Shear Rupture
BG= Bolt Group Shear Failure
SR= Shear Rupture through Plate Net Area
PFY= Plate Flexural Yielding

Table 4-3 - Bolted Tests with Three Vertical Rows of Bolts Experimental Results Compared to Predicted Values

Test -	Measured Resistance kN	Observed Failure Mode -	Design Method -	Unfactored Predicted Resistance Based on Probable Material Properties kN	Predicted Failure Mode -	Measured/ Predicted Ratio -	Unfactored Predicted Resistance Based on Measured Material Properties kN	Predicted Failure Mode -	Measured/ Predicted Ratio -
1	652	SR	AISC Extended	583	PFY	1.12	597	BG	1.09
			Modified Method	583	PFY	1.12	605	PFY	1.08
2	1834	SR	AISC Extended	1455	BLS	1.26	1534	BLS	1.20
			Modified Method	1455	BLS	1.26	1534	BLS	1.20
8	614	SR	AISC Extended	583	BG	1.20	597	BG	1.03
			Modified Method	583	PFY	1.05	605	PFY	1.01
10	1954	SR	AISC Extended	1455	BLS	1.34	1534	BLS	1.27
			Modified Method	1455	BLS	1.34	1534	BLS	1.27

Failure Modes:

BLS= Block Shear Rupture
BG= Bolt Group Shear Failure
PFY= Plate Flexural Yielding
SR= Shear Rupture through Plate Net Area

Table 4-4 - Comparison of Predicted Resistance for Observed Failure Mode

Test -	Method -	Observed Failure Mode -	Measured Connection Resistance kN	Predicted Resistance for Observed Failure Mode with AISC Equation kN	Predicted Resistance for Observed Failure Mode with CISC Equation kN
1	AISC Extended	SR	652	630	654
2	AISC Extended	SR	1834	1556	1686
5	AISC Extended	SR	501	503	567
6	AISC Extended	SR	1910	1699	1984
7	AISC Extended	SR	508	503	567
8	AISC Extended	SR	614	630	676
9	AISC Extended	SR	1970	1699	1984
10	AISC Extended	SR	1954	1556	1984

Failure Modes

BLS= Block Shear Rupture
BG= Bolt Group Shear Failure
SR= Shear Rupture through Plate Net Area
PFY= Plate Flexural Yeilding

Table 4-4 presents a summary of the measured connection resistance compared with the predicted resistance for the observed failure mode. Shear rupture through the net area of the shear tab being the observed failure mode in all tests, the predicted resistance for this failure is presented as calculated by the AISC 14th Edition (2011) method and the CISC Manual 10th Edition (2010) equation using measured material properties based on Clause 13.11 of CSA S16-09 (2009). Using the AISC Manual (2011) equations for net shear rupture, the predicted

resistance underestimated the measured connection resistance in all cases except for Test 5. However, the CISC Manual (2011) equation using measured material properties overestimated the shear tab capacity for all shallow connections, Tests 1, 5, 7 and 8

4.2.1 Connections with Two Vertical Rows of Three Bolts

Both double vertical row of bolts connections of W310x60 test beams, Tests 5 and 7, with three bolt lines exceeded the predicted connection resistance determined using $\phi = 1.0$ and the measured yield and ultimate strength values. The maximum beam end rotation values relative to the supporting column face were also exceeded compared to the targeted rotation values for both these flexible support condition tests. The rotations are being monitored during the experiments in order to reach the targeted rotation at the ultimate predicted resistance of the connection, but since this ultimate resistance is surpassed, the rotations are increased proportionally with the applied load. This justifies the fact that targeted rotations are surpassed in every experiment.

The beam end rotation observed for Test 5 is greater than the relative beam end rotation observed for Test 7. The test process for Test 5 did not include horizontal LVDTs at the top and bottom flanges to calculate the beam rotation relative to the column face and therefore Test 5 rotations where monitored throughout the testing by using the inclinometer readings of the instruments placed on the beam and test column. For this reason, the Test 5 relative rotation, calculated by subtracting the absolute column rotation to the absolute beam rotation, both measured with the inclinometers, does not provide very accurate results and can partially explain the very large beam rotation found in Test 5. Test 5 is associated to a W360x122 column size while Test 7 had a much stiffer W360x314 column support in terms of flexure. The different column members do not seem to have any influence on the connection capacity since the observed shear capacities are practically identical and both failure modes are identical.

As observed in Figure 4-1, picturing the shear tab for Test 5 after failure, once the test bolts had been removed it is noticeable that shear deformations have occurred around the bolt holes in the shear tab and that these deformations are greater in the vertical row of bolts closest to the face of the supporting column whereas the predicted failure modes was shear tab flexural yielding for both design method. Also, significant shear deformations were noticeable between the bolt holes through the column of bolts closest to the supporting column. Similarly, as shown

in Figure 4-2 picturing Test 7 at failure, shear deformations can be observed as well as shear rupture through the first line of bolts whereas the predicted failure modes were shear fracture of the bolt group by the AISC (2011) method and shear plate flexural yielding by the modified method.

Figure 4-1 - Test 5 after Failure

Figure 4-2 - Test 7 after Failure

As described in Section 3.4, strain gauges were placed on the shear tab to measure onsets of shear and flexural yielding. In both tests the strain gauges placed at 45° indicated shear yielding in the shear tab before the other strain gauges indicated flexural yielding of the plate. Figure 4-3 contains a graph of the beam rotation relative to the supporting column face against the connection shear. This plot demonstrates that very similar maximum connection shears were obtained in both experiments but at unequal relative rotation values. It is noticeable that in order to reach its maximum 0.0382 radian relative rotation maximum, red curve, Test 7 beam needed to achieve an absolute rotation of 0.0561 radians, green curve, as measured with the inclinometers placed on its flanges. This curve absolute rotation of Test 7 is very similar to the Test 5 derived relative rotation, blue curve, which indicated that the relative rotation observed with LVDTs for Test 5 would have sensibly matched Test 7 relative rotation curve.

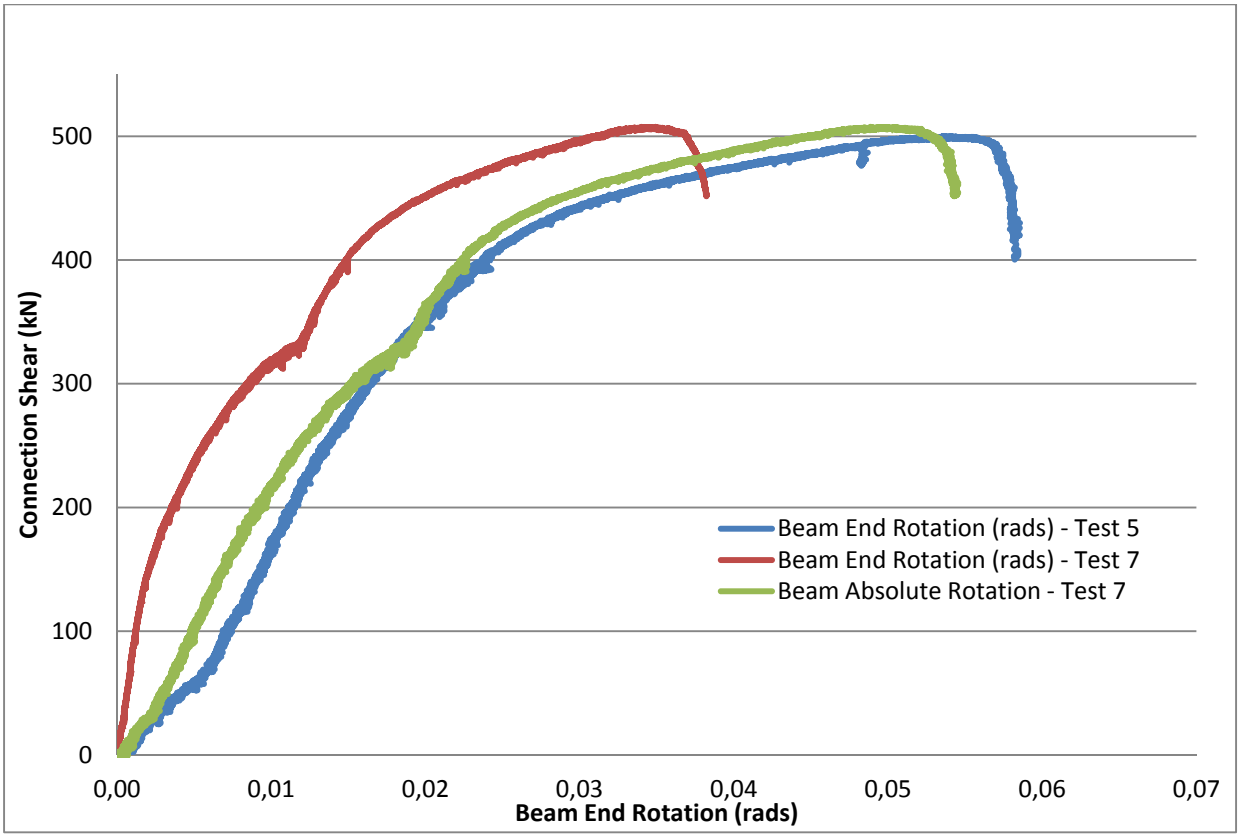

Figure 4-3 - Comparison of Tests 5 and 7 Connection Shear vs. Beam End Rotation

For this group, as observed in Figure 4-4, the strain gauges indicate that shear yielding, SG4 in Test 5 and SG10 in Test 7, occurred in the shear tab prior to the onset of flexural yielding

in SG2 and SG7 for Test 5 and SG2 and SG6 for Test 7, and this being the case for both Tests 5 and 7. Refer to Appendix A for diagrams of exact strain gauge positioning for each test.

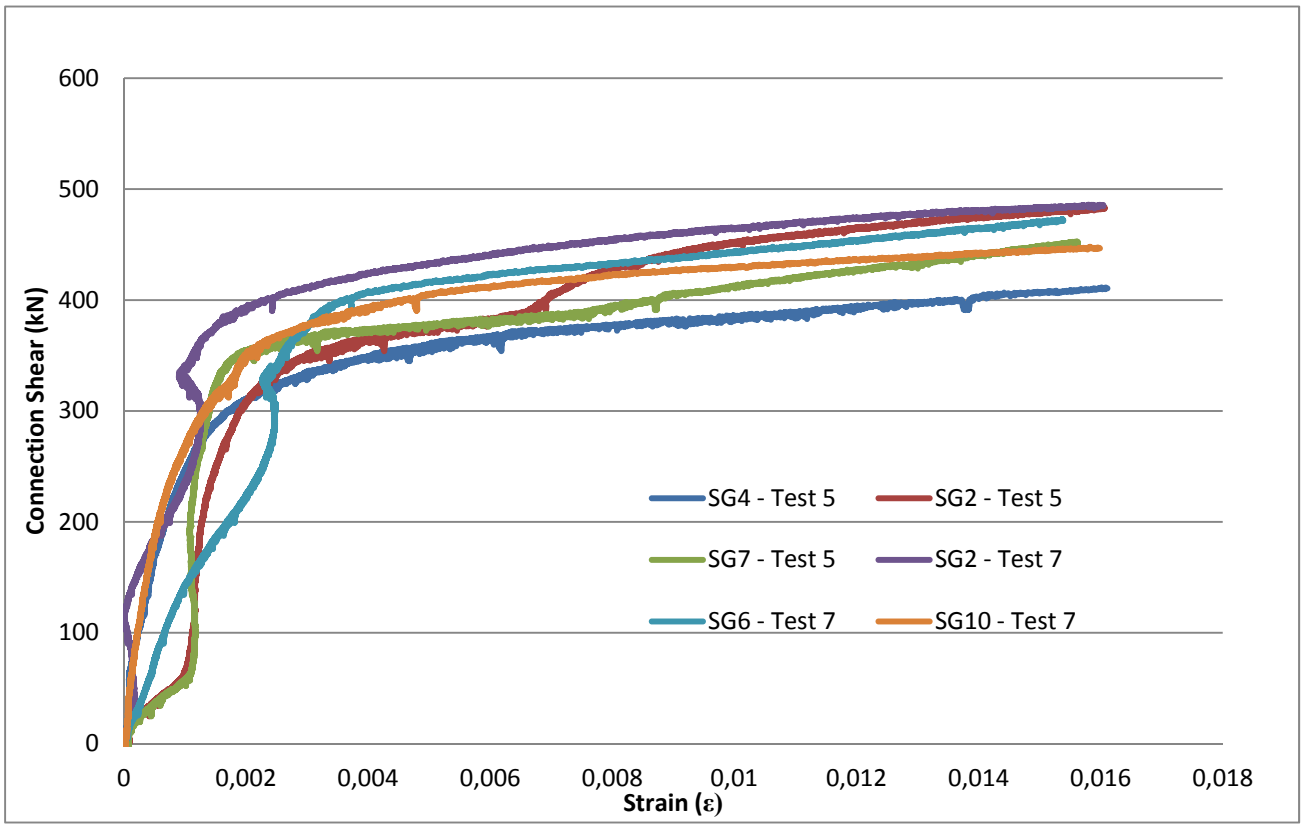

Figure 4-4 - Comparison of Tests 5 and 7 Connection Shear vs. Strain

4.2.2 Connections with Three Vertical Rows of Three Bolts

Test 1 and Test 8, with three vertical lines of bolts and W310x74 beams, exceeded the predicted connection resistance determines using $\phi = 1.0$ and the measured yield and ultimate strength values. The beam end rotation relative to the supporting column face values were also exceeded compared to the targeted rotation values. Bolted shear tab Test 1 was welded onto a rigid support as opposed to Test 8 which was welded onto a flexible support, refer to Appendix A for test specimen schematics.

The maximum beam end rotation relative to the supporting column observed for Test 1 is greater than the maximum relative rotation observed for Test 8. This difference in relative beam end rotation could be explained by the difference between the types of supports. The flexible

support being a connection into the web of a full-span column, as in the case of Test 8, has a strong tendency to rotate with the shear connection. The rotation capacity of the connection itself is similar in both tests, as observable by looking at shear tab deformations in Figures 4-5 and 4-6, but the relative beam end rotation is lower for Test 8 since the column rotates with the connection as depicted in Figure 4-7 where the absolute rotation of Test 8 beam is very similar to relative rotation of Test 1. In this case, the different column members seem to have little influence on the connection capacity since the observed shear capacity for Test 1 is 8% greater than the maximum shear measured in Test 8.

It was observed that, during Test 1, as depicted in Figure 4-5, picture taken once the test was completed, a weld fracture of approximately 25mm in length of the shear tab to column weld at the top of the shear tab occurred after the shear and flexural yielding of the shear tab towards the end of the test but slightly before the net shear rupture of the shear tab occurred. In contrast fracture of the weld was not observed in Test 8, although the location of the weld versus the first vertical row of bolts was different, as such likely resulted in less strain demand on the weld. In both tests, shear deformations around the bolt holes could be observed after removing the bolts. Also, both these bolted connections resulted in shear yielding along the line of the bolt holes which increased to shear fracture through the net area of the plate in the vertical row of bolts closest to the support column.

The predicted failure mode for Test 1 was shear fracture of the bolt group for the AISC Extended Method (2011) and shear tab flexural yielding by the proposed modified method.

Figure 4-6 shows the failure modes observed for Test 8. Similar to Test 1, it is noticeable that shear deformations have occurred around bolt holes, mainly along the vertical row of bolts closest to the supporting member. Also, shear fracture through the net area of the shear tab occurred along the same column of bolts. Once again, the predicted failure mode for this connection was shear fracture of the bolt group by the AISC Extended Method (2011) and shear tab flexural yielding by the modified method.

Figure 4-5 - Test 1 after Failure

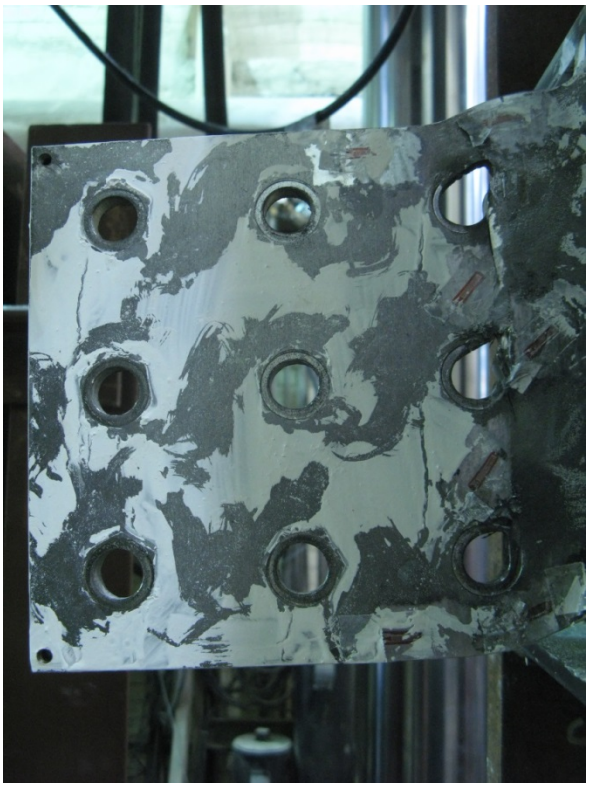

Figure 4-6 - Test 8 after Failure

Figure 4-7 plots the test beam end rotation relative to the column face against the connection shear for both Tests 1 and 8. This plot illustrates that very similar beam end rotation relative to the test column face were obtained at the point of maximum connection capacity.

For this group of connections, as pictured in Figure 4-8, strain gauges readings indicated that shear yielding, SG4 for both tests, occurred in the shear tab before the onset of flexural yielding was observed in SG2 and SG7 for Test 1 and SG2 and SG6 for Test 8, this being the case for both Tests 1 and 8. Refer to Appendix A for diagrams of exact strain gauge positioning for each test.

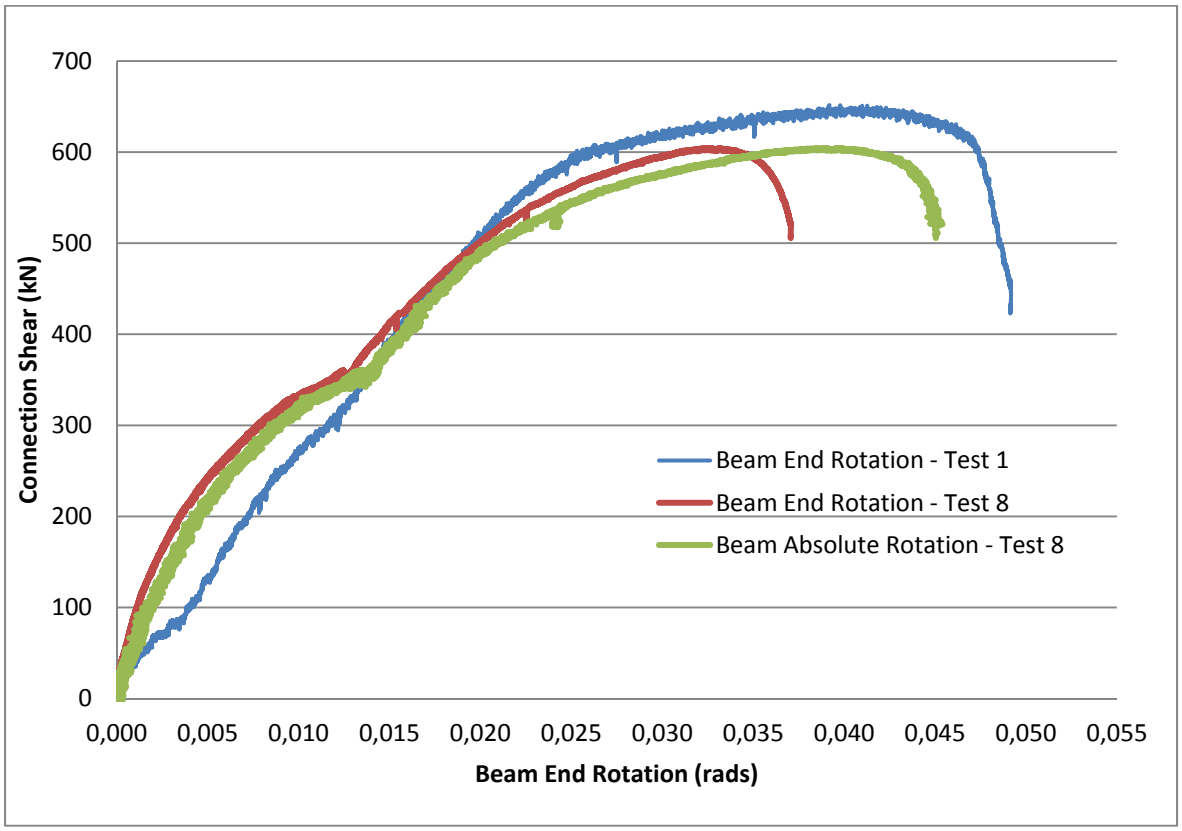

Figure 4-7 – Comparison of Tests 1 and 8 Connection Shear vs. Beam End Rotation

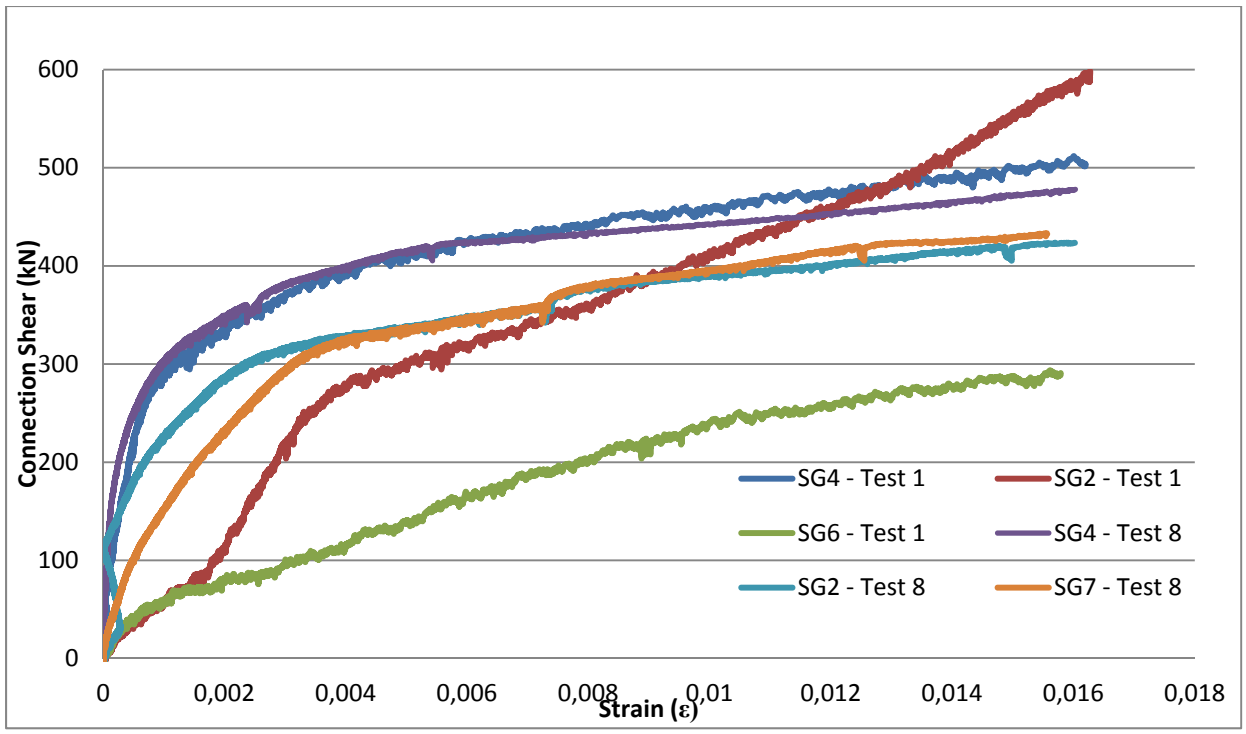

Figure 4-8 - Comparison of Tests 1 and 8 Connection Shear vs. Strain

4.2.3 Connections with Two Vertical Rows of Six Bolts

Test 6 and Test 9 double column connections of W610x140 test beams with six vertical bolt lines both exceeded the predicted connection resistance determined using $\phi = 1.0$ and the measured yield and ultimate strength values. The maximum beam end rotation values relative to the supporting column face were also exceeded compared to the targeted rotation values. Both these bolted shear tab connections had flexible supports. The targeted rotations set for Test 9 was attained and surpassed unlike Test 6 where the relative rotation targeted at ultimate was 0.020 rad and the maximum rotation reached was 0.0153 rad. The beam absolute rotation observed for Test 9 is greater than the beam absolute rotation observed for Test 6; this could be explained by the difference in relative rigidity of both supporting column members. Test 6 is associated to a W360x122 column size and Test 9 had a much heavier column being a W360x314. In this case, the relative rigidity of the column members, the W360x314 is approximately 7 times stiffer in terms of weak axis flexure than the W360x122, seems to have very little influence on the connection capacity since the observed shear capacity for Test 9 is 3% greater than the maximum shear measured in Test 6 as depicted in Table 4-1.

As pictured in Figure 4-9, in Test 6, a weld fracture could be observed along the entire length of the shear tab to top stiffener weld. This weld fracture has caused a significant load drop near the maximum shear capacity of the connection which was well beyond the predicted connection capacity. This weld fracture might have been caused by the extensive deformations suffered by the column and the top and bottom stiffeners. It is also noticeable that the failure mode of Test 6 is shear rupture through the net area of the shear tab. Shear deformations around bolt holes can also be observed mainly along the first row of bolts closest to the column.

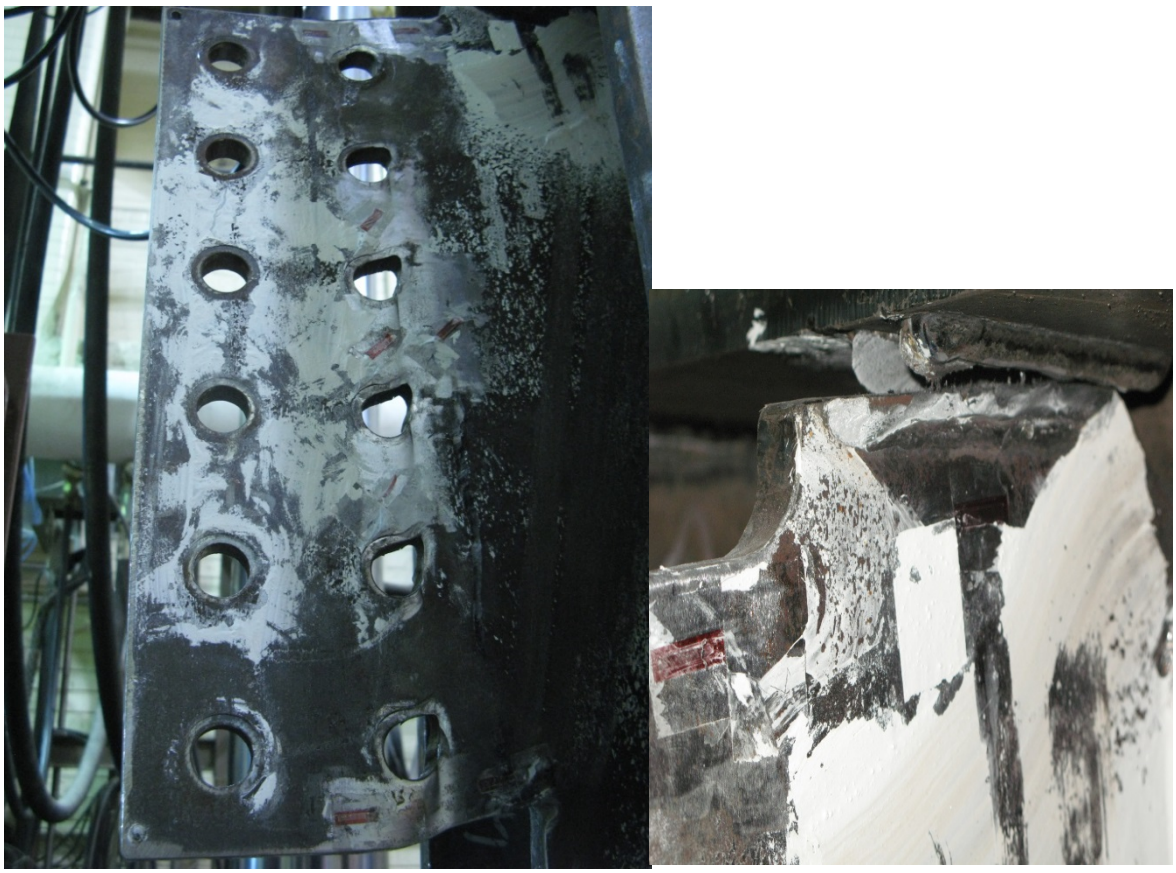

Figure 4-9 - Test 6 after Failure

The loading on the beam also resulted in a significant amount of weak axis bending in the supporting column as depicted in Table 4-1. This moment was calculated as described in Section 3.4.2.2. The weak axis bending capacity of the column member is M_p = 253kNm and the calculated moment induced in the column is M_p = 272.6 kNm. Therefore, this weak axis moment generated in the column exceeded the column capacity by roughly 20% causing the column to yield in flexure as depicted in Figure 4-10. This flexural yielding occurred at loads beyond the

predicted ultimate capacity of the shear tab connection using measured yield and ultimate strength values of the material. The rotation imposed to the column, as read by the inclinometer placed on top of the stiffener on the opposite side of the connection, was as large as 0.424 radians. However, the accuracy of this reading is doubtful since the stiffener supporting the inclinometer, which was placed on the opposite connection side, was severely deformed during the experiment.

Figure 4-10 - Test 6 Column Showing Signs of Yielding

The predicted failure mode for Test 6 and Test 9 was block shear rupture of the shear tab for both design methods. In this case, as previously mentioned, this failure mode was not the governing failure mode observed during the experiment, but, as observed in Figure 4-11, permanent damage was made to the bolt atop the connection in the vertical bolt line closer to the test column.

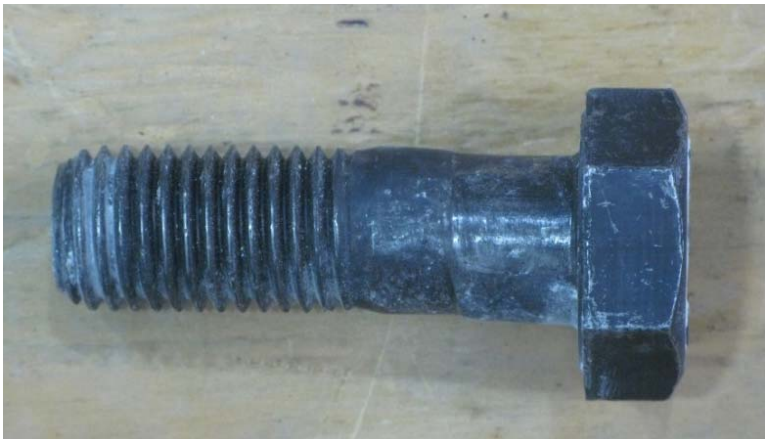

Figure 4-11 - Damaged Bolt after Test 6

With respect to Test 9, shear deformations could also be observed around bolt holes but, as opposed to Test 6, no weld fracture occurred at the top shear tab to stiffener weld. As pictured in Figure 4-12, shear rupture through the net area of the shear tab is the observed failure mode while shear fracture of the bolt group was predicted by the AISC (2011) method and shear tab block shear rupture was predicted by the modified method. The column being a much more rigid shape in terms of flexure for this Test, W360x314 Test 9 column is approximately 7 times stiffer in terms of flexural stiffness (EI_y/L) than the W360x122 Test 6 column, no flexural yielding occurred in the column itself as opposed to strain gauge readings indicating clear flexural yielding in the shear tab at the top and bottom stiffener interfaces.

Figure 4-13 shows a graph of the test beam end rotation relative to the column face against the connection shear for Tests 6 and 9 as well as the absolute beam rotation curves for both tests. The load drop shown in the curves of Test 6 represents the time at which the weld between the top stiffener and the shear tab fractured as depicted in Figure 4-7. This weld fracture affected the beam end rotation curve minimizing the maximum rotation attainable. For this particular reason and due to the relative column shaft stiffness, it is believed that Test 6 connection would have reached higher rotation values had this weld not fractured and maybe reached the targeted rotation at ultimate.

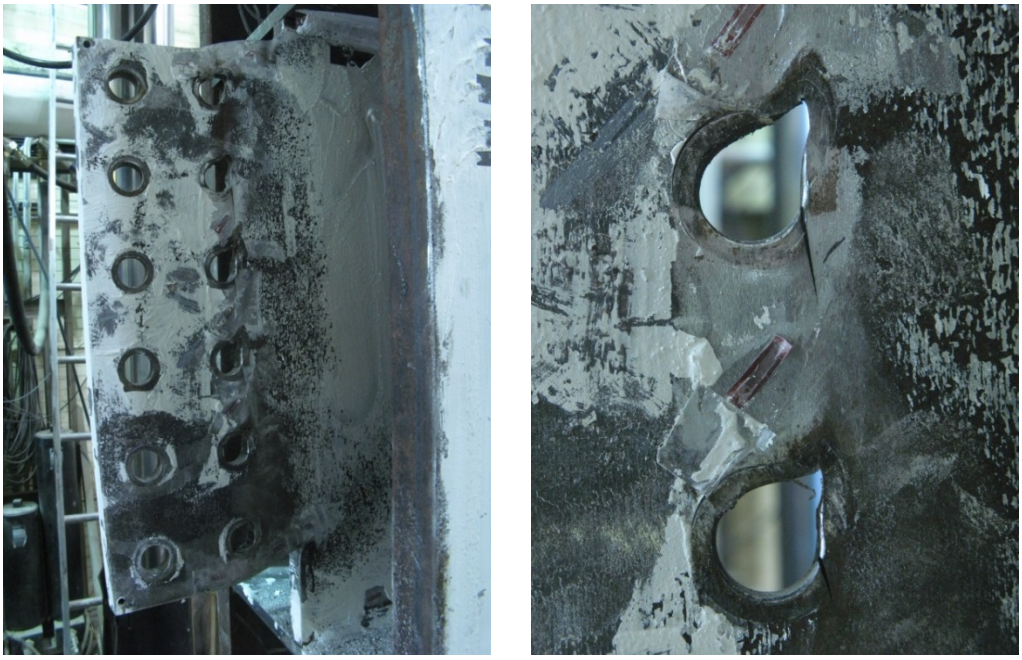

Figure 4-12 - Test 9 after Failure

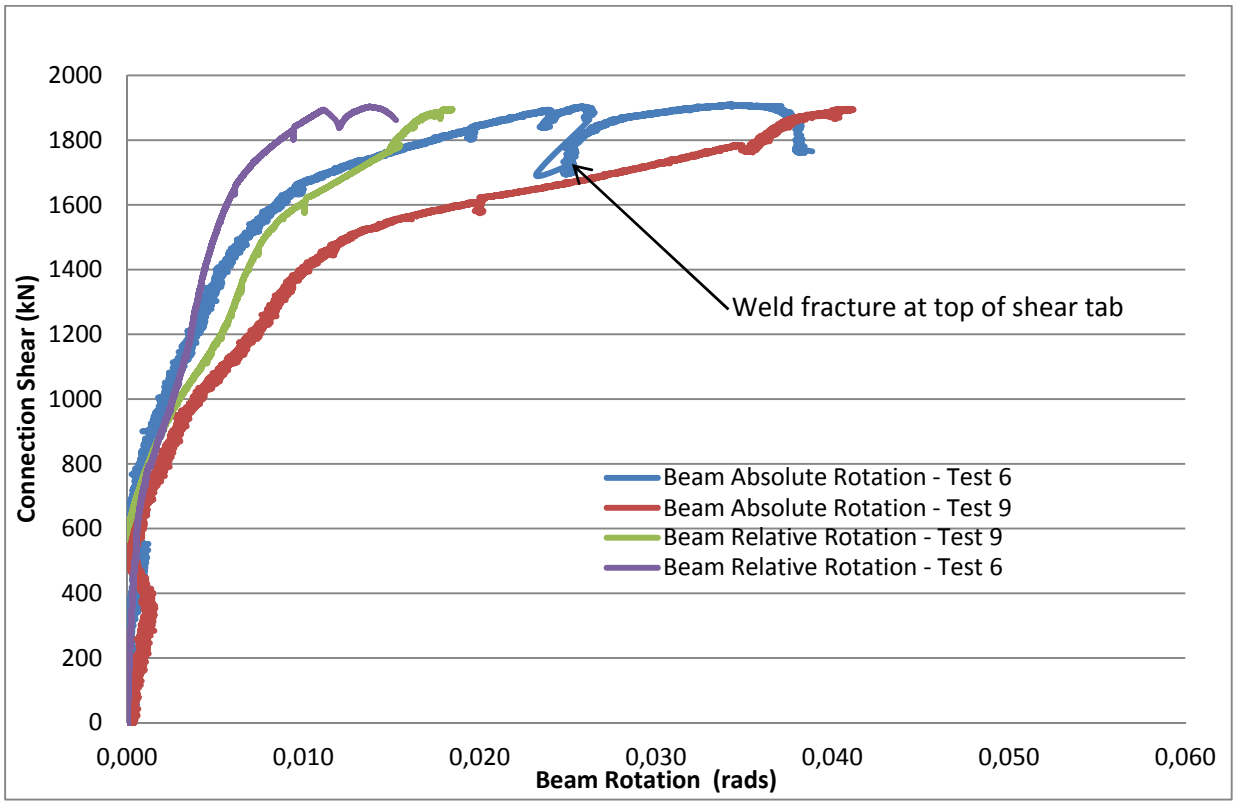

Figure 4-13 - Comparison of Tests 6 and 9 Connection Shear vs. Beam End Rotation

Once again, in both tests, as plotted in Figure 4-14, the strain gauges on the shear tabs indicate that shear yielding, depicted as SG6 for Test 6 and SG4 for Test 9, occurred in the plates prior to onsets of flexural yielding were observed, labelled as SG2 and SG8 for both tests. Note that SG2 in Test 6 malfunctioned and is therefore not plotted. Refer to Appendix A for diagrams of exact strain gauge positioning for each test.

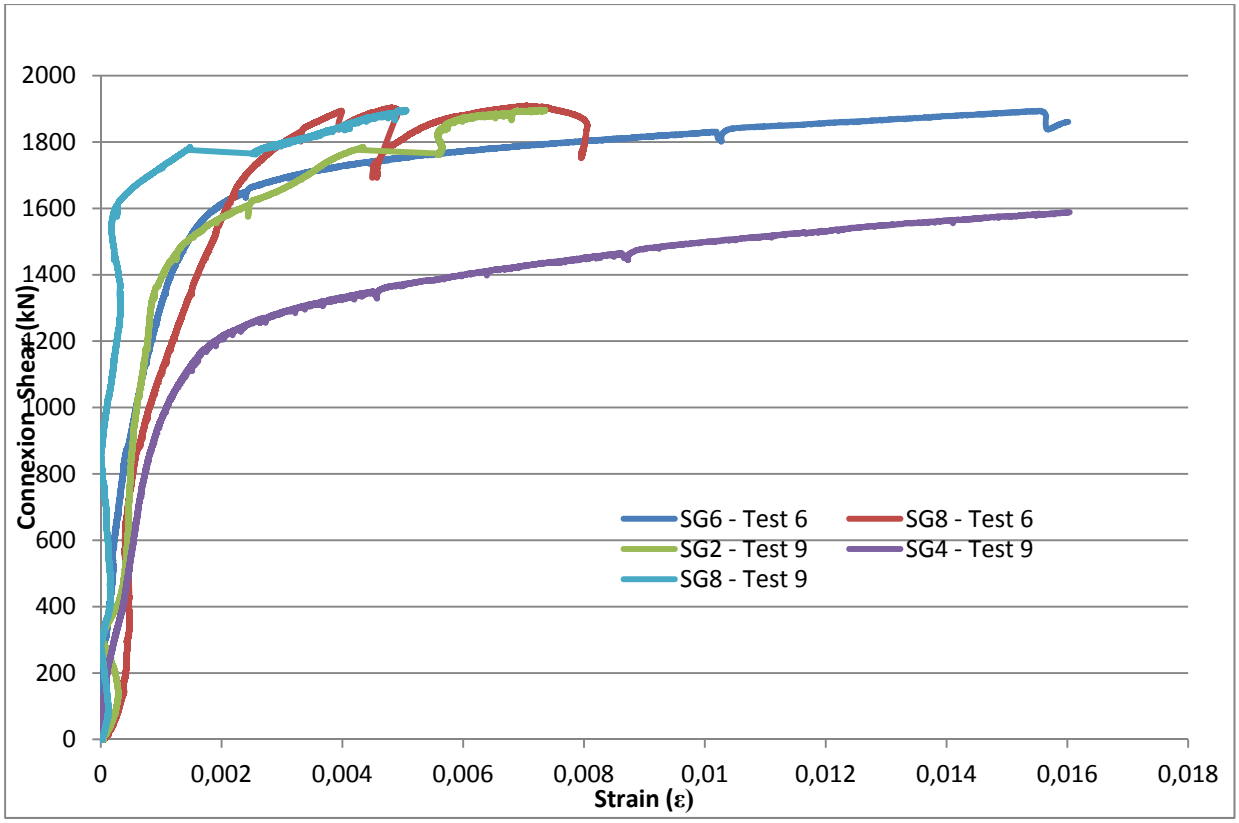

Figure 4-14 - Tests 6 and 9 Comparison of Connection Shear vs. Strain

4.2.4 Connections with Three Vertical Rows of Six Bolts

Test 2 and Test 10 triple vertical lines of six bolts connections of W610x140 test beams exceeded the predicted connection resistance determined using $\phi = 1.0$ and the measured yield strength and ultimate strength values. The beam end rotation values relative to the supporting column face were also exceeded compared to the targeted rotation values. Bolted shear tab Test 2 had a rigid support as opposed to Test 10 which was welded to a flexible support. The maximum beam end rotation relative to the supporting column observed for Test 10 is greater than the maximum relative rotation observed for Test 2. In this case, the different sizes of the column

members seem to have very little influence on the connection capacity since the observed shear capacity for Test 10 is only 7% greater than the maximum shear measured in Test 2.

Figure 4-15 - Test 2 after Failure

It was observed that, during Test 2 as depicted in Figure 4-15, a weld fracture of approximately 25mm in length between the top of the shear tab and the test column occurred after the yielding of the shear tab towards the end of the test. This weld fracture might be the cause of Test 2 not reaching the same connection resistance as Test 10. In both tests, shear deformations around the bolt holes could be observed after removing the bolts. Also, both these bolted connections resulted in shear yielding along the bolt holes which increased to shear fracture through the net area of the plate in the vertical row of bolts closer to the support column this being the failure mode of both the connections. The predicted failure mode was block shear rupture of the shear tab for Test 2 and Test 10 as both the design methods predicted the same failure mode.

Figure 4-16 - Test 10 after Failure

As for Test 10, shear yielding deformations could also be observed around bolt holes but, as opposed to Test 2, no weld fracture occurred at the top shear tab to stiffener weld. As pictured in Figure 4-16, the observed failure mode is shear yielding increasing into shear rupture through the net area of the shear tab in the vertical line of bolts closest to the supporting column.

Figure 4-17 plots the test beam end rotation relative to the column face against the connection shear for both Tests 2 and 10. This graph illustrates that the maximum connection shears of both connections were reached at similar relative rotation levels. It can be observed that in order to reach and exceed the targeted rotation relative to the column face, Test 10 beam needed to withstand a level of absolute rotation, measured with the beam inclinometers, practically equivalent to the Test 2 beam relative rotation.

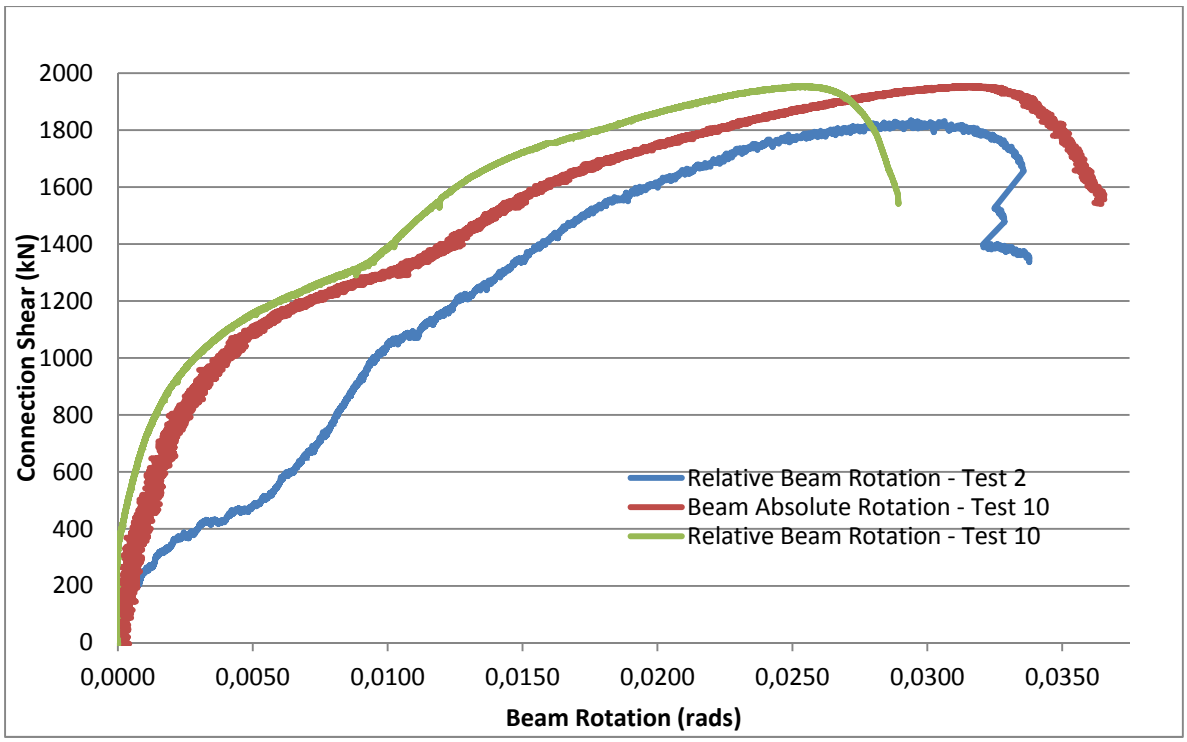

Figure 4-17 - Comparison of Tests 2 and 10 Connection Shear vs. Beam Rotation

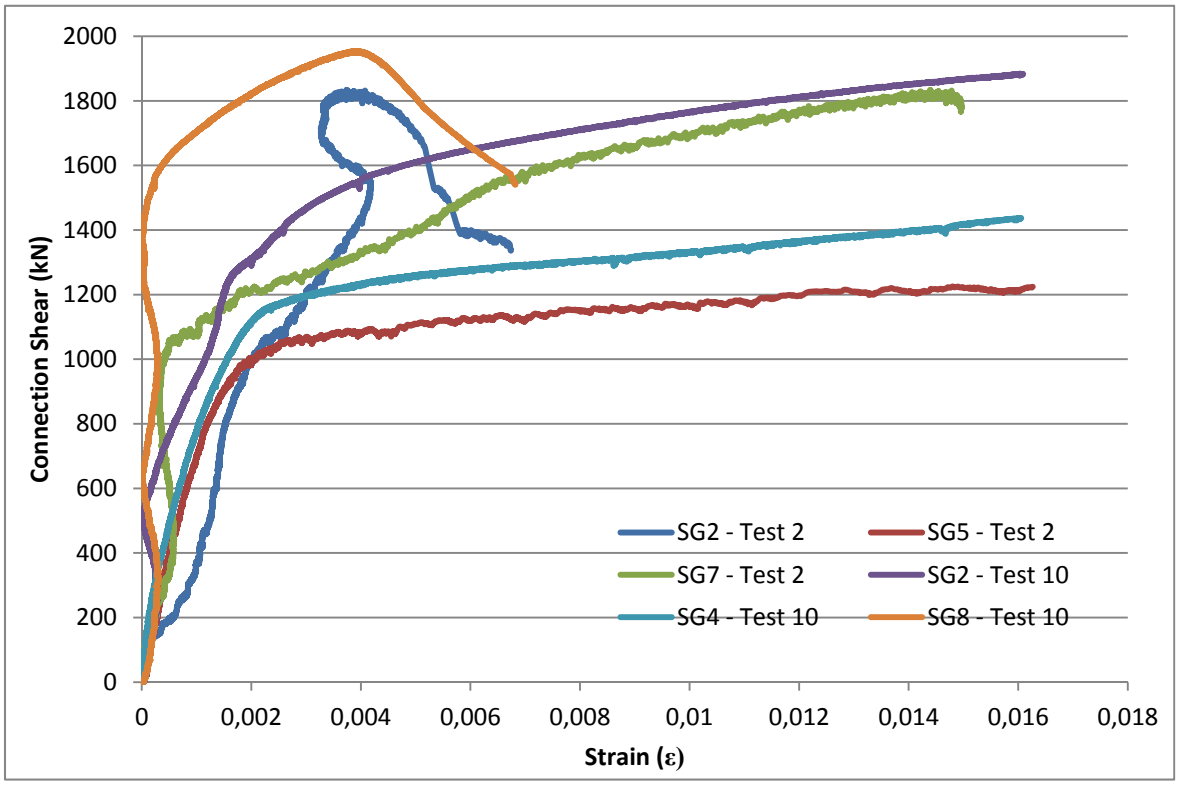

Figure 4-18 - Comparison of Tests 2 and 10 Connection Shear vs. Strain

Again, as plotted in Figure 4-18, the strain gauges indicate that shear yielding, strain gauge SG5 in Test 2 and SG4 in Test 10, occurred in the shear tab prior to the onset of flexural yielding; observed on strain gauges SG2 and SG7 in Test 2 and SG2 and SG8 in Test 10. Refer to Appendix A for diagrams of exact strain gauge positioning for each test.

4.2.5 Connections with Single and Double Vertical Rows Welded Retrofit

Both these retrofit welds were partial C-shape welds around the perimeter of the shear tab where it makes contact with the beam web. Both weld retrofit connections for Test 3 and Test 4 well surpassed the predicted maximum unfactored capacity of their bolted counterparts as determined by Marosi (2011) with $\phi = 1.0$ and using the measured yield and ultimate strength values. Also, these welded connections have reached relative beam rotation levels beyond their targeted rotation values. In both tests, the bolts were removed from the bolt holes once the retrofit welds were performed. Thus, when comparing the unchanged shear tab parameters and by replacing the bolts with a retrofit weld, the connection still performs beyond the expected rotation and resistance objectives. The shear tab capacity does not seem to be reduced by this field weld repair.

As shown in Figure 4-19, the failure mode for Test 3 is net shear fracture through the vertical edge distance of the bolt hole. Since, the top and bottom legs of the partial C-shape weld end in line with the centerline of the bolt hole this is quite possibly the reason why this corresponds with where the vertical edge distance shear fracture initiated. It was also observed during Test 3, and illustrated in Figure 4-19, that a weld fracture of approximately 38 mm in length at the top of the weld between the shear tab and the test column occurred after the yielding of the shear tab towards the end of the test once the predicted connection capacity was well surpassed.

Figure 4-19 - Test 3 after Failure

Regarding Test 4, as shown in Figure 4-20, the experimental failure mode observed is a fracture of the shear tab to column flange weld and extensive shear deformations. This time the retrofit weld shape did not coincide with the centerline of the erection bolt holes. Therefore, no vertical edge distance fracture was observed for this experiment.

Both configurations began to yield in flexure relatively early on into the testing highlighting the stiffness of the retrofit welded connections in the low shear load ranges, even though this type of connection showed great flexibility and rotation allowance in the higher shear load range. This weld pattern put a greater strain demand on the part of the shear tab near the column weld because the section of plate within the perimeter of the weld group did not deform and redistribute the stress early in the test as a bolt group would allow.

Figure 4-20 - Test 4 after Failure

Figures 4-21 and 4-22 illustrate the test beam end rotation relative to the column face against the connection shear respectively for Tests 3 and 4. In Figure 4-21, representing Test 3, a plateau is noticed. The lack of data between those points indicates that there has been slippage in the instrument either on the top or the bottom flanges of the test beam. Therefore, the subtraction between the rotation values of these two data points is to be subtracted to the maximum rotation value reached in the experiment. This means that the maximum rotation reached for Test 3 is 0.0235 – (0.0270-0.0219) = 0.0184. Also, early flexural yielding of the plate explains the lack of rotation in the connection at low shear load ranges, up to 60kN.

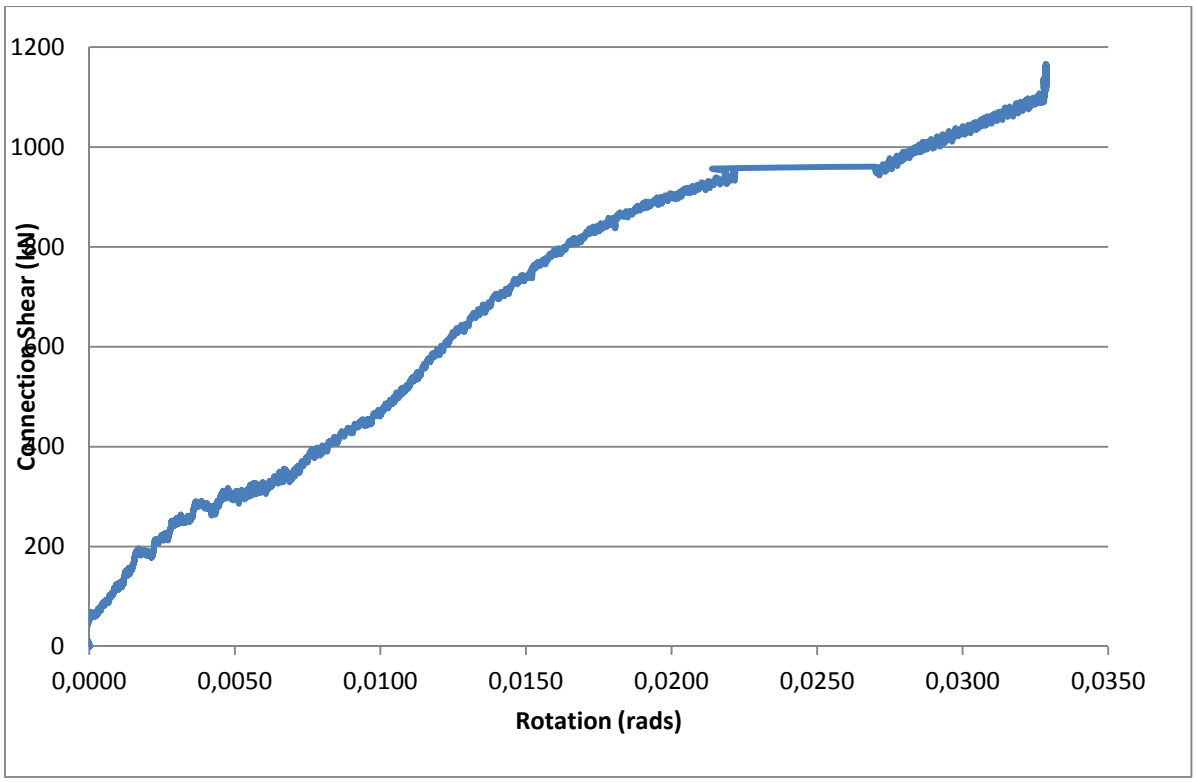

Figure 4-21 - Test 3 Connection Shear vs. Beam End Rotation Relative to Column Face

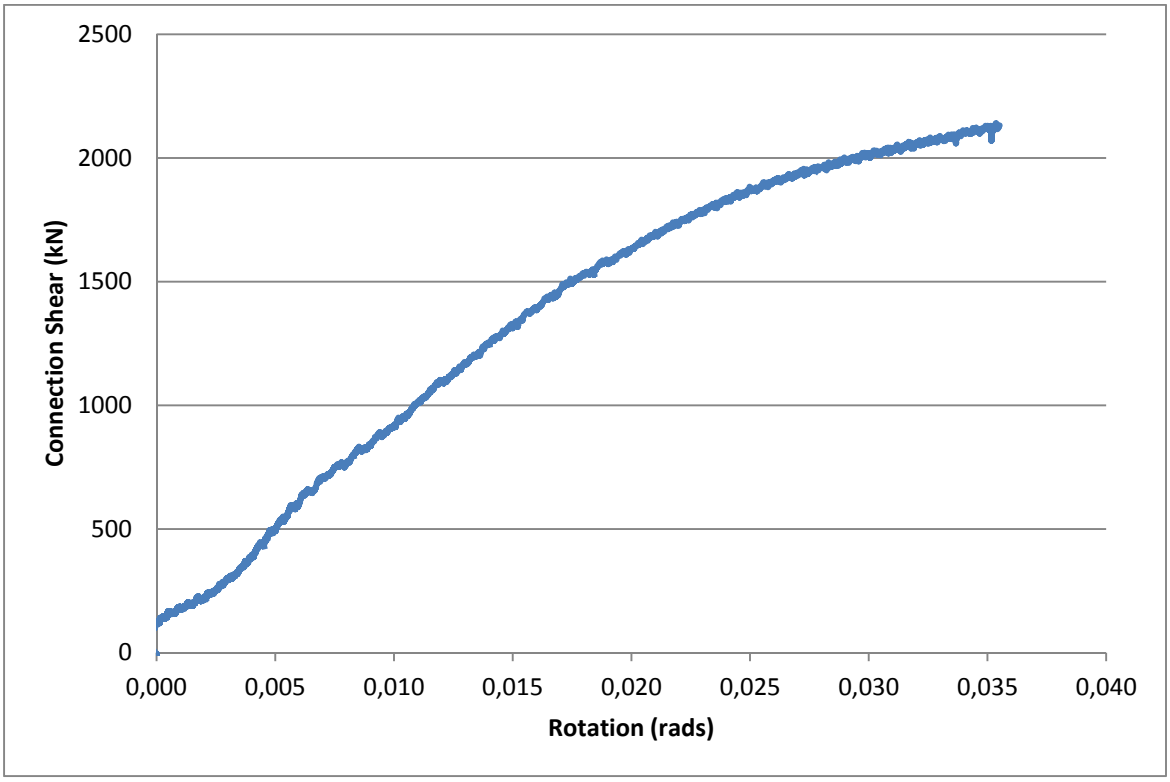

Figure 4-22 - Test 4 Connection Shear vs. Beam End Rotation Relative to Column Face

Conversely to the all the bolted shear tab connections in this research program and as shown in Figure 4-23, in both experiments the strain gauges, SG1 and SG8, indicated that flexural yielding occurred in the shear tab before the onset of shear yielding was observed, strain gauge SG5 in both configurations. Refer to Appendix A for diagrams of exact strain gauge positioning for each test.

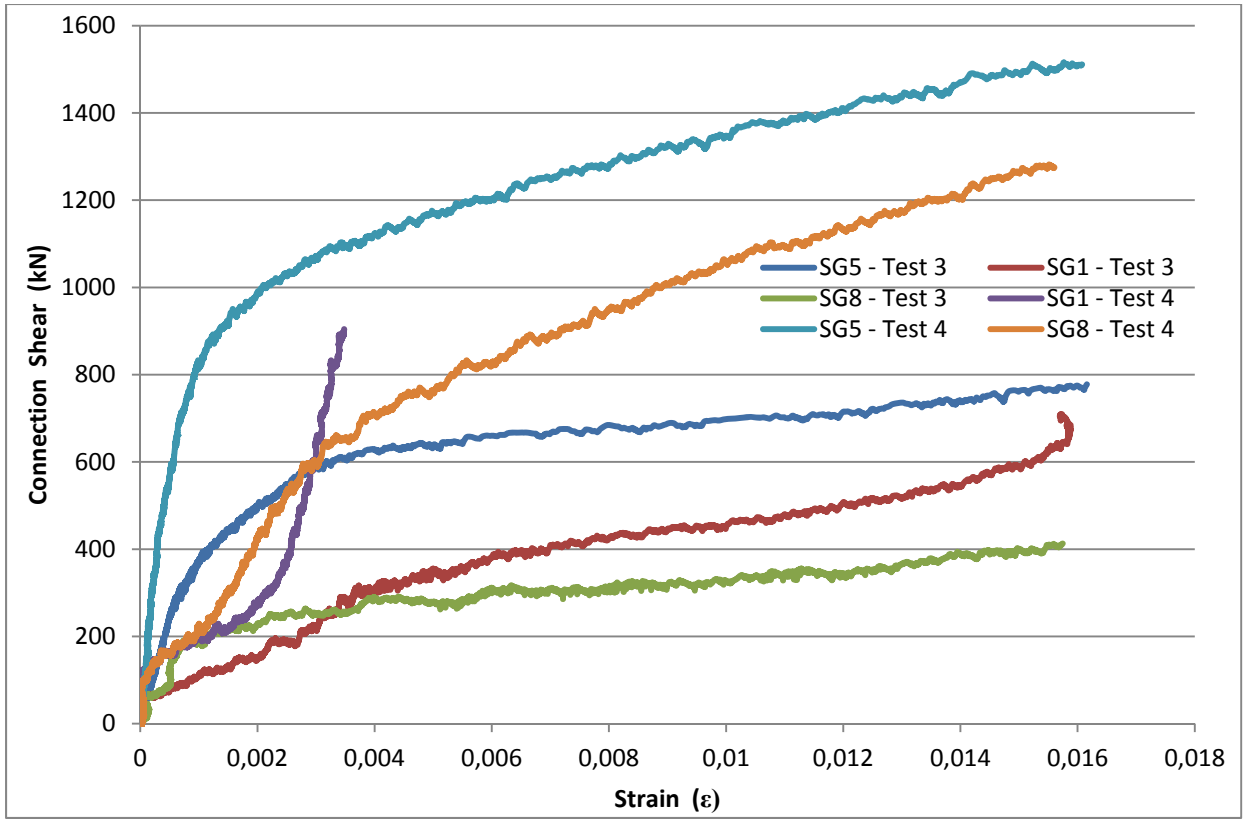

Figure 4-23 Comparison of Tests 3 and 4 Connection Shear vs. Strain

4.3 Comparisons

The comparisons expressed in this section are regrouped in five main sections divided as follows: predicted values and experimental results, rigid support and flexible support effects, beam size effect, comparison of double and triple vertical rows of bolts tests and comparison of welded shear tabs with or without bolt holes. Frequent references will be made to the results described in the research of Marosi (2011). These references are permissible since both research programs were performed using similar experimental conditions.

4.3.1 Predicted Values and Experimental Results

In some cases where the AISC (2011) extended shear tab design method predictions differed from the Modified Method predictions, the Modified Method came closest to the observed experimental results in terms of predicted failure mode, predicted resistance based on nominal material properties and based on measured material properties. Table 4-5 contains a summary of the observed failure modes, the measured connection resistances and the measured-to-predicted ratios for every bolted test.

The AISC (2011) extended method predicted a shear fracture of the bolt group for two tests, a failure mode that was not observed for the test specimens described herein, while this failure mode was never predicted by the modified method. These experimental results outline the main difference between the modified method and the extended design method which lies in the bolt group strength.

These observations on the bolt group shear strength indicate that the proposed increase in the single bolt shear strength of the modified method should be strongly considered. This proposal consists of increasing the single bolt ultimate shear strength factor from $0.583F_u$ to $0.62F_u$ based on the work of Kulak et al. (1987).

The results acquired in all eight of the bolted tests were predicted with equal or better accuracy using the proposed modified method compared to the AISC (2011) 14^{th} Edition extended shear tab design method in terms of measured-to-predicted connection resistance ratios.

For example, in the case of Test 1, the AISC extended method predicted a fracture of the bolt group as the failure mode unlike the modified method which predicted flexural yielding of the shear tab. The predicted-to-measured maximum connection shear ratio was of 1.08 for the modified method as opposed to 1.09 for the AISC (2011) method. The variation observed in this case does not seem major, although bolt group shear strength was definitely not an observed failure mode. Therefore, the author recommends that this method should be considered as a replacement of the actual CISC (2010) single plate connection design approach for conventional and extended configurations.

As summarized in Table 4-6, the results gathered in this research project reflect the findings of Marosi (2011). The modified design method always gives an equal or better prediction of the bolted connection resistance and of the observed failure mode.

Table 4-5 - Summary of Measured Connection Resistances and Observed Failure Modes

Test -	Method -	Observed Failure Mode -	Measured Connection Resistance kN	Unfactored Predicted Resistance Based on Probable Material Properties kN	Measured / Predicted Ratio -	Predicted Failure Mode -	Unfactored Predicted Resistance Based on Measured Material Properties kN	Measured / Predicted Ratio -	Predicted Failure Mode -
1	AISC Extended	SR	652	583	1.12	BG	597	1.09	BG
	Modified Method			583	1.12	PFY	605	1.08	PFY
2	AISC Extended	SR	1834	1455	1.26	BLS	1534	1.20	BLS
	Modified Method			1455	1.26	BLS	1534	1.20	BLS
5	AISC Extended	SR	501	363	1.38	PFY	440	1.14	PFY
	Modified Method			363	1.38	PFY	440	1.14	PFY
6	AISC Extended	SR	1910	1455	1.31	BLS	1676	1.14	BLS
	Modified Method			1455	1.31	BLS	1676	1.14	BLS
7	AISC Extended	SR	508	363	1.40	PFY	440	1.15	PFY
	Modified Method			363	1.40	PFY	440	1.15	PFY
8	AISC Extended	SR	614	583	1.05	BG	597	1.03	BG
	Modified Method			583	1.05	PFY	605	1.02	PFY
9	AISC Extended	SR	1970	1455	1.35	BLS	1676	1.18	BLS
	Modified Method			1455	1.35	BLS	1676	1.18	BLS
10	AISC Extended	SR	1954	1455	1.34	BLS	1534	1.27	BLS
	Modified Method			1455	1.34	BLS	1534	1.27	BLS

Failure Modes

BLS= Block Shear Rupture

BG= Bolt Group Shear Failure

SR= Shear Rupture through Plate Net Area

PFY= Plate Flexural Yeilding

Table 4-6 - Summary of Bolted Connection Results for Marosi (2011) and D'Aronco (2013)

Test	Design Method	Predicted Failure Mode	Observed Failure Mode	Measured / Predicted Ratio **Measured** Properties
D'Aronco 1	AISC Extended	BG	SR	1.09
	Modified Method	PFY		1.08
D'Aronco 2	AISC Extended	BLS	SR	1.20
	Modified Method	BLS		1.20
D'Aronco 5	AISC Extended	PFY	SR	1.14
	Modified Method	PFY		1.14
D'Aronco 6	AISC Extended	BLS	SR	1.14
	Modified Method	BLS		1.14
D'Aronco 7	AISC Extended	PFY	SR	1.15
	Modified Method	PFY		1.15
D'Aronco 8	AISC Extended	BG	SR	1.03
	Modified Method	PFY		1.02
D'Aronco 9	AISC Extended	BLS	SR	1.18
	Modified Method	BLS		1.18
D'Aronco 10	AISC Extended	BLS	SR	1.27
	Modified Method	BLS		1.27
Marosi 1	AISC Extended	PF*	SR / PF *	1.38
	Modified Method	PF*		1.22
Marosi 2	AISC Extended	BG	SR / PF *	1.29
	Modified Method	PF*		1.21
Marosi 7	AISC Extended	SR	SR / PF *	1.30
	Modified Method	SR		1.30
Marosi 8	AISC Extended	SR	SR / PF *	1.21
	Modified Method	SR		1.18
Marosi 13	AISC Extended	SR	SR / PF *	1.15
	Modified Method	SR		1.15

	AISC Method	Modified Method
Mean	1.19	1.17
Standard Deviation	9.17%	7.13%

Failure Modes:

BG= Shear Fracture of Bolt Group

BLS= Block Shear Rupture

PF= Plate Flexure with Von Mises Shear Reduction

SR= Shear Rupture through Plate Net Area

PFY= Plate Flexural Yielding

* Failure mode replaced by PFY in AISC (2011) 14th Edition Manual considering same interaction of stresses

4.3.2 Beam Size Effect

The beam size did not appear to have any influence on the progression of the yielding in the shear tab connections. No matter the beam size, onsets of flexural and shear yielding were mainly dictated by the nature of the connection whether they were bolted or welded. All bolted connections displayed shear yielding in the shear tab before the onsets of flexural yielding were observable, unlike welded connections which typically showed flexural yielding of the single plate before the appearance of shear yielding.

A tendency is established throughout the experimental results in terms of the effect of beam depths when comparing the measured-to-predicted connection resistances ratios not dependent of the support condition or of the number of bolt vertical rows in the connection. The analysis of Table 4-5 illustrates that the measured-to-predicted connection resistance ratio increases as the beam size increases. Thus, the smallest measured-to-predicted ratio by the modified method of the four bolted W310 beams was of 1.02 and the largest was 1.15. Conversely, the smallest measured-to-predicted ratio by the modified method of the four bolted W610 tests was of 1.14 and the largest was 1.27.

4.3.3 Comparison of Double and Triple Vertical Row of Bolts Connections

The principal objective of comparing these two configurations in laboratory experiments was to observe the rotational behavior of the triple row bolted test in order to establish whether or not this configuration allowed enough rotation to be considered as a ductile connection and to determine whether it provided increased shear resistance. The shear tabs were designed so that the plate thickness and weld sizes remained the constant, focusing on the effect of the bolt group only.

As previously mentioned, all experiments surpassed their predicted connection resistances with ratios up to 1.27 when compared to predicted resistances using measured material properties. When examining Tables 4-2 and 4-3 no particular tendency can be outlined with measured-to-predicted ratios in relation with these two bolt arrangements. The ratios reached are close enough to affirm that the addition of an extra vertical row of bolts to the bolt configuration while keeping the other connection parameters constant has very little effect.

Most importantly, both bolted arrangements attained their targeted beam end rotation relative to the supporting element. Even though the rotation allowed by the triple vertical row arrangement was slightly lower than its two vertical row of bolts counterpart the results obtained suggest that both these bolt patterns allowed enough rotation in order for the connections to fail in a ductile and safe manner avoiding sudden collapses.

4.3.4 Comparison of Welded Shear Tabs with and without Bolt Holes

The comparable retrofit weld shear tab connection results from experiments described herein with those performed by Marosi (2011) are summarized in Table 4-7. Since the partial retrofit welds themselves did not have the same exact shape in the tests used for comparisons in this section, Marosi's partial L-shape and partial C-shape welds were slightly smaller, the measured connection resistances cannot be discussed. However, the focus is set on the measured beam end rotation relative to the column face. In both cases, the partial C-shape weld retrofit showed no damage and resisted shear loads greater than predicted values as calculated with the AISC (2011) and CISC (2010) design methods.

The rotation allowed by the partial L-Shape weld of Marosi's (2011) Test 11 is twice the rotation achieved by the partial C-Shape weld connection of Test 3. In the case of these smaller shear tabs, this difference can be explained by the fact that the L-Shape weld tested by Marosi (2011) did not have a horizontal leg at the top of the shear tab which naturally leads to a more flexible detail. In addition, another explanation resides in the fact that the shear tab without bolt holes does not deform to the same extent as the shear tab having all the originally planned bolt holes, and thus is stiffer.

Table 4-7- Experimental Results of Retrofit Welded Connections

Test	Description	Measured Connection Resistance	Measured Relative Beam End Rotation
-	-	kN	rads
D'Aronco 3	Partial C-Shape Weld Single Row of 6 Holes	1166	0.018
Marosi 11	Partial L-Shape Weld Single Row of 6 Holes	854	0.035
D'Aronco 4	Partial C-shape Weld Double Row of 6 Holes	2283	0.036
Marosi 10	Partial C-Shape Weld Double Row of 6 Holes	1850	0.034

Regarding the partial C-shape weld Test 4 and Marosi (2011) Test 10 equivalents of double row connections, the relative beam end rotation results are very similar. Both configurations, with and without bolt holes, allow for beam rotations greater than the targeted values and to values almost identical. The difference in maximum shear loads resisted by these connections is believed to be a combination of a smaller C-shape weld in the case of Marosi (2011) Test 10 and the absence of bolt holes in Test 4.

Due to the ductile behavior of the arrangement without bolt holes, it seems that if replacing the shear tab on site and using retrofit welds is the only option available to the erector, the author believes that it is not necessary to drill holes other than the ones essential for the erection of the framing members.

4.4 Coupon Measurements

4.4.1 Testing Methodology

Coupon measurements are taken in order to obtain the material strengths of the steel members used in the experiments. For this research project, coupons were cut from all plates used as shear tabs and seven coupons were cut from the web and flanges of the test beams as pictured in Figure 4-24.

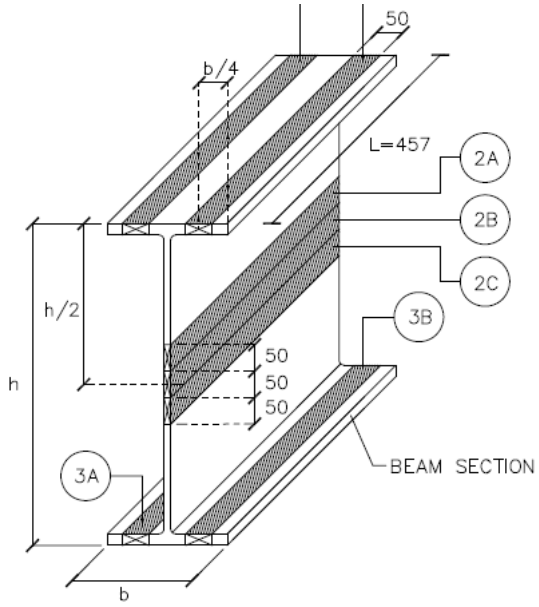

Figure 4-24 - Coupons taken from Test Beam Web and Flanges (Courtesy: DPHV)

Once the rectangular coupon blanks were cut from the plates and beams they were machined with a 203 mm gauge length in accordance with the tensile test procedures of the ASTM A370 Standard (ASTM, 1995).

Before proceeding with the testing process each coupon was instrumented with strain gauges at both faces of the gauge (G) section in order to determine the modulus of elasticity. Using a micrometer, the width and thickness of each coupon was measured in three different positions along the gauge length to obtain that average cross-sectional area. Then, the gauge length of 203mm of each coupon was marked at both ends in order to be able to measure the coupon elongation after the destructive tensile test. An extensometer was attached to the coupons along the gage length for an additional level of precision in terms of elongation measurement; as well, the LVDT built in to the actuator was used to measure elongation.

The measurements were performed on a 1000kN actuator. In order to perform these tensile tests, hydraulic grips were used to hold the grip sections of the coupons. This type of tensile stress records the engineering yield and ultimate stresses for each specimen and both static and dynamic data were documented. In order to acquire the static values, the tests were paused for one minute 5 times throughout the loading by holding the displacement of the actuator piston. The crosshead displacement rates were set to 0.0026 mm/s in the elastic range and to 0.026 mm/s in the post-elastic region.

4.4.2 Shear Tabs

Three coupons were tested for each different shear tab thicknesses. The results gathered were plotted in a typical stress-strain graph for each coupon and the average yield and ultimate stresses were calculated. Figure 4-25 illustrates a typical engineering stress-strain curve for a shear tab coupon. The material used for all plates was ASTM A572-Grade 50 steel.

Table 4-8 is a summary of the mechanical properties of each plate used for the shear tabs. The tests in which those shear tabs have been used are also listed in Table 4-8.

Table 4-8 - Mechanical Properties of Shear Tab Plates

		Plate 1	Plate 2	Plate 3	Plate 4	Plate 5	Plate 6
Shear Tabs	$F_{ySTATIC}$ (MPa)	369	392	393	478	424	497
	$F_{uSTATIC}$ (MPa)	532	494	517	548	492	574
	Elongation (%)	19	22	22	17	17	17
	E (MPa)	201	203	203	200	206	208
	F_u/F_y	1.44	1.26	1.31	1.15	1.16	1.16
	Tests Used	3	1	2, 4	5, 7	8	6, 9, 10

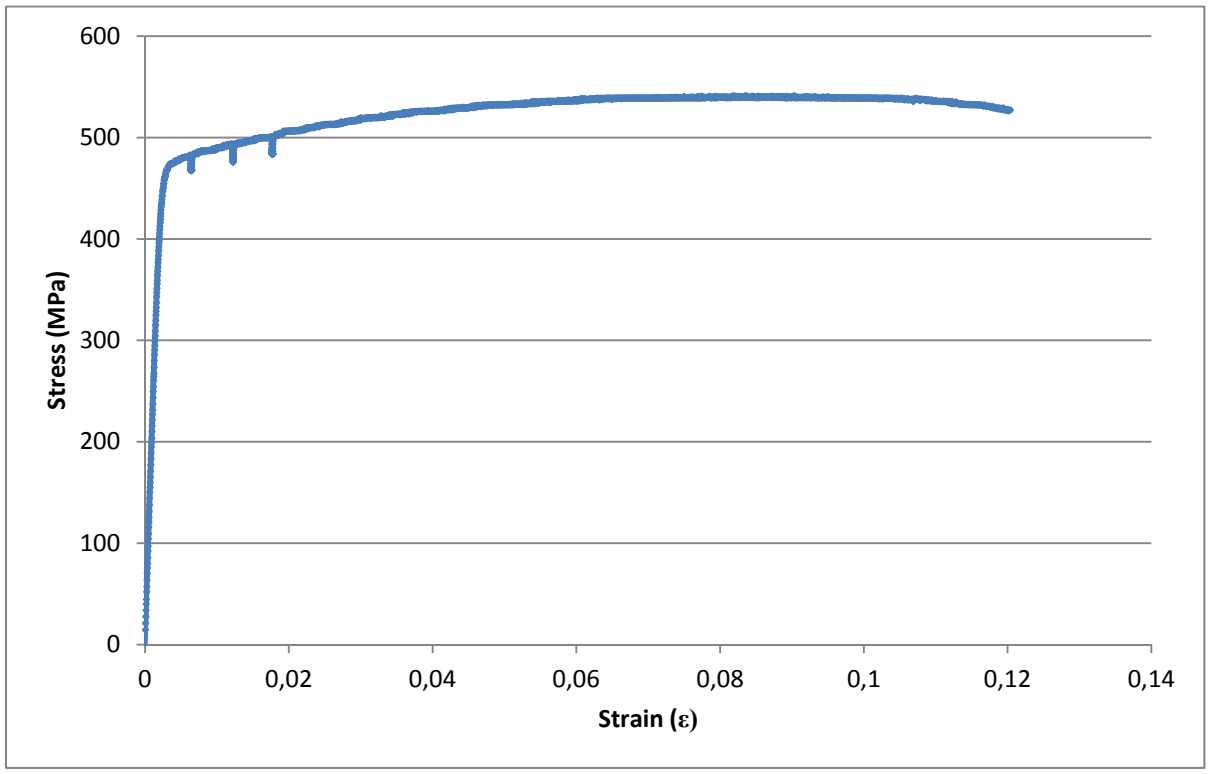

Figure 4-25 - Typical Engineering Stress-Strain Curve of a Shear Tab Coupon

4.4.3 Test Beams

Seven coupons were tested for each different beam size, two from each beam flange and three from the web. The results gathered were plotted in a typical stress-strain graph for each coupon and the average yield and ultimate strengths were calculated. Figure 4-26 illustrates a typical engineering stress-strain curve for a beam flange coupon. The material used for all test beams was ASTM A992-Grade 50 steel.

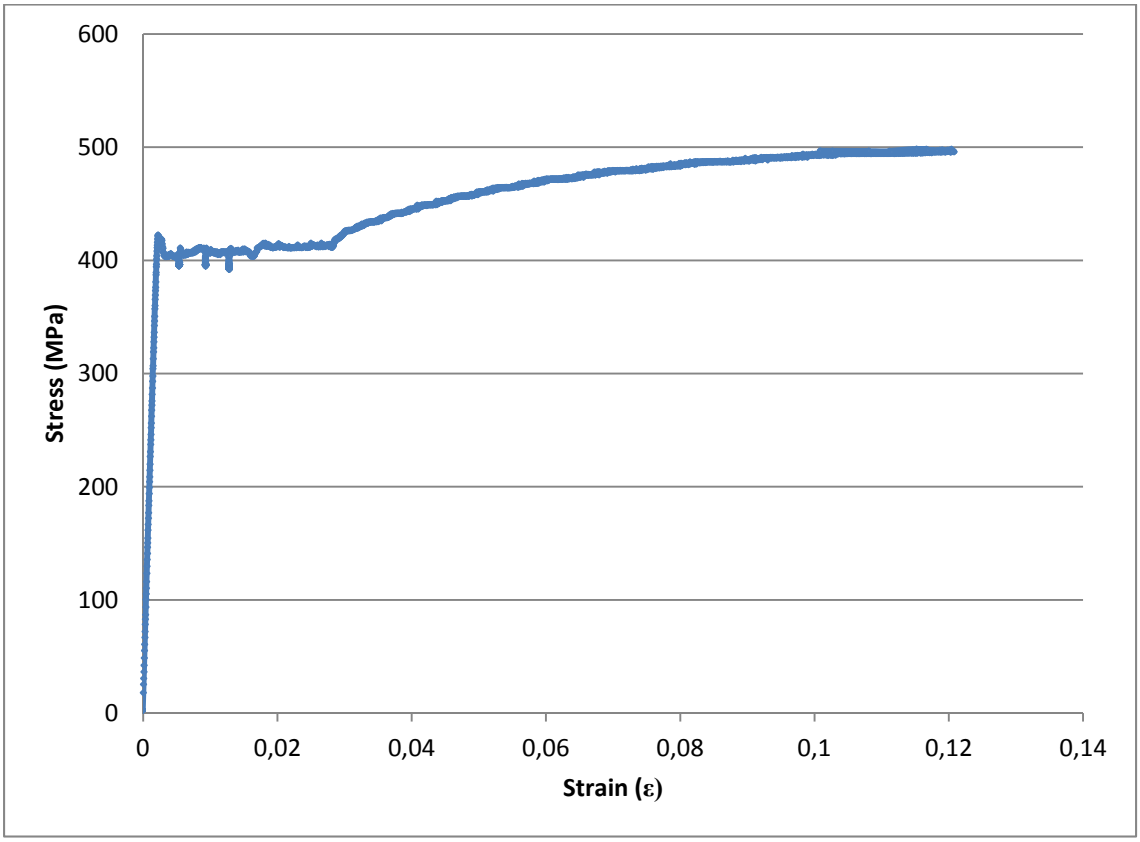

Figure 4-26 - Typical Engineering Stress-Strain Curve of a Beam Flange Coupon

Table 4-9 and Table 4-10 respectively represent the material properties for the beam flange coupons and the beam web coupons used in all the tests. The tests in which those beams were used are also listed in these two tables.

4.4.4 Material Behavior

All the test beam coupons and the shear tab coupons both exceeded the minimum specified yield and ultimate strengths and the stress-strain curves showed easily noticeable elastic regions, yield plateaus, increase in stress due to strain hardening and ultimately plastic

deformation of the gauge length and rupture. The author recommends the use of Grade 50 (50ksi) material for the shear tab connections since testing has proven that considerable deformations occurred in the connections sign that this material possessed sufficient ductility to meet the targeted rotations in each specimen.

Table 4-9 - Mechanical Properties of Test Beam Flanges

		Beam 1 *	Beam 2 *	Beam 3	Beam 4	Beam 5	Beam 6	Beam 7
Beam Flanges	$F_{ySTATIC}$ (MPa)	388	380	361	390	360	366	364
	$F_{uSTATIC}$ (MPa)	551	487	490	502	497	478	490
	Elongation (%)	28	29	17	24	27	26	22
	E (MPa)	204	206	207	207	205	208	205
	F_u/F_y	1.34	1.42	1.36	1.29	1.38	1.31	1.34
	Tests Used	2	3, 4	1	6	9, 10	8	5, 7

* Coupon measurements taken from Marosi (2011) since beams were reused

Table 4-10 - Mechanical Properties of Test Beam Webs

		Beam 1 *	Beam 2 *	Beam 3	Beam 4	Beam 5	Beam 6	Beam 7
Beam Web	$F_{ySTATIC}$ (MPa)	434	440	382	409	390	389	399
	$F_{uSTATIC}$ (MPa)	570	527	489	510	500	487	502
	Elongation (%)	23	28	17	25	28	27	23
	E (MPa)	207	215	205	209	209	212	208
	F_u/F_y	1.31	1.20	1.28	1.25	1.28	1.25	1.26
	Tests Used	2	3, 4	1	6	9, 10	8	5, 7

* Coupon measurements taken from Marosi (2011) since beams were reused

CHAPTER 5: BENDING MOMENT DEMAND ON BOLT GROUP AND COLUMS

5.1 Overview

This chapter contains the findings obtained on the subjects of flexural bending moment demand on shear tab bolt groups and on the shear tab support conditions focusing particularly on the connections to the flexible columns. The results obtained from the experiments described in Section 4.2 are used to formulate design recommendations for the bending moments that must be resisted by columns with shear tabs connected to the column webs. The influence of the presence of stiffeners in those connections is examined through finite element analysis developed in SAP2000.

5.2 Bending Moment Demand on Bolt Group

This section will present the results found for the bending demand on shear tab connections bolt groups and the effective eccentricity for the design of these bolt groups. The objective is to compare the eccentricity calculated using the results computed in the laboratory with the effective connection eccentricities suggested in the AISC Manual 14th Edition (2011).

As explained in Section 2.2, Muir and Thornton (2011) describe that the use of shear tab connections develop negative moments at the supporting column face. This suggests that the inflexion point can be located on the span side of the bolt group as shown in Figure 5-1 which represents a typical moment diagram for a flexible support condition shear tab connection. A similar moment diagram would be observed for a rigid support condition with a negative moment at the face of the column. This moment diagram was reported by Astaneh-Asl when defining appropriate design eccentricity values for the bolt group and welds, as described in Section 2.2 (see Figure 2-3).

In the 2011 AISC design procedure, the bending moment acting in the bolt group must be considered such that premature failure of the bolts is prevented prior to reaching the desired shear capacity. By examining the failure loads of bolt groups in past test programs, Muir and Thornton determined that this objective can be attained by using an effective design eccentricity taken

equal to the distance between the bolt group and the welds. However, this eccentricity actually exists on the side of the bolt group that is opposite to the column.

As described in section 2.3, the same bending moment is also used to verify the shear tab. The remaining detailing requirements of the procedure essentially aim at developing ductile rotation in the connection such that the moment demand on the bolt group and the column remains small as the beam deflects. For instance, maximum plate thickness is specified to promote plowing of the bolts rather than bolt shear failure and the specified minimum weld size ensures that shear plate yielding will develop without failure of the welds.

However, apart from clarifications allowing designers to design the columns without considering an axial force without eccentricity, the AISC method is relatively silent regarding the bending moment that must be considered for the design of the columns and do not offer a precise design methodology to evaluate this bending moment. Results obtained in this test program can be used to validate the bolt group design moments assumed in the AISC method and assess the bending moment demand imposed on the columns.

For the flexible support condition reproduced in the laboratory, the moment diagram depicted in Figure 5-1 can be obtained from the free-body diagram (FBD) shown in Figure 5-2. As depicted in the FBD, the top and bottom load cells which carry respectively tension and compression loads, were relied on to monitor the horizontal reactions in the test column during the loading of the shear tab connections. Moments in the columns as well as moments acting in the beams can therefore be obtained from these measurements. Similarly, for the rigid support conditions, the bending moment diagram in the beam up to the column face can be obtained from the loads that were applied at the beam tip and by the 12MN load frame.

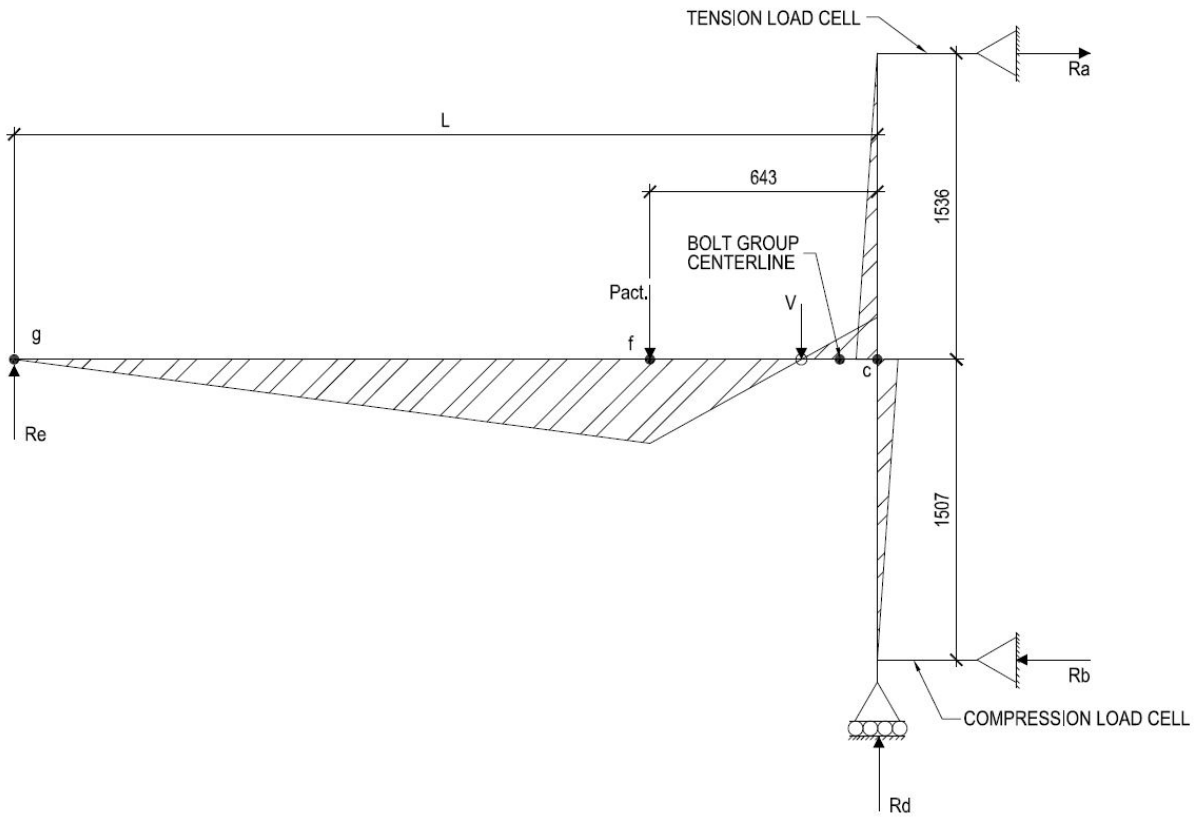

Figure 5-1 – General Moment Diagram for Flexible Support Condition

The free-body and beam bending moment diagrams illustrated in Figures 5-1 and 5-2 also identify the two critical eccentricities as measured from the point of zero moment: 1) the eccentricity e that induces the moment in the bolt group, i.e. the distance between the point of zero moment and the centerline of the bolt group which is the actual bolt group eccentricity, and 2) the eccentricity leading to the bending moment imposed on the columns, e_{CALC}, i.e. the distance between the point of zero moment and the centerline of the column.

By considering the equilibrium of forces at point ‘’g’’, which is positioned at the far end of the beam at the position of the tip actuator, and by performing the sum of moments around that point, the negative moment at the face of the column can be calculated. Similarly, by computing the sum of moments around point ‘’f’’, the maximum moment in the beam can be defined. Knowing the moment at the column face and the maximum beam moment, the inflexion point, e_{CALC}, can be determined.

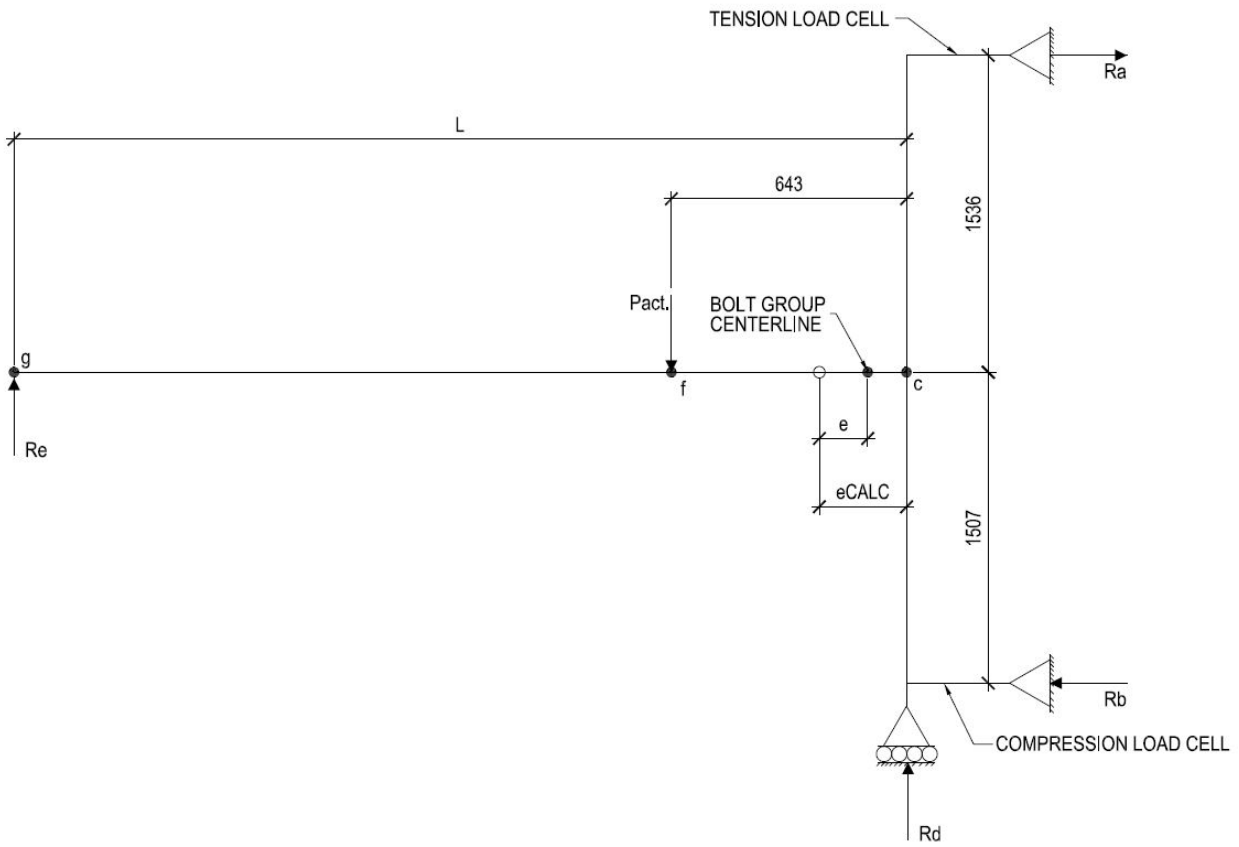

Figure 5-2 – General Free-Body Diagram for Flexible Support Condition

The values described are summarized in Table 5-1 for all ten tests conducted in the laboratory. The calculations have been performed at two load steps; the calculated nominal shear capacity of the shear tab connection using the modified design method, $V_{nominal}$, and the ultimate shear load reached resisted by the connection during the tests, $V_{ultimate}$.

The table also gives the value of the effective eccentricity that should be used for design of the bolt group, as specified in the 2011 AISC method, e_{AISC}. For Tests 1 to 4 representing rigid support conditions, this eccentricity corresponds to the distance between the centerline of the bolt group to the face of the column. In the case of a flexible support condition in Tests 5 to 10, the design eccentricity as per AISC should be taken as the distance between the bolt group and the centerline of the column. As discussed in Chapter 3, however, considering that stiffeners were used with the shear tabs, a shorter value corresponding to the distance between the bolt group and the tip of the column flanges was used. That second group of design eccentricities is compared to the measured values in Table 5-2.

Table 5-1 - Calculated Eccentricity and Connection Moment with Effective Design Eccentricity as per AISC 2011

Test	Test Beam	Test Column	Shear Load at Connection		Effective Design Bolt Group Eccentricity e_{AISC} (mm)	Actual Bolt Group Eccentricity e (mm)	Calculated Eccentricity e_{CALC} (mm)
1	W310x74	W360x196	$V_{nominal}$ (kN)	583	127	140	267
			$V_{ultimate}$ (kN)	652		140	267
2	W610x140	W360x196	$V_{nominal}$ (kN)	1455	127	216	343
			$V_{ultimate}$ (kN)	1834		216	343
3	W610x140	W360x196	$V_{nominal}$ (kN)	503	98	245	343
			$V_{ultimate}$ (kN)	1166		245	343
4	W610x140	W360x196	$V_{nominal}$ (kN)	1006	158	185	343
			$V_{ultimate}$ (kN)	2283		185	343
5	W310x60	W360x122	$V_{nominal}$ (kN)	363	229	48	277
			$V_{ultimate}$ (kN)	501		57	286
6	W610x140	W360x122	$V_{nominal}$ (kN)	1455	229	73	302
			$V_{ultimate}$ (kN)	1910		24	253
7	W310x60	W360x314	$V_{nominal}$ (kN)	363	290	91	381
			$V_{ultimate}$ (kN)	508		95	385
8	W310x74	W360x314	$V_{nominal}$ (kN)	583	328	83	411
			$V_{ultimate}$ (kN)	614		95	423
9	W610x140	W360x314	$V_{nominal}$ (kN)	1455	290	91	381
			$V_{ultimate}$ (kN)	1970		5	295
10	W610x140	W360x314	$V_{nominal}$ (kN)	1455	328	90	418
			$V_{ultimate}$ (kN)	1954		62	390

Regarding the rigid support condition tests, Tests 1 to 4, the actual eccentricity of the bolt group, in the case of Tests 1 and 2, or weld group in the case of Tests 3 and 4, is constant for both shear loads computed, nominal calculated shear capacity of the connection and ultimate shear load. However, the actual eccentricity in all cases is greater than the effective design eccentricity

suggested by the AISC Manual 14th Edition (2011) extended configuration shear tab connection design method.

This general trend can be attributed to the fact that very stiff column support conditions that were present, which likely favored the development of larger negative moments at the beam end. For the bolted connections, the difference is much smaller for the smaller beam of Test 1 (140 *vs* 127 mm) compared to deeper beam section of Test 2 (216 *vs* 127 mm). Much larger bending moments also developed in Test 3 (245 *vs* 98 mm) with the welded connection with the narrower shear tab. For the wider welded connection of Test 4, the difference between design and measured eccentricities is small (185 *vs.* 158 mm).

With regards to the flexible support condition tests, Tests 5 to 10, the position of the point of inflexion in the beam moment diagram seems to shift along the beam span towards the bolt group when the loading increases from the calculated nominal shear capacity of the connection to the ultimate shear load. It is noticeable that with shallow beams, W310 shapes, the actual eccentricity increases with the increase in the applied shear load at the connection as opposed to the deeper beams, W610 shapes, where the actual eccentricity decreases with the increase of the applied shear load at the connection.

When comparing measured and effective design eccentricity values in Tables 5-1 and 5-2, it is clear that the design eccentricity suggested by AISC Manual 14th Edition (2011) extended shear tab configuration design method tends to overestimate the actual eccentricity in the bolt groups combined with flexible support conditions. The results obtained indicate that it would be more appropriate to consider a design eccentricity of the bolt group as the distance between the centerline of the bolt group and the tip of the column flanges instead of the centerline of the column. For all specimens, this design eccentricity is comparable to or greater than the measured value at the specimen ultimate load, suggesting that this approach would be realistic yet on the conservative side.

Table 5-2 - Comparison of Actual Eccentricity with Effective Design Eccentricity at Tip of Column Flanges

Test	Test Beam	Test Column	Shear Load at Connection		Effective Design Bolt Group Eccentricity e (mm)	Calculated Eccentricity e_{CALC} (mm)	Actual Eccentricity of Bolt Group e (mm)
5	W310x60	W360x122	$V_{nominal}$ (kN)	363	89	277	48
			$V_{ultimate}$ (kN)	501		286	57
6	W610x140	W360x122	$V_{nominal}$ (kN)	1455	89	302	73
			$V_{ultimate}$ (kN)	1910		253	24
7	W310x60	W360x314	$V_{nominal}$ (kN)	363	89	381	91
			$V_{ultimate}$ (kN)	508		385	95
8	W310x74	W360x314	$V_{nominal}$ (kN)	583	127	411	83
			$V_{ultimate}$ (kN)	614		423	95
9	W610x140	W360x314	$V_{nominal}$ (kN)	1455	89	381	91
			$V_{ultimate}$ (kN)	1970		295	5
10	W610x140	W360x314	$V_{nominal}$ (kN)	1455	127	418	90
			$V_{ultimate}$ (kN)	1954		390	62

5.3 Bending Moment Demand on Columns

It was demonstrated that for the flexible support tests, as represented in Figure 5-1, that a certain amount of weak axis flexural moment was introduced in the supporting columns by the shear tab connections. These moments are generally ignored in the design of the columns, but based on the findings presented herein a negative bending moment is transferred to the columns. This section will present the results found for the columns and the interpretation of these findings.

As depicted in the general free-body diagram of Figure 5-2, the flexural moment induced in the supporting column's weak axis can be calculated with the use of the top and bottom load cells. The bending moments in the columns have been determined for all possible beam/column combinations; both beam sizes combined with both column sizes. Therefore, the moment diagrams have been prepared for Tests 5, 6, 7 and 9. Each of these moment diagrams graphs

contain four curves representing respectively the moment in the column at 25%, 50%, 75% and 100% of the ultimate shear load reached by the shear tab connections during the test.

The main objective of the research program being to monitor and observe the behaviour of the shear tab connection plates themselves, the flexible support connections were designed by taking the eccentricity in the connection at the tip of the column flanges, as described in Section 3.3.2. The remaining eccentricity, equal to a half flange width, was distributed as a couple in the top and bottom column stiffeners. Therefore, by using these assumptions in the design calculations of the connections, a fixed amount of negative flexural bending was to be expected in the supporting columns.

As plotted in Figure 5-3, representing the column moment diagram for Test 5, the development of the bending moment in the test column is proportional to the increase in the connection shear load. Therefore, the moment increase is near constant throughout the loading process.

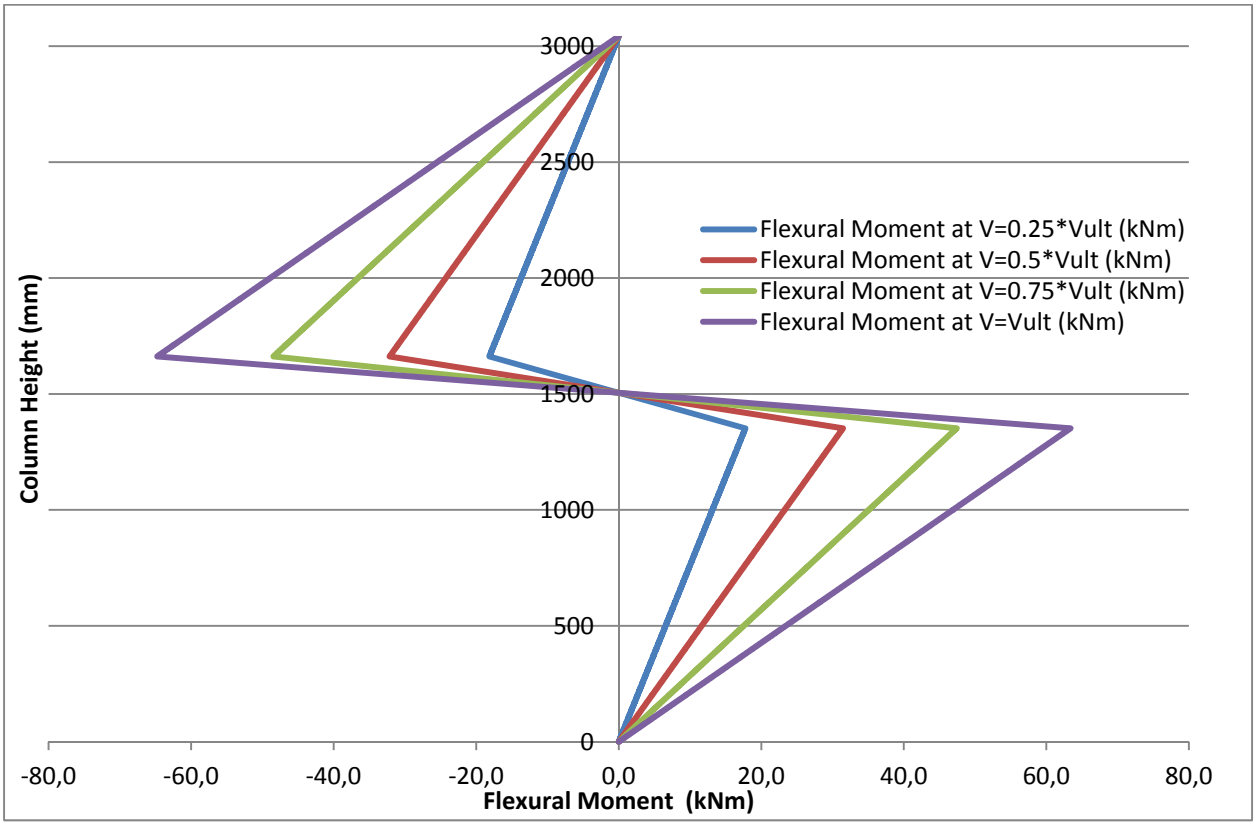

Figure 5-3 - Test 5 Column Moment Diagram at Various Load Levels

As mentioned in Section 5.2.1, part of the observed moment in the column was predictable and expected due to the method used to design the shear tabs. The maximum observed moment in the column aligned with the column stiffeners was nearly 71kNm. In this case, the plastic flexural capacity of the column in its weak axis is M_{py}=252kNm. The expected negative moment induced in the column for this test was slightly higher than the measured moment. This can be explained since the eccentricity assumed in the design for this test was of 89mm+229mm=318mm which was higher than the calculated eccentricity, e_{CALC}=286mm as shown in Table 5-1. Hence, the design assumptions taken were realistic and conservative.

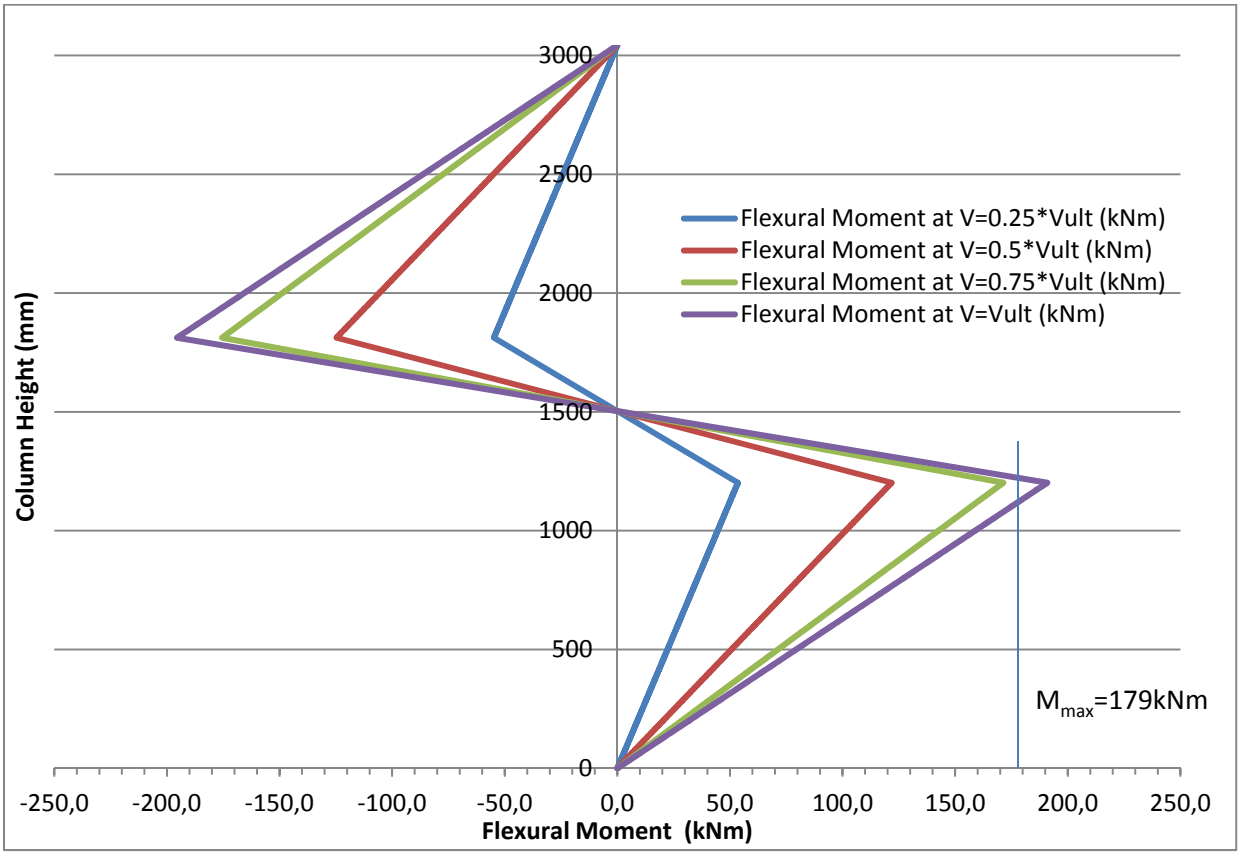

Figure 5-4 - Test 6 Column Moment Diagram at Various Load Levels

As for the Test 6, also a W360x122 column, it was described in Section 4.2.3 that signs of flexural yielding were observed on the column flanges in line with the W610x140 test beam bottom flange. As shown in Figure 5-4, which contains a graph of the moment diagram for the Test 6 column, the allowable weak axis bending moment in the supporting member was surpassed during the test. This nominal allowable moment, of a magnitude of 179kNm, is calculated using the interaction equation which accounts for both the compression load in the

column and the flexural moment. The maximum observed moment in the column aligned with the column stiffeners was nearly 192kNm. As it was observed in the laboratory, the yielding in the column only occurred in a position aligned with the beam's bottom flange where the column also withstands a compressive load.

Unlike the Test 5 column, the bending moment in the column of Test 6 increased earlier during the test, however this increase was not proportional to that in the connection shear load. Again, a portion of the observed moment was to be expected due to the design assumptions previously described. The expected negative moment induced in the column for this test also was higher than the measured moment. This can be explained since the eccentricity assumed in the design for this test was of 89mm+229mm=318mm which was higher than the calculated eccentricity, e_{CALC}=253mm as shown in Table 5-1. Again, this indicates that the design assumptions taken were realistic and conservative.

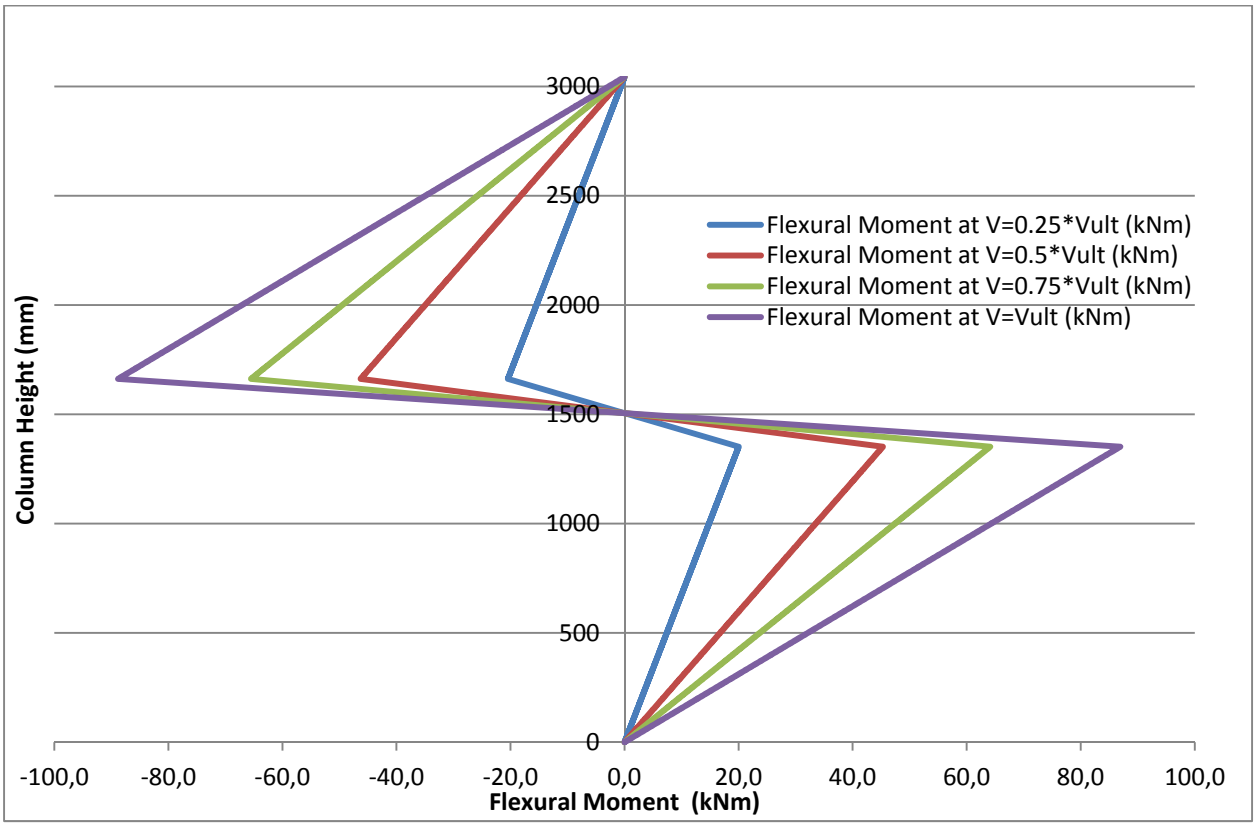

Figure 5-5 - Test 7 Column Moment Diagram at Various Load Levels

Regarding Test 7, which had a W360x314 column and a W310x60 beam, Figure 5-5 shows a plot of the column moment diagram at various percentages of the ultimate shear load carried by the shear tab connection.

In the case of Test 7 as well as Test 5, the moment was developed in the column proportionally with the increase of the shear applied at the connection. However, due to the relatively low ultimate shear load, the bending moment was well below the weak axis plastic bending capacity of the column which is 1122kNm. The maximum observed moment aligned with the column stiffeners was nearly 92kNm. Once again, the expected negative moment induced in the column for this test which was 173kNm, was higher than the measured moment.

Figure 5-6 contains a plot of the moment diagram for the column of Test 9, which was composed of a W360x314 column and a W610x140 beam. Again, as observed in Tests 5 and 7, the flexural moment of the column increased proportionally with the increase of the shear load applied at the connection.

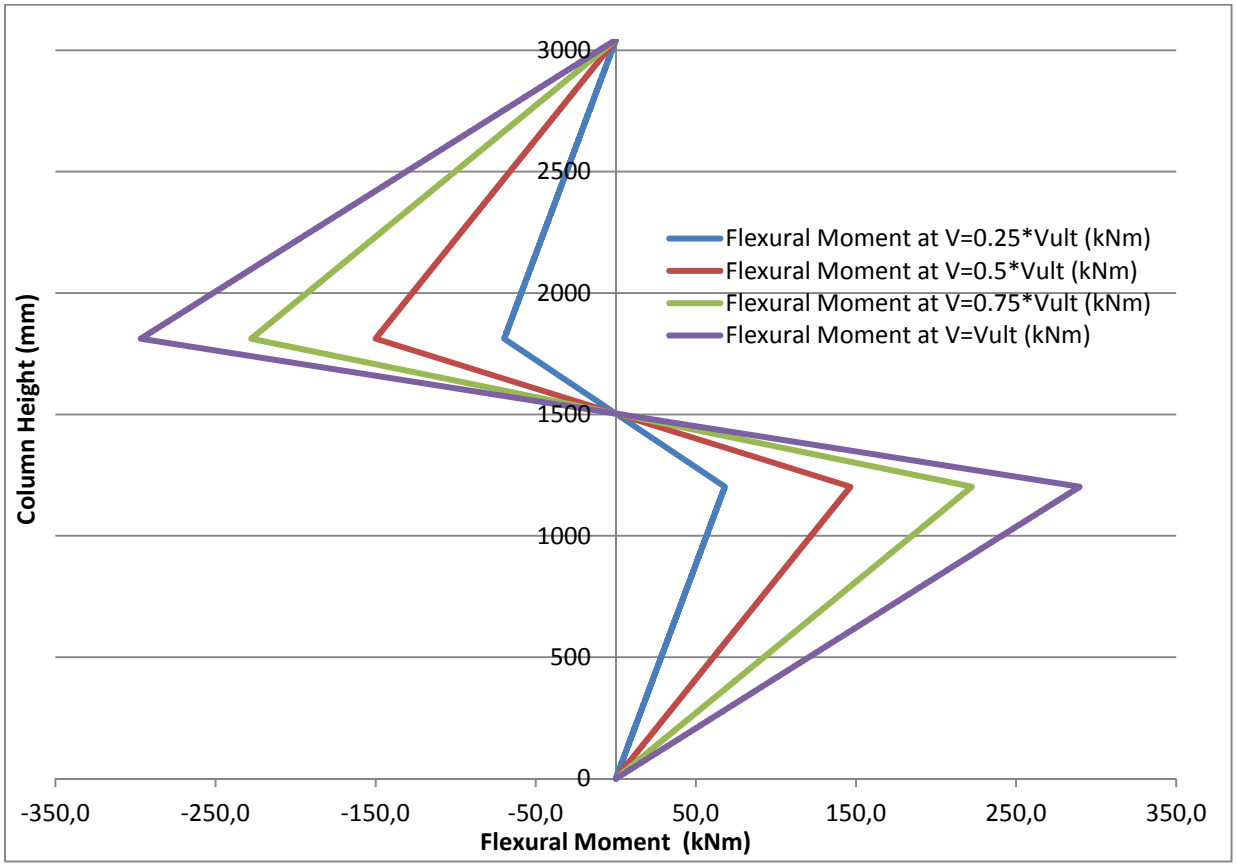

Figure 5-6 - Test 9 Column Moment Diagram at Various Load Levels

Again, due to the relatively low ultimate shear load, the bending moment is well below the weak axis plastic bending capacity of the column which is 1122kNm. The maximum observed moment aligned with the column stiffeners was nearly 270kNm. Again, the expected negative moment induced in the column for this test was slightly higher than the measured moment. This can be explained since the eccentricity assumed in the design for this test was of 89mm+290mm=379mm which was higher than the calculated eccentricity, e_{CALC}=295mm as shown in Table 5-1. Hence, the design assumptions taken were realistic and conservative.

5.4 Finite Element Analyses

The intent of the finite element analyses presented in this section was to clarify the effect of the column stiffeners used at the top and bottom ends of the shear tabs on the weak axis flexural bending generated in the supporting column. Their effects on the shear tab connection itself are also examined.

Therefore, a typical test in which no plastic deformations had occurred in the column during the laboratory experiment was outlined as the main model for the analysis; as such, Test 5 was chosen. The analyses presented were performed using CSI SAP2000 v.15. Two models are created: a simple frame model and a finite shell element model. The former is used essentially as a reference for validating the second one. Simplified boundary and loading conditions are considered in both models. These conditions do not exactly match those that prevailed in the test but are deemed sufficient to examine the effects of the column stiffeners.

5.4.1 Frame Element Model

The model shown in Figure 5-7 is built with the shapes used for Test 5 of this research program, a W360x122 column combined with a W310x60 beam. The load applied is the calculated nominal shear capacity of the connection as per the modified design method. The displacement at the far end of the beam was not included in the model and the shear tab connection was represented as a node, instead of a pin or a spring with a relative rigidity. This is a simplified model which includes a fully rigid beam to column connection and neglects the displacement at the tip actuator. This simplified model was used since it provides bending moments in the column with very similar amplitudes to those measured in Test 5. The intent of this model was to verify the results obtained with the shell FE model which will be presented in

Section 5.3.2. Figure 5-7 depicts the frame elements used in the model as well as the top and bottom elements which represent the load cells used to monitor the horizontal reactions in the test column.

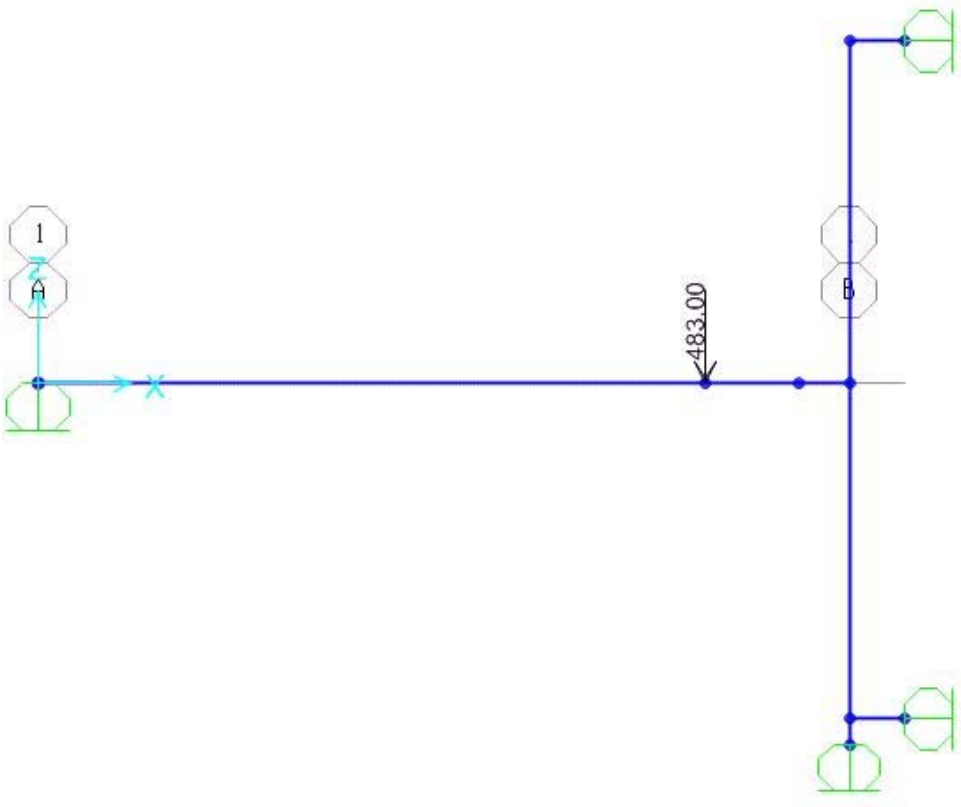

Figure 5-7 - Test 5 Frame Element Model

Figure 5-8 and Figure 5-9 respectively represent the moment diagram of the assembly result of the frame element and the joint loads observed with this model. These values were used to validate the shell model presented in Section 5.3.2.

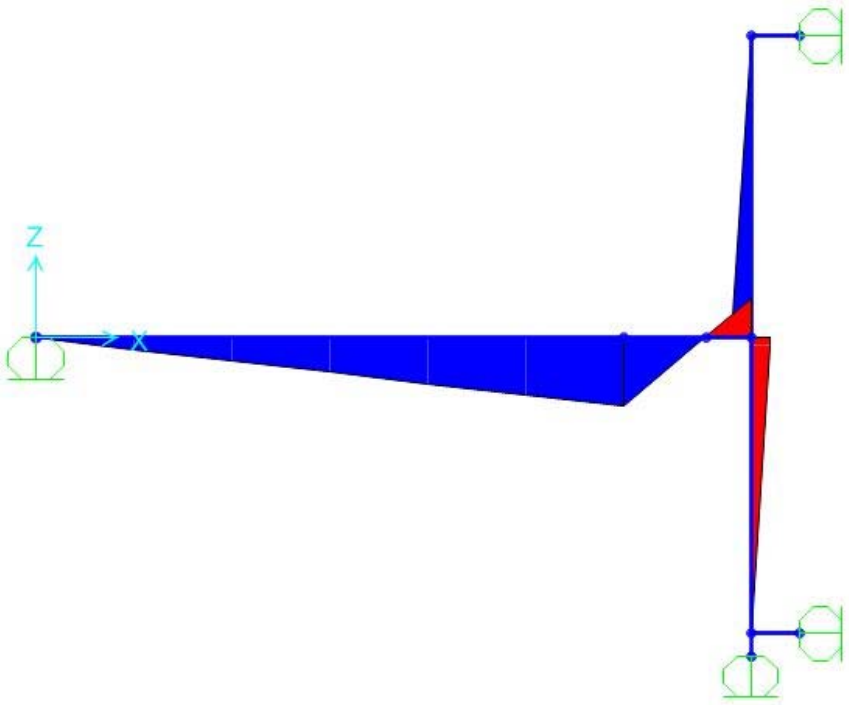

Figure 5-8 - Test 5 General Moment Diagram

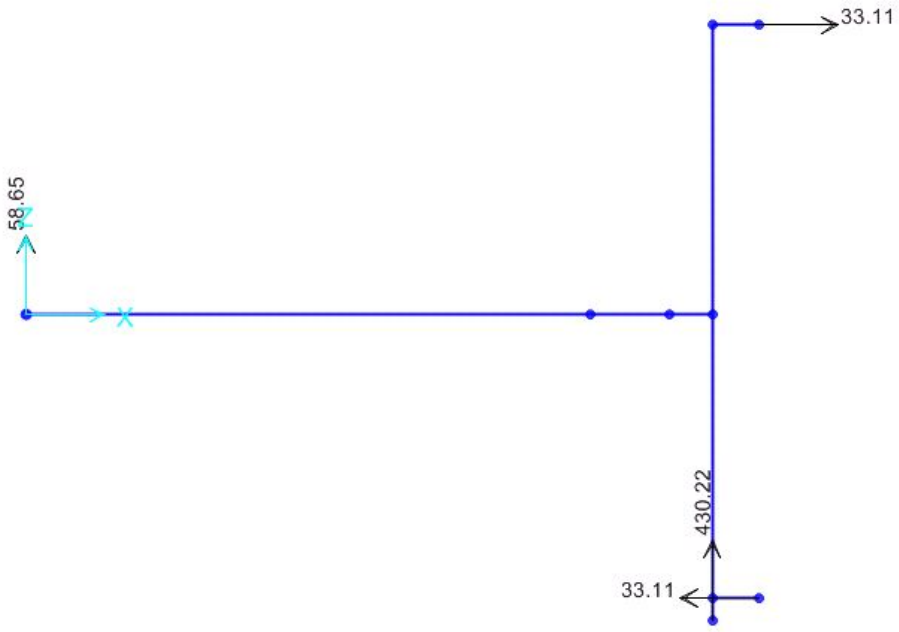

Figure 5-9 - Test 5 Joint Reactions (kN)

The horizontal reactions observed in the stick model presented in this section were very similar to the actual values measured in the laboratory for Test 5. At the calculated nominal shear

strength of the shear tab connection, the bending moment observed in the column by the FE frame model was 49.9kNm.

5.4.2 Shell Element Models

The models shown in this section were built reproducing the members used for Test 5 of this research program. Three different models will be presented in order to monitor the effect of the column stiffeners on the flexural moment induced in the supporting column. The base shell FE model built with both the top and bottom column stiffeners in place was validated with the frame model presented in Section 5.3.1. These three models are as follows: 1) both top and bottom column stiffeners in place, 2) bottom column stiffener only and 3) no column stiffeners. These three models did not allow displacement of the joint at the far end of the assembly.

5.4.2.1 Model 1: Top and Bottom Column Stiffeners

The shell analysis described in this section includes a column with top and bottom stiffeners in place. Figure 5-10 depicts the un-deformed model showing the W310x60 beam and the W360x122 column and its base plate.

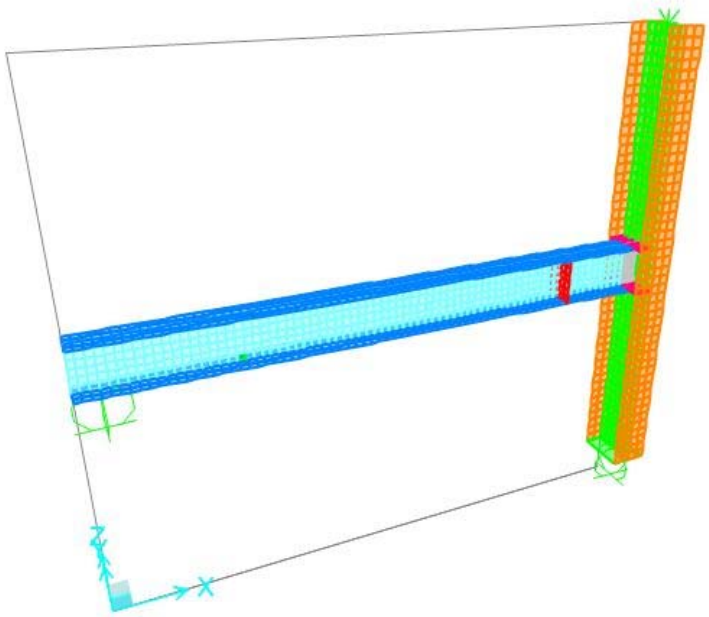

Figure 5-10 - Test 5 Shell Model 1 with Top and Bottom Column Stiffeners

Figure 5-11 pictures the joint reactions observed in the shell model 1. Using the same nominal connection shear capacity as the frame element model, these are almost identical to the

values obtained with the calibration frame element model (Figure 5-9). The weak axis bending moment induced in the column with this arrangement is 50kNm.

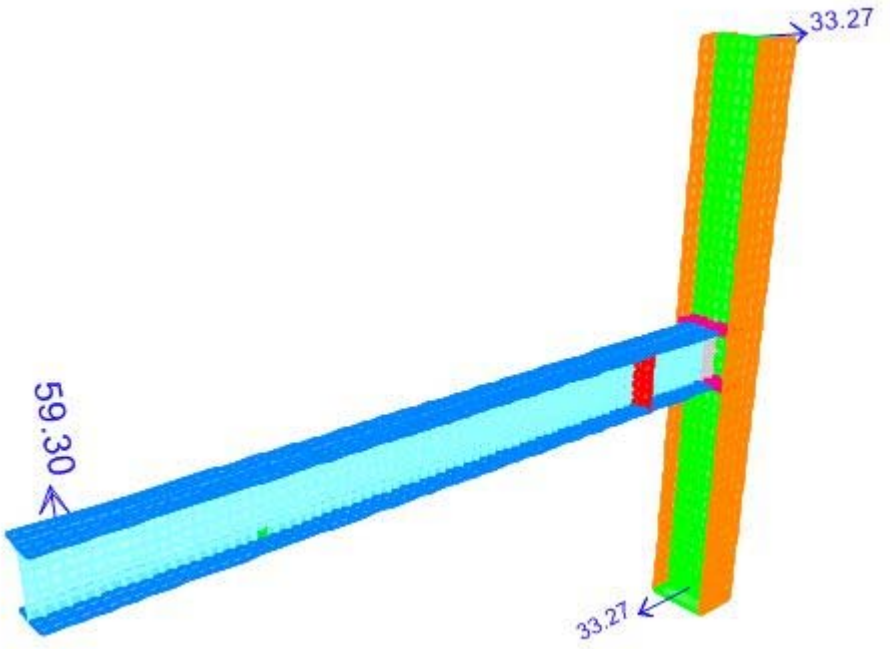

Figure 5-11 - Test 5 Shell Model 1 Joint Reactions (kN) with Top and Bottom Column Stiffeners

5.4.2.2 Model 2: Bottom Column Stiffener Only

The shell model shown in Figure 5-12 depicts the un-deformed W310x60 beam and the W360x122 column and its base plate. The top column stiffener was removed from this analysis to monitor the effect this has on the moment induced by the connection in the column member. Once again, this model was run with a loading equivalent to the nominal shear capacity of the shear tab connection. The idea of using the bottom column stiffener only was to insure the stability of the shear plate particularly in buckling on its bottom horizontal edge, but without having the unwanted couple effect of the stiffeners transferring a moment to the column member.

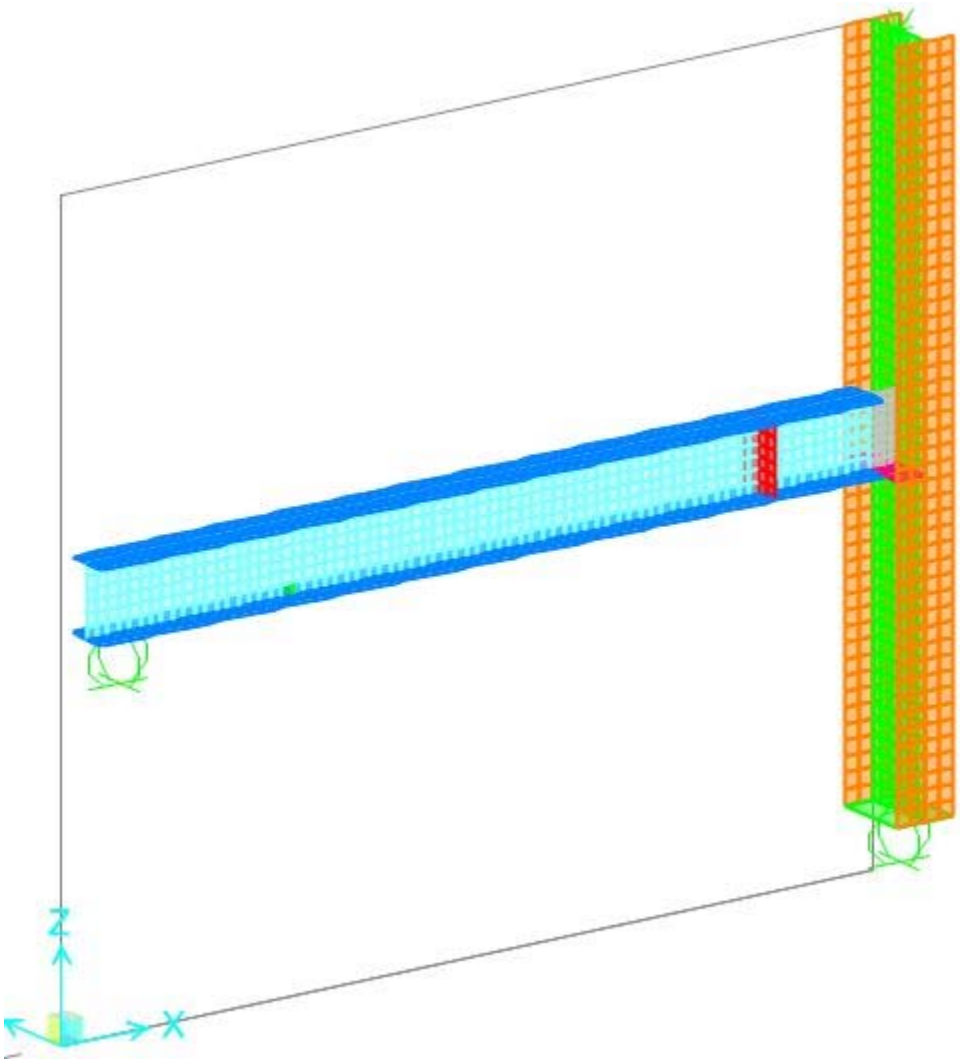

Figure 5-12 - Test 5 Shell Model 2 with Bottom Column Stiffener Only

Figure 5-13 illustrates the joint reactions observed in the shell model 2. Using the same nominal connection shear capacity as the shell model presented in Section 5.3.2.1, the joint reactions obtained are 24.05kN, which is 28% smaller than with Model 1. The weak axis bending moment induced in the column with this arrangement is 36.1kNm.

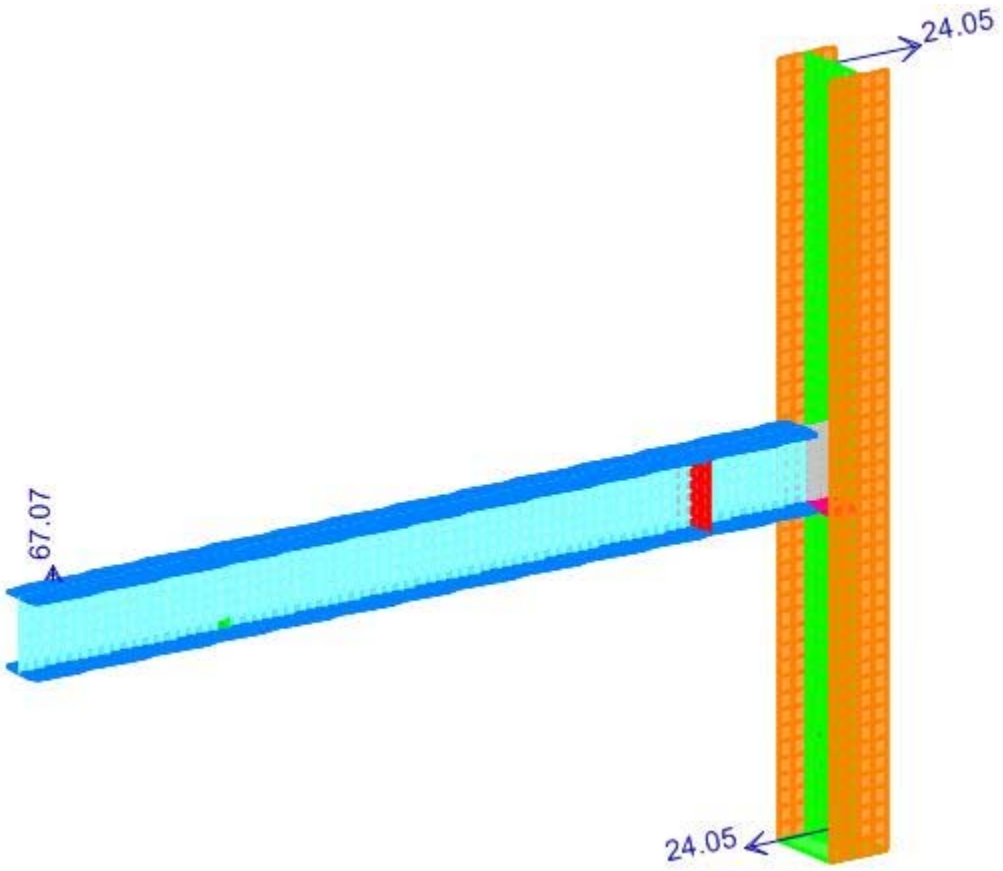

Figure 5-13 - Test 5 Shell Model 2 Joint Reactions (kN) with Bottom Stiffener Only

5.4.2.3 Model 3: No Column Stiffeners

The shell analysis described in this section includes a column without top and bottom stiffeners. Figure 5-14 depicts the un-deformed model showing the W310x60 beam and the W360x122 column. This model aims to reduce to a minimum the bending moment induced in the column using the same nominal shear capacity, as an applied load, as for the previous models. According to the 2011 AISC method, with the removal of the stiffeners, an increased effective design eccentricity would need to be considered for the bolt group in this case, with a value equal to the distance between the bolt group and column centerline. In order to achieve that same capacity, the shear tab plate parameters such as its thickness and weld size to the column web would need to be modified because the shear tab was no longer supported by the stiffeners. Due to the increased eccentricity, the bolt group could also need to be modified, by adding an extra vertical row of bolts for example.

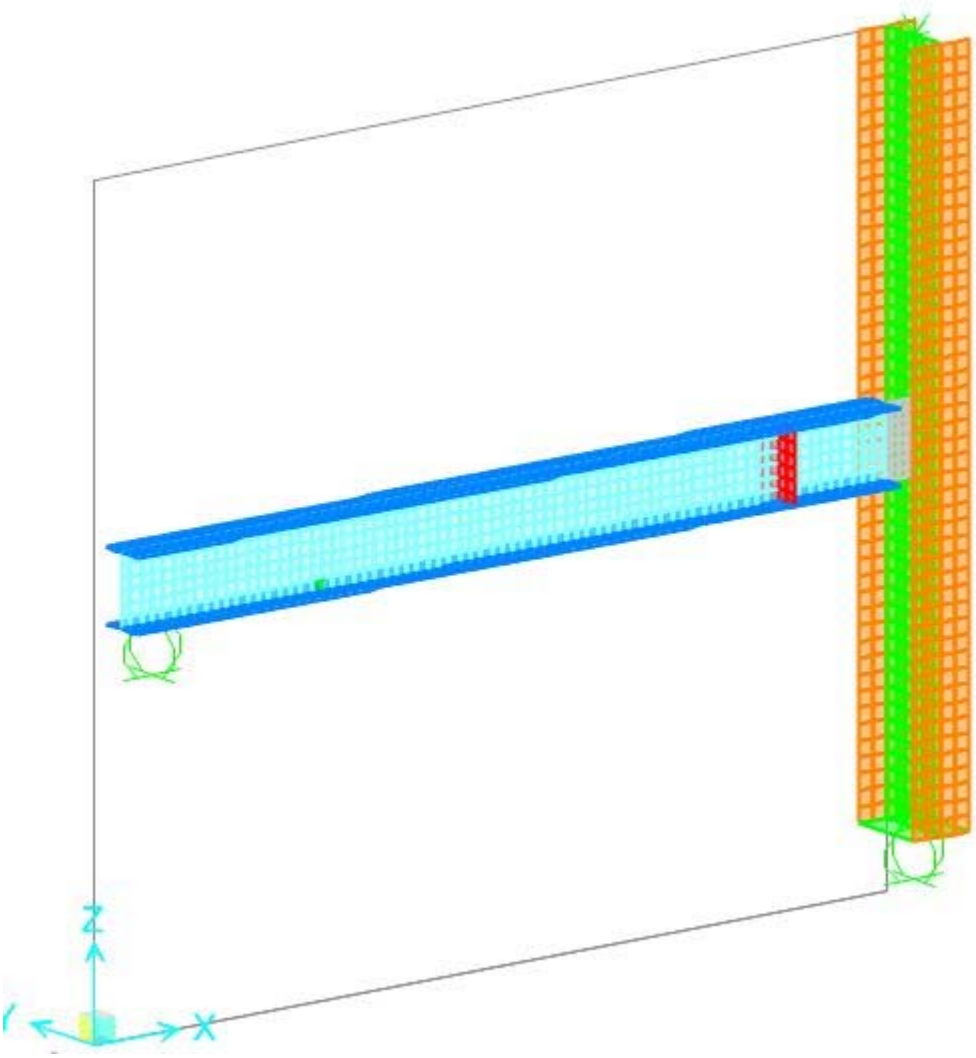

Figure 5-14 - Test 5 Shell Model 3 without Column Stiffeners

Figure 5-15 pictures the joint reactions observed in the shell model without column stiffeners. Using the same nominal connection shear capacity as the shell model presented in Sections 5.3.2.1 and 5.3.2.2, the joint reactions obtained are of 15.95kN which is 52% smaller than with Model 1. The weak axis bending moment induced in the column with this arrangement is 24kNm, which is the lowest moment observed in all three shell models. Without considering stability issues for the shear tab and column web behaviour, avoiding the use of column stiffeners lowers the flexural moment induced in the column by the connection.

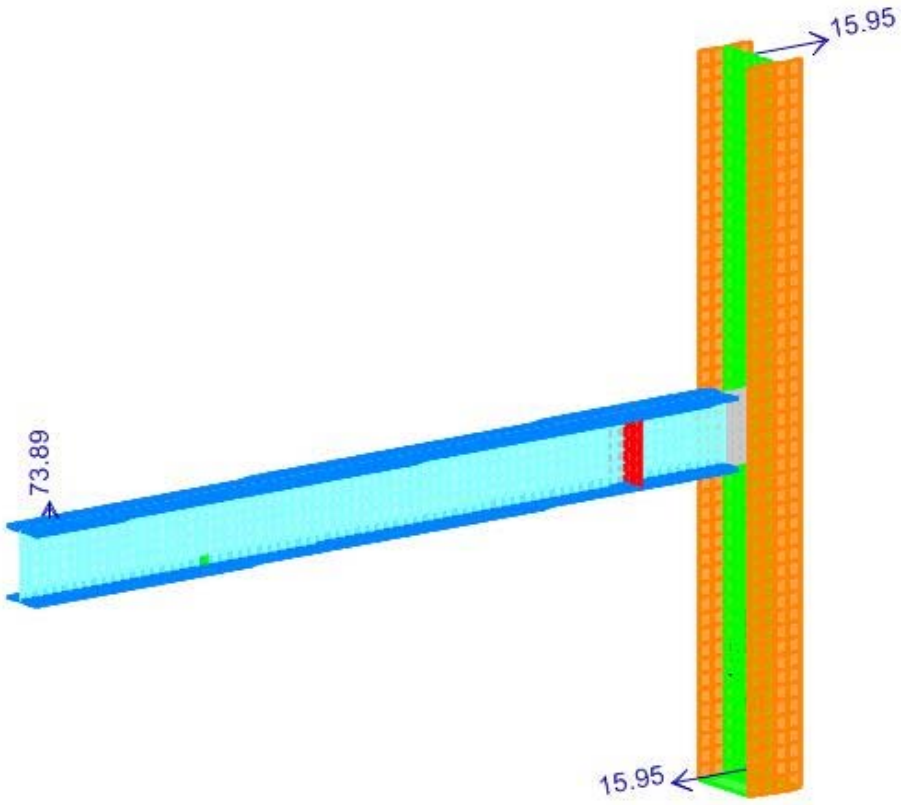

Figure 5-15 - Test 5 Shell Model 3 Joint Reactions (kN) without Column Stiffeners

5.5 Comparison of Rigid and Flexible Supports

As described in Section 1.1 the classification of rigid and flexible supports is based on the capability of the connection to follow the rotation of the supported framing member. A rigid support defines a situation where the connection is restrained from following the rotation of the supported member. Conversely a flexible support will provide some stiffness to the connection but should allow an increased rotation in comparison to the rigid support. In the case of this research, column strong axis connections were considered as the rigid supports and column weak axes connections were considered as flexible supports. The relative rigidity Inertia/Length ratios reveal that the rigid support, W360x196 stub column, is approximately 30 times stiffer than the W360x122 full-span column and approximately 5 times stiffer than the W360x314 full-span column.

The deformations in the shear tabs after the experiments were similar for both support conditions as depicted in Figure 5-16. It can be affirmed that the support condition had little or no

effect on the deformation behavior of the tested shear tabs including the observed failure mode since all bolted connection tests suffered extensive shear deformation of the plate which carried on to shear fracture through the net area of the plate.

For connections with two vertical rows of bolts, comparisons should be made between Tests 5, 6, 7 and 9 of this research which were tested on flexible supports and Tests 2 and 8 of the research by Marosi (2011) which were tested on rigid supports. As shown in Table 5-3, in all cases, the predicted connection capacities were surpassed as well as the targeted beam end rotations.

Table 5-3 – Shear Resistance Summary of Bolted Connections with Two Vertical Rows of Bolts of Marosi (2011) and D'Aronco (2013)

Test	Design Method	Predicted Failure Mode	Observed Failure Mode	Measured / Predicted Ratio **Measured** Properties
D'Aronco 5	AISC Extended	PFY	SR	1.14
	Modified Method	PFY		1.14
D'Aronco 6	AISC Extended	BLS	SR	1.14
	Modified Method	BLS		1.14
D'Aronco 7	AISC Extended	PFY	SR	1.15
	Modified Method	PFY		1.15
D'Aronco 9	AISC Extended	BLS	SR	1.18
	Modified Method	BLS		1.18
Marosi 2	AISC Extended	BG	SR / PF *	1.29
	Modified Method	PF*		1.21
Marosi 8	AISC Extended	SR	SR / PF *	1.21
	Modified Method	SR		1.18

Failure Modes:

BG= Shear Fracture of Bolt Group
BLS= Block Shear Rupture
PF= Plate Flexure with Von Mises Shear Reduction
SR= Shear Rupture through Plate Net Area
PFY= Plate Flexural Yielding
* Failure mode no longer considered in AISC (2011) 14th Edition Manual

a)  b) 

Figure 5-16 - Comparison of Shear Tab Deformation for Rigid and Flexible Supports; a) Rigid Supporting Column, b) Flexible Supporting Column

For connections with three vertical rows of bolts, comparisons should be made between Tests 1 and 2 which had rigid supports and Tests 8 and 10 which were performed with flexible support conditions. Once again, in all cases, the predicted connection shear using measured material properties was well surpassed as was the targeted beam end rotation. As previously mentioned, the relative rigidity Inertia/Length ratios reveal that the rigid support, W360x196 stub column, is approximately 30 times stiffer than the W360x122 full-span column and approximately 5 times stiffer than the W360x314 full-span column.

In terms of rotation allowance, the flexible support does not seem to allow significant greater connection rotation than its opposite rigid support.

As for bolt group and weld group eccentricities, it has been found that the AISC Manual 14th Edition (2011) extended configuration shear tab design method does not accurately predict the actual eccentricity to be resisted by the bolt group and weld group. The theoretical eccentricity to be considered in the design of welded and bolted shear tab connections with rigid supports underestimates the actual eccentricity computed with the test results. However, shear fracture of the bolt group or of the weld group has never been observed in the tests. As for the flexible support tests, the theoretical eccentricity dictated by the AISC Manual 14th Edition (2011) design method overestimates the actual eccentricity observed with the test results. Test

results indicate that it would be more appropriate to consider the connection eccentricity as the distance between the centerline of the bolt group to the tip of the column flanges instead of the centerline of the column.

Although negative bending moments were expected for both support conditions which are usually neglected in the column design, it was found that the main difference between the shear tab connection to rigid and flexible supports lies in the magnitude of the flexural bending that is generated in the column weak axes in the case of flexible supports. As depicted in Table 5-4, the findings indicate that moments imposed to columns could be well predicted using the AISC 2011 total reference design eccentricity. When compared to the calculated design eccentricity, the ratio of test eccentricity over reference eccentricity indicates that the reference eccentricity is slightly conservative. Also, these negative bending moments could be due to the presence of top and bottom stiffeners at the shear tab to column interface. The author believes that the stiffness that these plates create in the columns diminishes the flexible behaviour of the support and attracts a significant amount of unwanted eccentricity in the support. A series of finite element analyses have been performed and tend to confirm that the column stiffeners do attract flexural moment in the column. These analyses confirm that when column stiffeners are not used, the weak axis bending moment generated in the column is lowered by more than 50%.

Table 5-4 - Summary Table of Flexible Support Condition Specimens at Ultimate Shear Capacity

Test	Effective Design Bolt Group Eccentricity from Tip of Column Flanges e (mm)	Effective Design Bolt Group Eccentricity Suggested by AISC e (mm)	Total Reference Design Eccentricity (mm)	Calculated Eccentricity e_{CALC} (mm)	Ratio of Calculated Eccentricity and Design Eccentricity
5	89	229	318	286	0.90
6	89	229	318	253	0.80
7	89	290	379	385	1.02
8	127	328	455	423	0.93
9	89	290	379	295	0.78
10	127	328	455	390	0.86
				Average=	0.88
				CoV=	0.10

CHAPTER 6: CONCLUSION

6.1 Summary

With the ambition to deepen the knowledge and knowhow on the behavior of shear tab connections detailed with double and triple vertical columns of bolts and their retrofit welded counterparts, a series of ten full-scale connection experiments was performed on two different beam sizes and support conditions. Eight of these full-scale experiments were double or triple column bolted connections, four of each, of which two were carried out on rigid supports and six on flexible supports. The remaining two tests were full-scale weld retrofit shear tab connection specimens without bolts carried out on rigid supports. These tests were performed to examine the ductility of this type of connection and their shear resistance since they are a preferable retrofit option on construction sites when connection elements do not align between framing members.

On the subject of the weld retrofit tests, the experimental process has revealed that this type of on-site retrofit connection possesses adequate ductility to exceed the rotational demand anticipated at the beam end. Although the two connections used for this series of experiments possessed no bolt holes except the mandatory erection holes, extensive deformations were observed in the shear tabs. The partial C-shape welds, designed using the instantaneous center of rotation method and the CSA S16 Standard to have the same factored resistance as the bolted connection that they replaced were able to resist loads greater than their bolted counterparts which had previously been tested by Marosi (2011). The performance of these retrofit connections indicates that the remaining verifications performed for the shear tab itself when designing the original bolted connection are also adequate. Therefore, the field weld retrofits are an adequate repair alternative for construction site misfits.

The predicted connection resistances for each bolted shear tab specimen were determined based on the AISC Steel Construction Manual 14th Edition (2011) extended configuration method for single plate connections. The CISC Handbook of Steel Construction (2010) conventional configuration method was not applicable due to limitations based on the number of vertical bolt columns (only one allowed) and the reliance on outdated design parameters in comparison to the most recent version of CSA S16 (2009). Consequently, the AISC (2011) design method was the

only documented approach available to predict the connection resistance of the laboratory connection specimens for this research.

However, in conjunction with work from Marosi (2011), an updated design method based on the AISC Steel Construction Manual 14th Edition (2011) extended configuration method was proposed for use in Canada. This method was originally shown by Marosi to be applicable to shear tab connections with one or two vertical columns of 10 bolts. The research carried out for this thesis has demonstrated that the application limits of this updated method can be extended to connections with three columns of bolts. This proposed method is mainly based on the design procedure depicted in the AISC Manual 14th Edition (2011) for extended shear tab configuration, but uses increased single bolt shear strength values when determining the shear resistance of the bolt group by omitting the reduction factor applied to account for uneven distribution of shear forces in extended connections.

The failure mode predicted by the existing AISC (2011) extended configuration design method for Tests 1 and 8 was a shear fracture of the bolt group, unlike the proposed design method which predicted flexural yielding of the shear tab as the failure mode. In all cases, the experimentally observed failure mode was found to be shear rupture of the plate where the bolt group showed no damage. However, the design procedure for these connections allowed that the shear tabs be detailed to control the design and to avoid failure by shear fracture of the bolt group, thus avoiding this brittle failure mode.

The proposed modified design method was found to be giving slightly better predictions in comparison with the AISC (2011) extended configuration method in terms of predicting the ultimate shear load resisted by the test connections. Thus, the average measured-to-predicted ratio observed with the AISC (2011) extended method is of 1.17 meanwhile the average ratio obtained with the modified method is of 1.15.

On the aspect of the support condition, whether it is a strong axis oriented stub column or a weak axis oriented full-span column, the shear tab connections performed higher than the expectations in both conditions. In both cases, the various test configurations all reached the targeted rotation values, with the exception of Test 6 which might be due to the yielding of the column. However, both design methods considered in this thesis were found to give slightly better predictions for rigid support condition tests as the mean predicted-to-measured connection

resistance ratio was of 1.15 for rigid support conditions and of 1.16 for flexible support conditions. Also, the shear tab connections of shallower beams reached higher connection resistances with rigid supports, unlike the connections of deeper beams which attained higher resistances when combined with flexible supports.

With regards to the bolt configuration, the difference between the number of vertical bolt rows in the connection had very little influence on the ultimate connection capacity and in all cases the predicted connection strength was surpassed. The findings indicate that the addition of a third vertical line of bolts, while keeping the other shear tab parameters constant, has little effect on the overall observed connection resistance in comparison with a two column configuration. However, in terms of rotation allowance, the connections having a configuration with two columns of bolts attained larger beam end rotation values than the configurations with three columns of bolts although both configurations exceeded their targeted rotation values.

It was found that in order to achieve the targeted beam end rotations relative to the column face at the connection, the absolute rotation of the beams needed to be much larger in the case of flexible support conditions due to the rotation of the columns. In all cases, for both bolted and retrofit weld experiments, the connections surpassed the predicted connection resistances and the targeted beam end rotations.

The material used for the beams and shear tabs was ASTM A572 grade 50 (345MPa) steel. This material grade is typical for structural steel members but the focus was made on the behavior of this grade of steel for the shear tabs. It was found experimentally that this grade of steel possessed sufficient ductility to exceed the rotational demands and to suffer general deformations throughout the tests.

The yielding patterns distinguished throughout the testing depended on the nature of the connection. In the case of welded connections, both the tested shear tabs gave evidence of flexural yielding before the onset of shear yielding. Conversely, in all of the bolted connections, the shear tabs experienced shear yielding prior to flexural yielding. These tendencies are accountable to the inequity of deformations of the bolt group and the weld group. The weld patterns put a greater strain demand on the section of the shear tab near the support column weld because the remaining of the plate does not deform and redistribute the stress early in the test as a bolt group would allow due to the difference in relative stiffness of those elements. The weld

group imposes initial rotational restraint to the shear tab causing the early flexural yielding of the plate unlike the bolt group which allows some rotation early in the process causing shear yielding to occur prior to flexural yielding.

In terms of connection eccentricity, calculations indicate that the effective design eccentricity to be considered in the design of welded and bolted shear tab connections with rigid supports suggested by the AISC underestimates the actual eccentricity computed with the test results. Since none of the weld groups has failed during the experiments, the efficiency and precision of the instantaneous center of gravity method cannot be discussed. However, it was found that the design eccentricities suggested for the weld group design by the AISC underestimate the actual weld eccentricity by a factor of 2.5 in the case of single vertical row connection and by a factor of 1.8 in the case of a double vertical row specimen. As for the flexible support tests, the effective design eccentricity dictated by the AISC Manual 14th Edition (2011) design method overestimates the actual eccentricity calculated using the test results. Findings indicate that it would be more appropriate to consider the connection eccentricity as the distance between the centerline of the bolt group to the tip of the column flange instead of the centerline of the column in the case of flexible support connections.

This indicates that when designing a shear tab connection framing into the weak axis of a column which requires column stiffeners, the author recommends that the shear tab can be assumed as terminating at the tip of the column flanges because of the stiffness brought to the connection by the top and bottom stiffeners. Hence, the design eccentricity which should be considered for the bolt group is the distance between the centerline of the bolt group and the tip of the column flanges. In order to provide adequate stiffness to the connection, the column stiffeners must be designed to account for twice the design eccentricity of the bolt group.

In addition, as suggested by previous studies, a negative weak axis bending moment was induced in the support columns. These moments are generally neglected in the design of the columns, which seems as an appropriate assumption for core columns but does not seem conservative for perimeter columns, especially when acting as a flexible support. It was found that the bending moments imposed to the columns could be very well predicted using the AISC 2011 reference design eccentricity, and that in a slightly conservative manner.

The flexible support connections were all stiffened connections and finite element analysis have indicated that the flexural effect in the column is partially due to the rigidity brought by the column stiffeners to the connection. Although the bending moments measured were found to be smaller than the expected column moments, the finite element analysis indicate that avoiding the use of these column stiffeners would decrease considerably the bending moment induced in the column. However, when column stiffeners are not used, the designer would need to consider local failure modes for the shear tab to account for instability in compression and consider the possibility of local web bending effects in the column.

6.2 Recommendations for Future Research

A certain level of interrogation remains about the use of top and bottom stiffeners in the case of shear tab to column web connections. This additional rigidity induced in the system by the above mentioned stiffeners diminish the flexible support effect for the shear tab connection. While the connection behavior remains very ductile, experimental testing of the behavior of shear tab connections to column webs without the use of stiffeners would provide a better understanding of the effect of the stiffener plates. If these stiffeners were removed from the connection, questions would be raised about the reaction of the column web and the stability of the shear tabs. In addition, a more extensive finite element analysis of these flexible support shear tab connections, with and without the use of stiffeners, would shed light on the stress distribution in the both the stiffeners and column web at various moments in the loading pattern.

As this research was aiming to clarify the behavior of shear tab connections framing in column webs, future tests on other types of flexible supports such as girder webs could extend or restrict the applicability of single plate connections. Investigating the introduction of accidental torsion in the girders would insure that proper analyses are undertaken in the design process of the girder member itself and its end connections.

Also, examining the effect of composite beams or the only presence of a concrete slab on top of the beams, which could influence the rotational ductility and shear resistance of the connections may be useful to improve the proposed design procedure.

BIBLIOGRAPHY

AISC [2003], *Steel Construction Manual: Load and Resistance Factor Design, 3rd Edition*. American Institute of Steel Construction. Chicago.

AISC [2005], *Steel Construction Manual: 13th Edition*. American Institute of Steel Construction. Chicago, IL.

AISC [2011], *Steel Construction Manual: 14th Edition*. American Institute of Steel Construction. Chicago, IL.

Ashakul, A. [2004], "Finite Element Analysis of Single Plate Shear Connections", Ph.D Dissertation, Virginia Polytechnic Institute and State University. Blacksburg.

Astaneh, Asl. [1989], "Demand and Supply of Ductility in Steel Shear Connections", Journal of Constructional Steel Research, 14, pp. 1-19.

Astaneh, Asl., Call, S.M., and McMullin, K.M. [1989], "Design of Single Plate Shear Connections", American Institute of Steel Construction Engineering Journal, Volume 26, 1st Quarter, pp. 21-32.

Astaneh, Asl., McMullin, K.M., and Call, S.M. [1993], "Behaviour and Design of Steel Single Plate Shear Connections", Journal of Structural Engineering, ASCE, Volume 119, No. 8, pp. 2421-2440.

Astaneh, Asl., Liu, J., and McMullin, K.M., [2002], "Behaviour and Design of Single Plate Shear Connections", Journal of Constructional Steel Research, Volume 58, pp. 1121-1141.

ASTM [2009], *ASTM A370-09 Standard Test Methods and Definitions for Mechanical Testing of Steel Products*. Volume 01.03. American Society for Testing and Materials. Philadelphia, PA.

AWS [2005], *AWS A5.20:2005 Specification for Carbon Steel Electrodes for Flux Cored Arc Welding.* American Welding Society. Miami, FL.

Baldwin Metzger, K. A. [2006], "Experimental Verification of a New Single Plate Shear Connection Design Model", M.Sc. Thesis, Virginia Polytechnic Institute and State University. Blacksburg, VA.

CISC [2006], *Handbook of Steel Construction, 9th Edition*. Canadian Institute of Steel Construction. Toronto, ON.

CISC [2010], *Handbook of Steel Construction, 10th Edition*. Canadian Institute of Steel Construction. Toronto, ON.

Creech, D.D. [2005], "Behavior of Single Plate Shear Connections with Rigid and Flexible Supports", M. Sc. Thesis, North Carolina State University. Raleigh.

CSA [1994], *CSA Standard S16-94 Design of Steel Structures*. Canadian Standards Association. Mississauga, ON.

CSA [2009], *CSA Standard S16-09 Design of Steel Structures*. Canadian Standards Association. Mississauga, ON.

Kulak, G.L., Fisher, J.W., and Struik, J.H.A. [1987], *Guide to Design Criteria for Bolted and Riveted Joints*. American Institute of Steel Construction. Chicago, IL.

Lipson, S.L. [1968], "Single-Angle and Single-Plate Beam Framing Connections". Proceedings of *Canadian Structural Engineering Conference*. pp. 141-162. Toronto, ON.

Marosi, M. [2011], "Behavior of Single and Double Row Bolted Shear Tab Connections and Weld Retrofits", M. Sc. Thesis, McGill University. Montreal, QC.

Muir, L.S. and Thornton, W.A. [2011] , '' The Development of a New Design Procedure for Conventional Single-Plate Shear Connections'', Engineering Journal, AISC, Volume , No.2, pp. 141-152.

Ricles, J.M. [1980], "The Behaviour and Analysis of Double Row Bolted Shear Web Connections", M.Sc. Thesis, University of Texis. Austin, TX.

Sherman, D.R. and Ghorbanpoor, A. [2002], "Design of Extended Shear Tabs", American Institute of Steel Construction Final Report, University of Wisconson, Milwaukee, WI.

Thornton, W.A. and Fortney, P.J. [2011], ''On the Need for Stiffeners and the Effect of Lap Eccentricity on Extended Single-Plate Connections'', Engineering Journal, AISC, Volume, No.2, pp. 117-126.

APPENDIX A: INSTRUMENTATION AND TEST SETUP

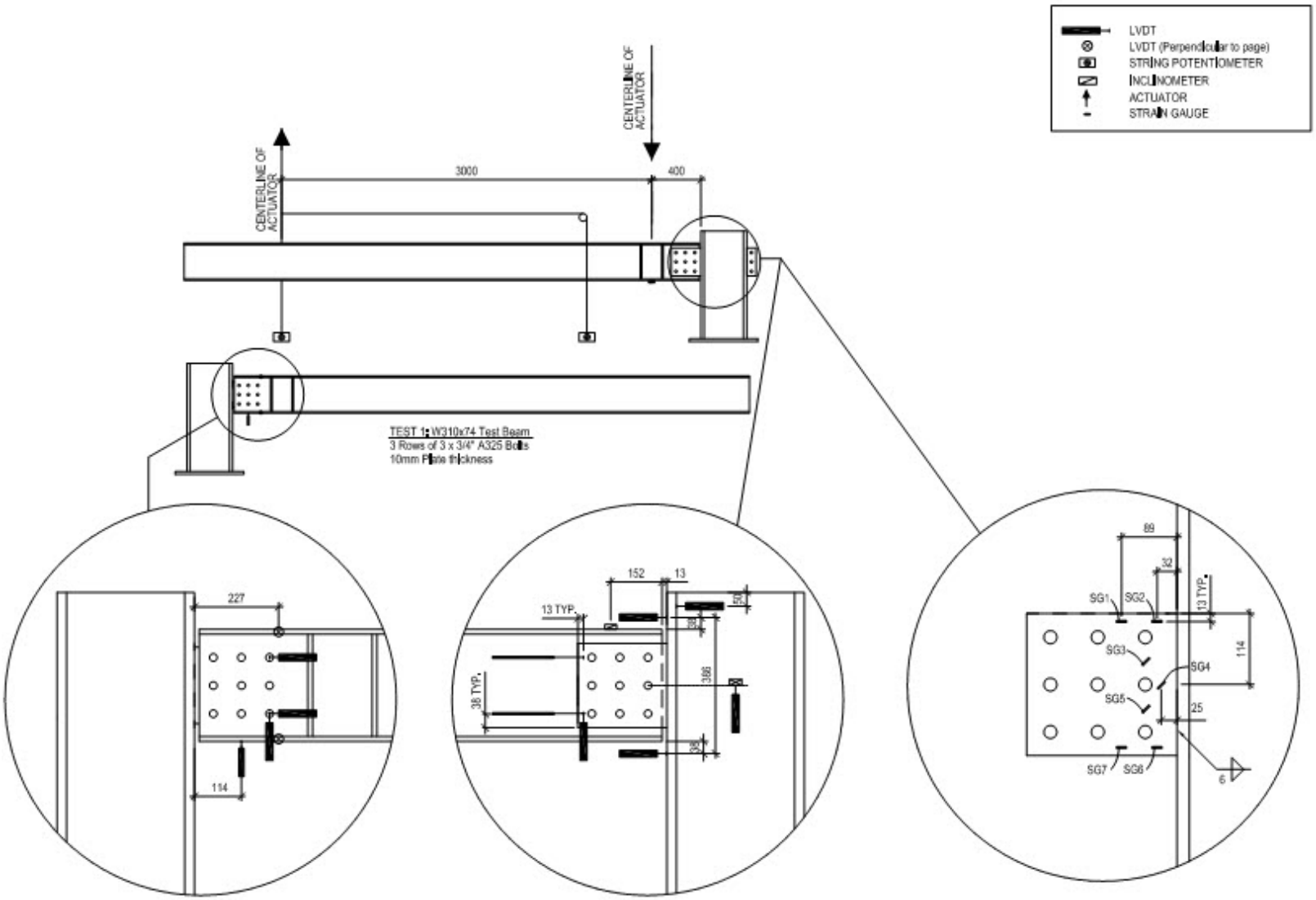

TEST 1 : Rigid Support Condition

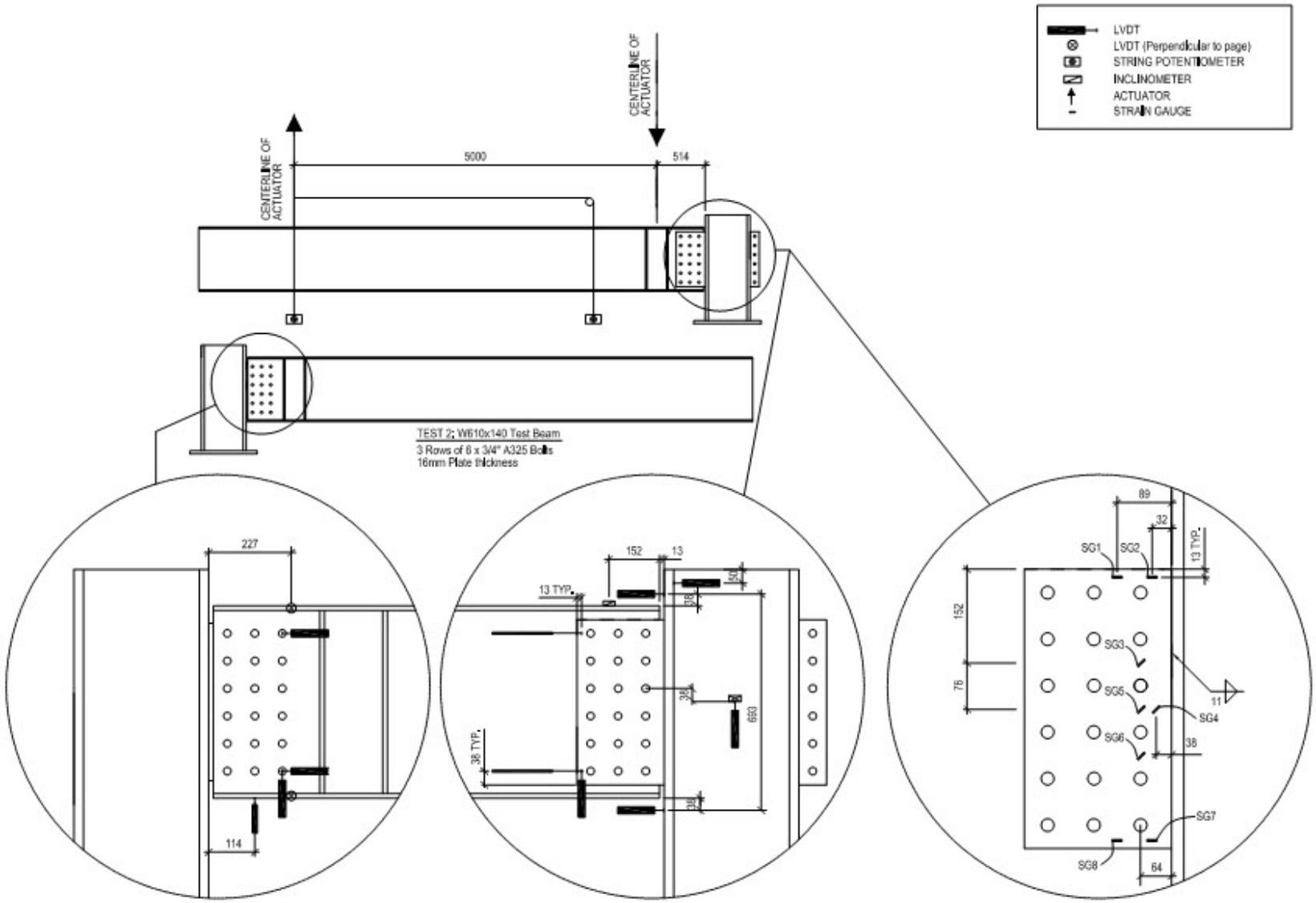

TEST 2 : Rigid Support Condition

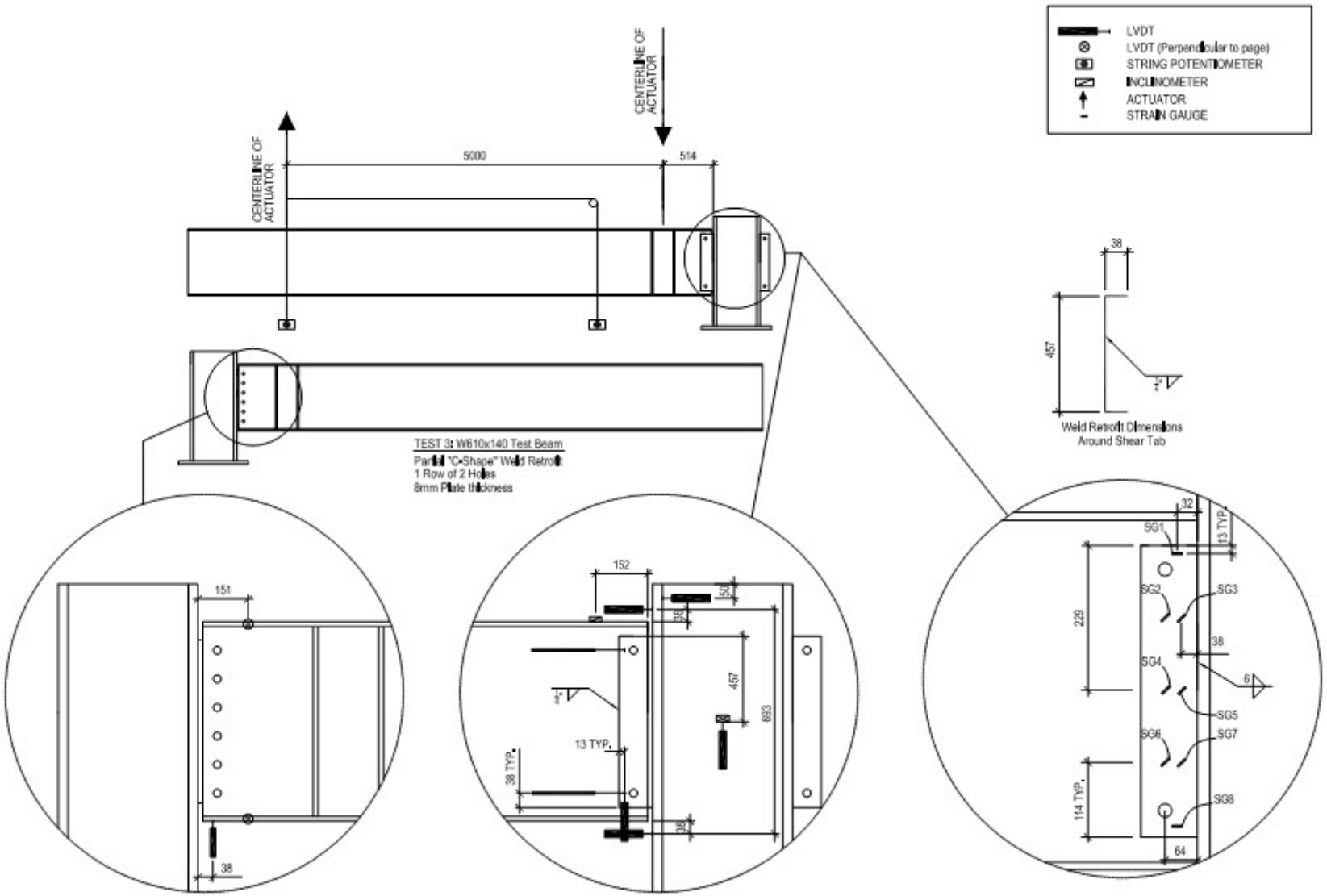

TEST 3 : Rigid Support Condition

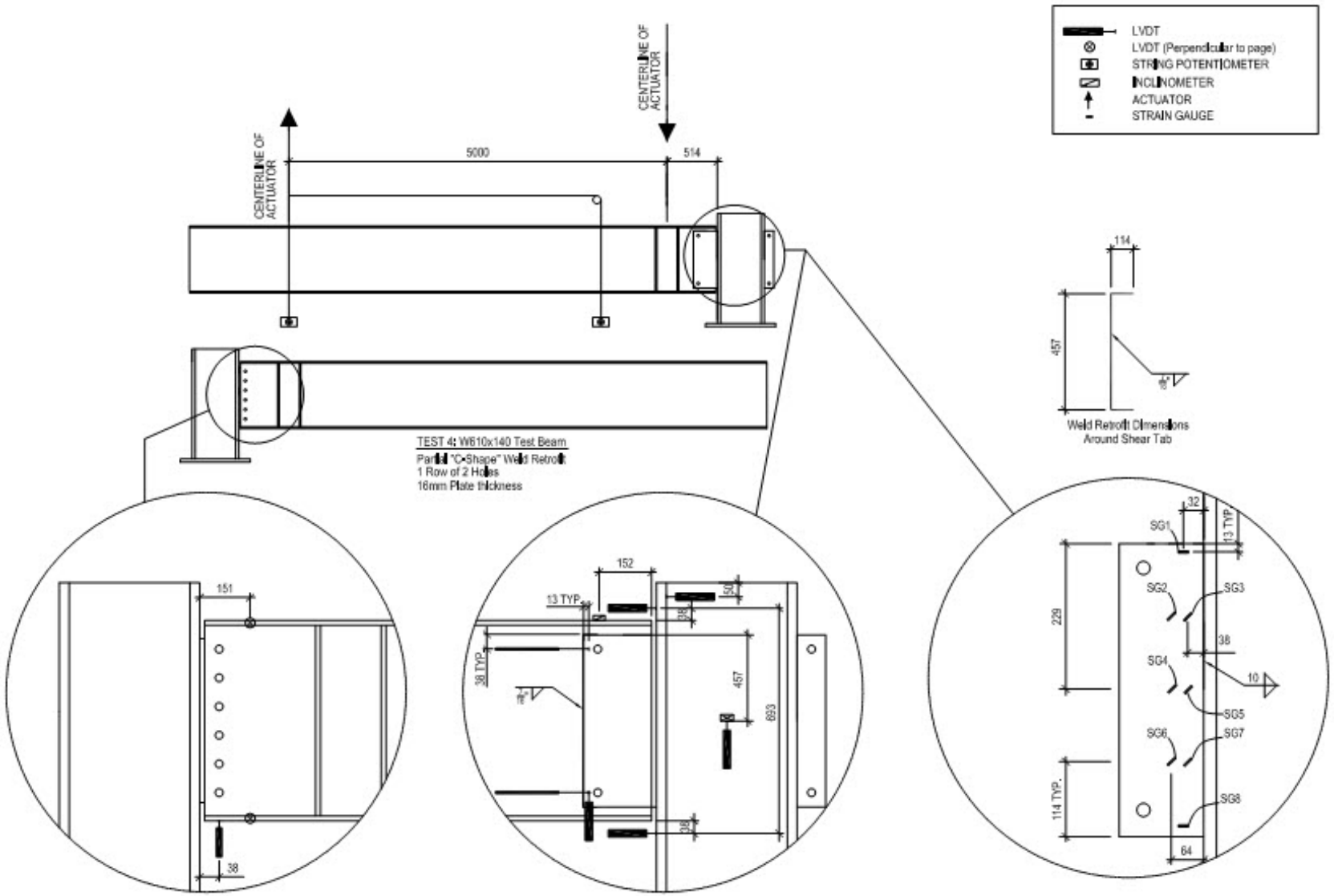

TEST 4 : Rigid Support Condition

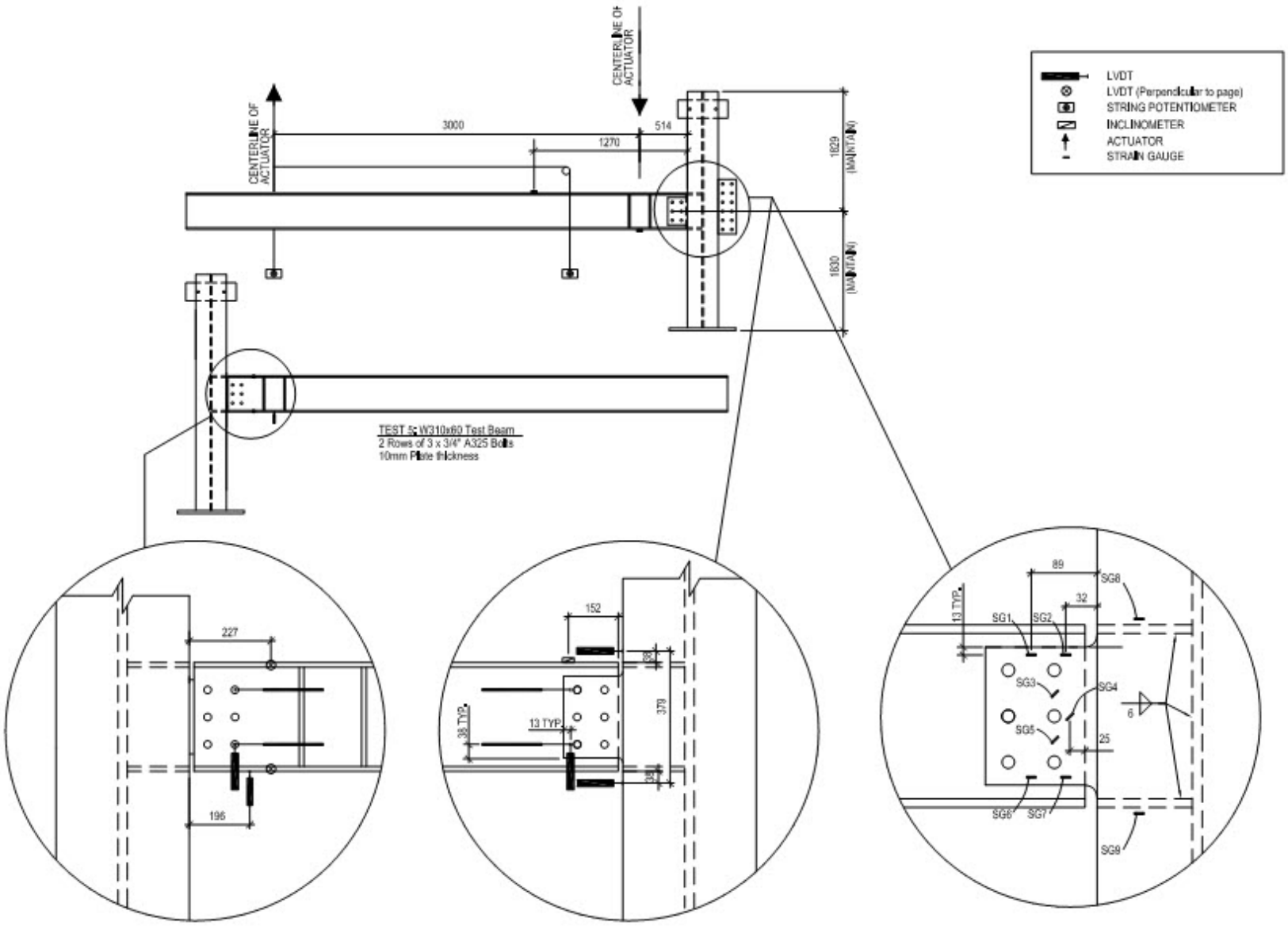

TEST 5 : Flexible Support Condition

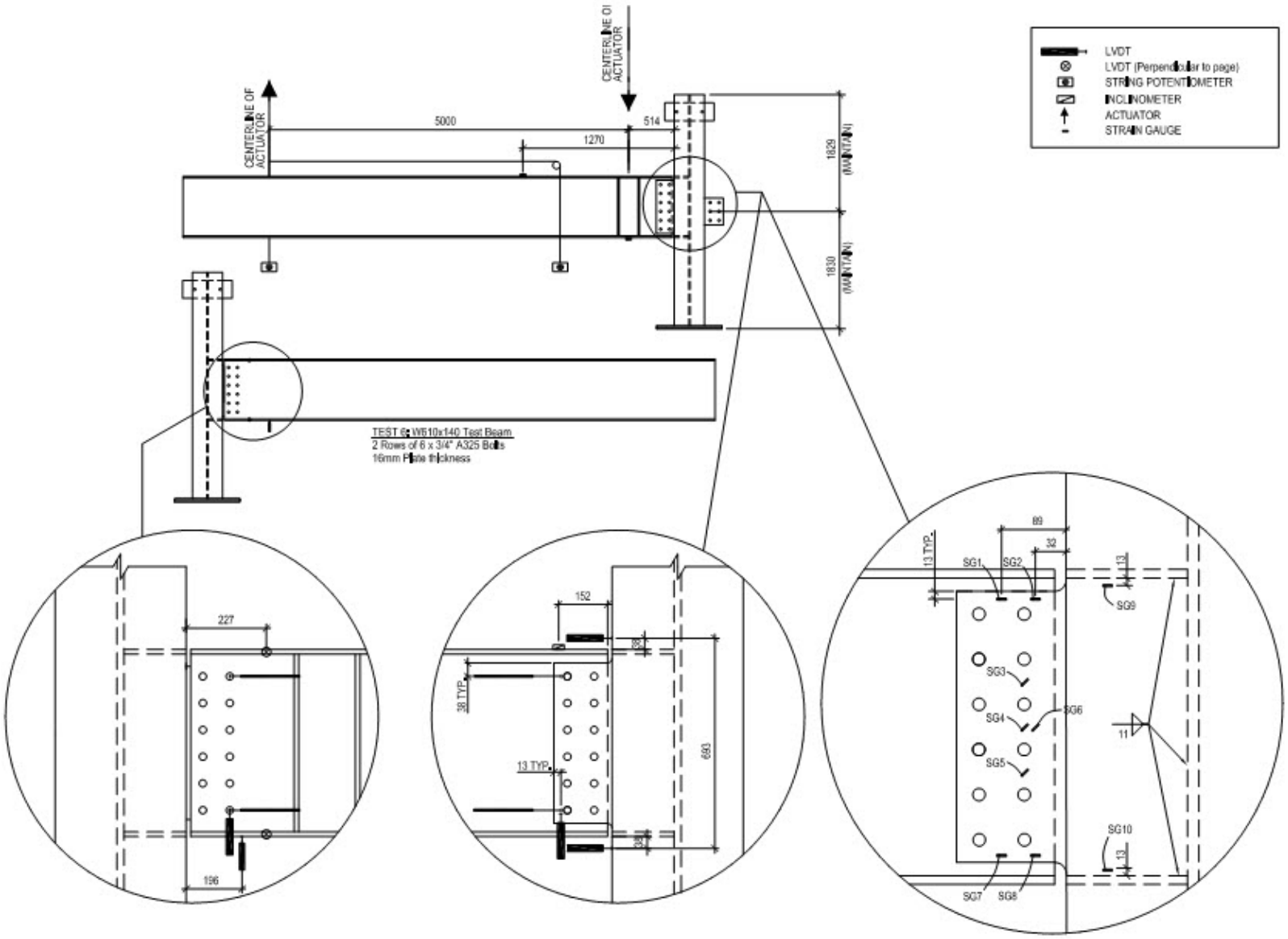

TEST 6 : Flexible Support Condition

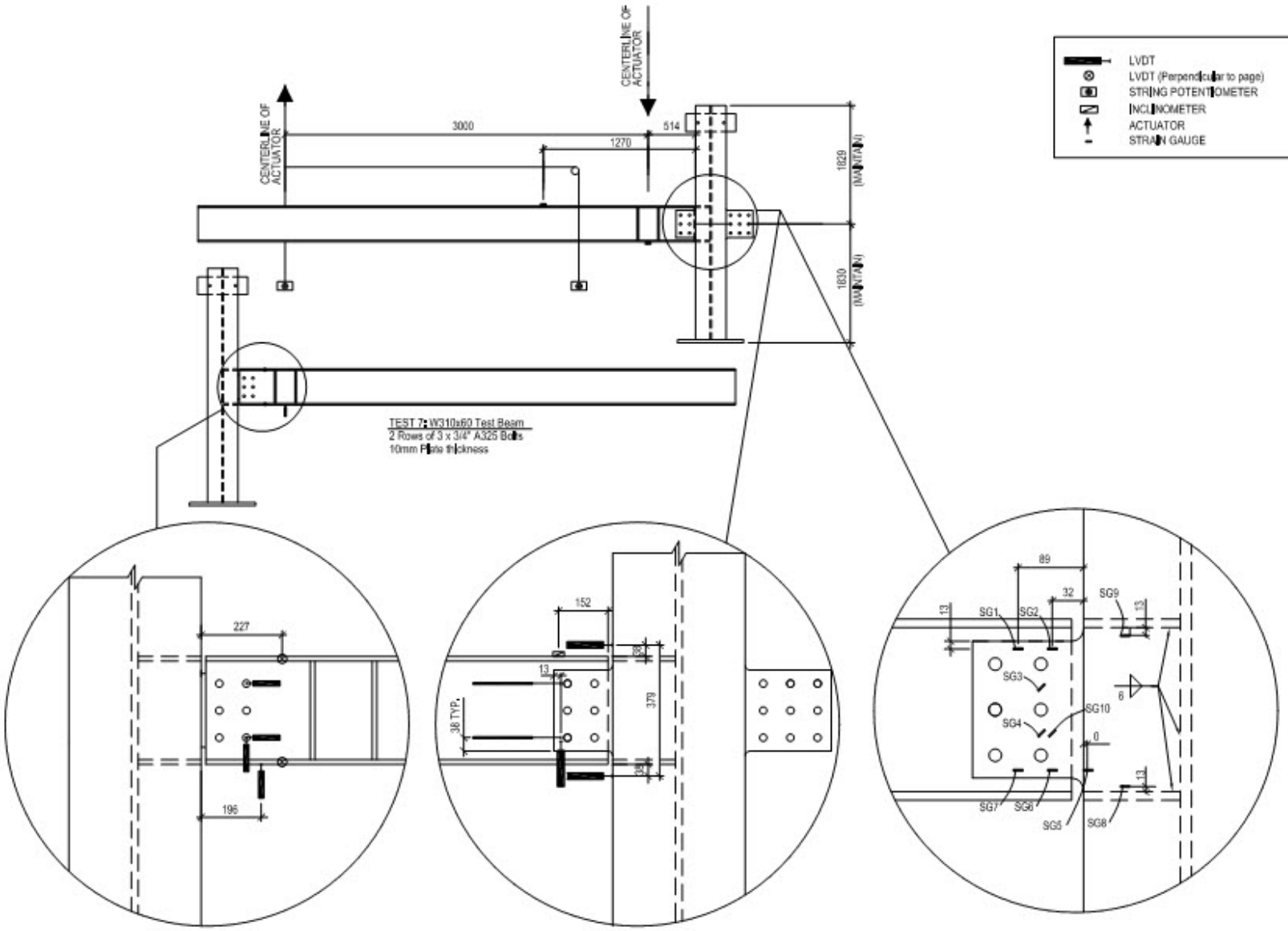

TEST 7 : Flexible Support Condition

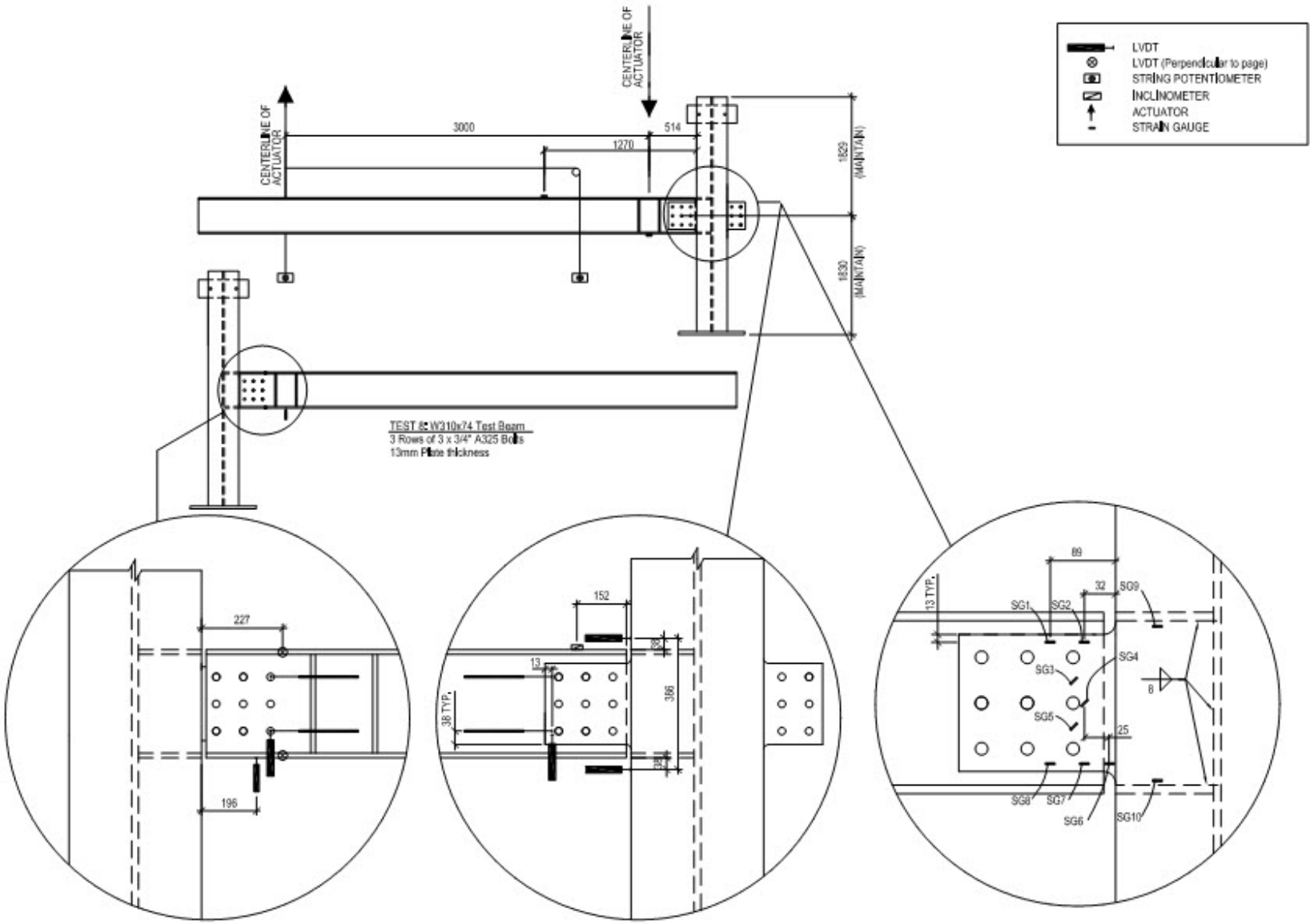

TEST 8 : Flexible Support Condition

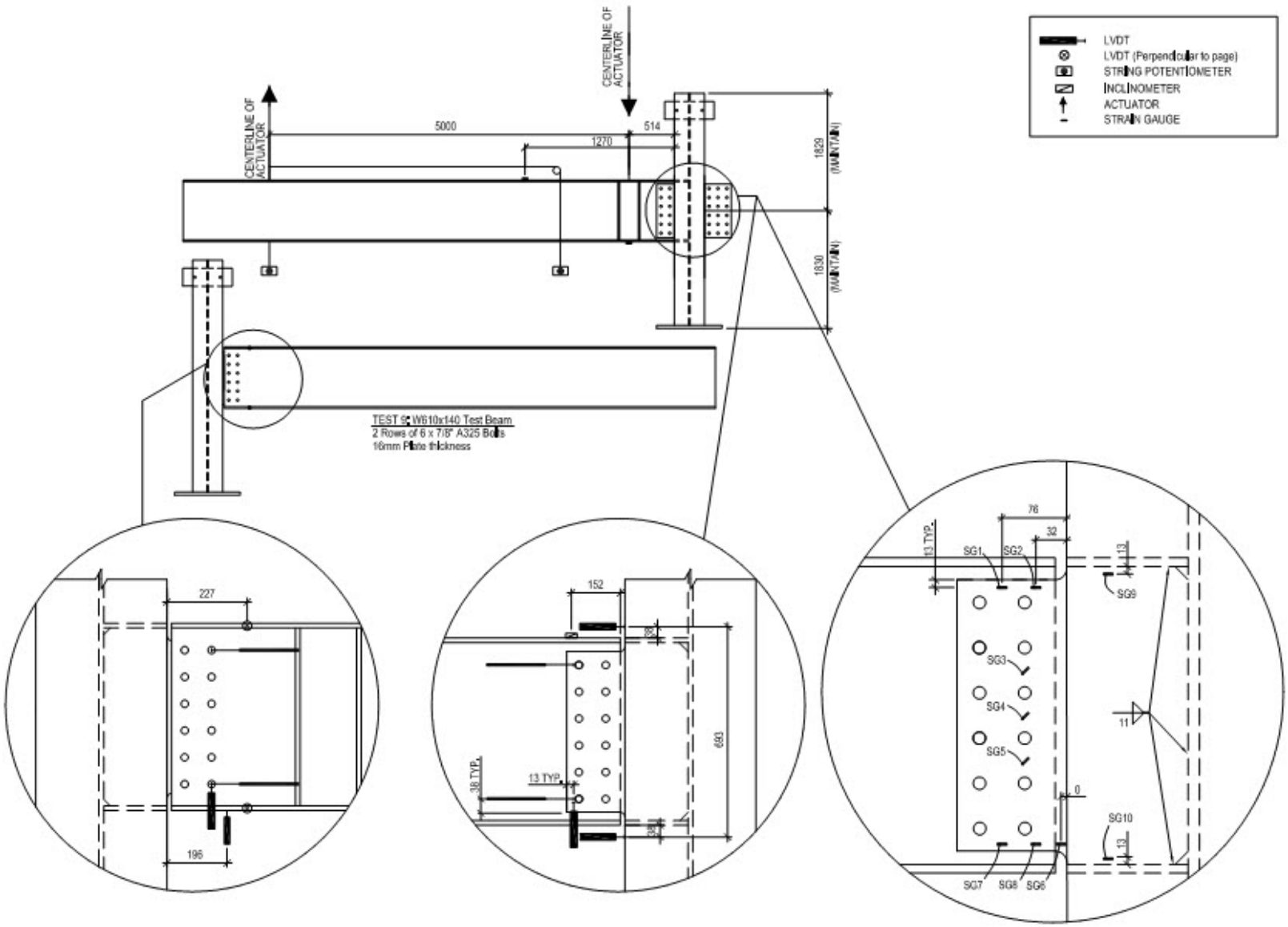

TEST 9 : Flexible Support Condition

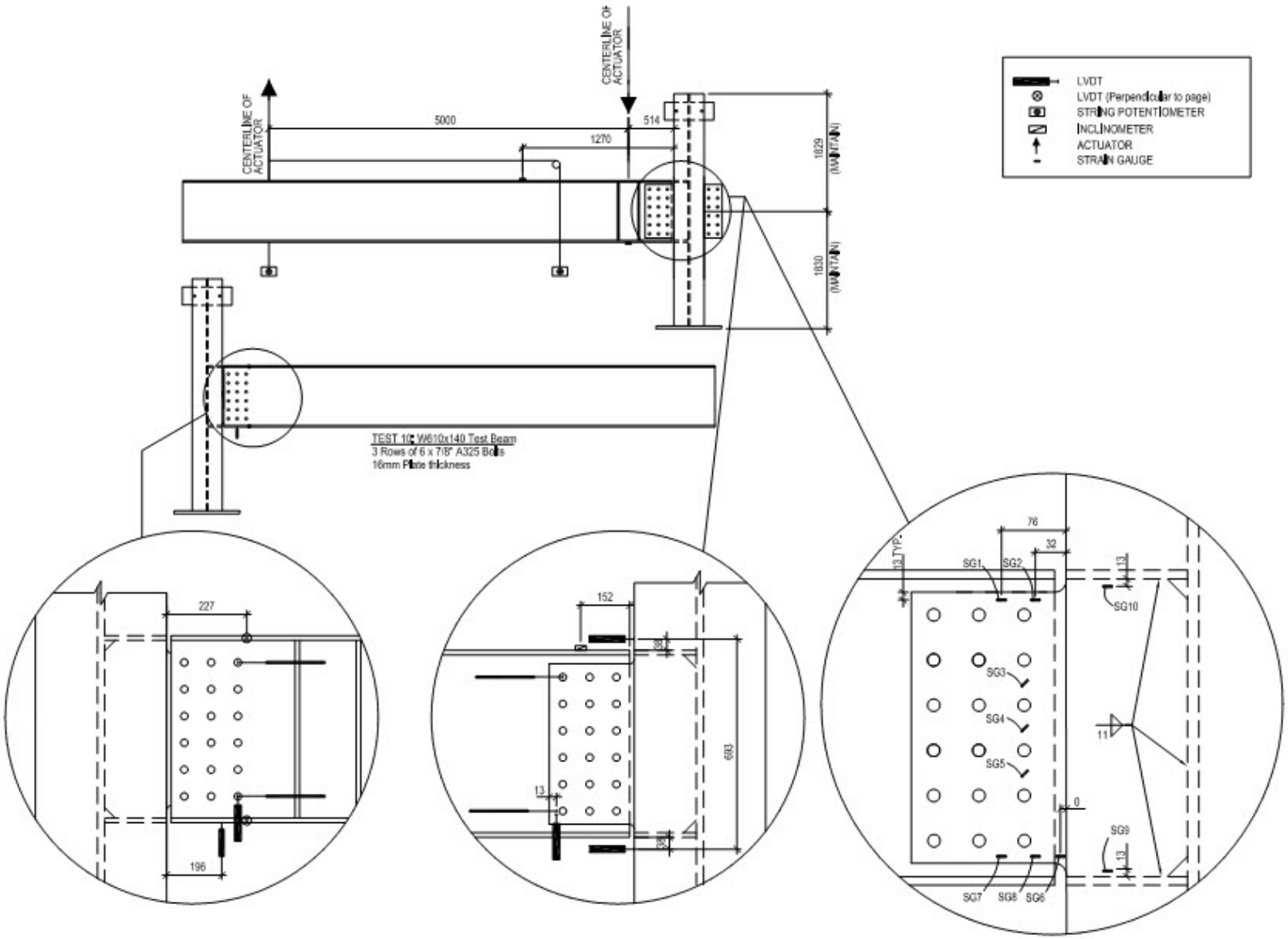

TEST 10 : Flexible Support Condition

APPENDIX B: MODIFIED METHOD: BOLTED SHEAR TAB PREDICTIONS

The calculations presented in this Appendix are based on the following parameters:

- Measured material properties have been used for both beam and plate for F_y, F_u and E.
- As described in Section 3.3.2, the eccentricity of the connection of the flexible support tests has been taken at the tip of the column flange.

TESTS 1 AND 8 - Modified Design Methode based on AISC Manual - 14th Edition - Extended Configuration

Bolt Parameters

Holes =	DRILLED	(Input PUNCHED or DRILLED)
Set Φ = 1.00?	yes	(Input YES or NO)
Bolt Type	A325	(Input A325 or A490)
Thread condition	excluded	(Input INCLUDED or EXCLUDED)
Shear planes	1	(Input 1 or 2)

Bolts / column =	3
# of col's =	3

	in.	mm	
d_b =	0.75	19.05	
d_h =	0.81	20.64	
Pitch =	3.00	76.20	
Gage =	3.00	76.20	
L_{ev} =	1.50	38.10	(Table J3.4 for $L_{ev\text{-}min}$)
L_{eh} =	1.50	38.10	(Table J3.4 for $L_{eh\text{-}min}$)

	ksi	MPa
F_{ub} =	120.00	827.37
*F_v =	74.40	512.97

Shear Resistance per Bolt

	kips	kN
$\Phi F_v A_b$ =	32.87	146.21
Φ =	1.00	

Bearing Strength of Bolt

	kips	kN
$\Phi 3.0 F_{up} d_b t_p$ =	80.93	359.99
$\Phi 3.0 F_u d_b t_w$ =	59.11	262.92
Φ =	1.00	

Governing Criterion

	kips	kN
Φr_n =	32.87	146.21
	BOLT SHEAR CONTROLS	

	in.	mm
Eccentricity, e_x =	5.00	127.00
Refer to AISC 14th edition:	Table 7-10	for C & C'
C =	4.34	
C' =	28.00	
Strength of the bolt group:	kips	kN
$\Phi R_n = C\Phi r_n$ =	**142.65**	**634.54**

Beam Parameters

Material Parameters

	ksi	MPa
F_{yp} =	55.4	382.0
F_{up} =	71.0	489.5
E =	29735.0	205015.6

Web Thickness

	in	mm
t_w =	0.37	9.40

Plate Parameters

Material Parameters

	ksi	MPa
F_{yp} =	56.9	392.0
F_{up} =	71.7	494.0
E =	29440.0	202981.6

Plate Layout

	in.	mm
t_p =	0.502	12.75
L_{total} =	9.00	228.60
a =	2.00	50.80
L_{gv} =	7.50	190.50
L_{nv} =	5.47	138.91
L_{nt} =	1.09	27.78
L_n =	6.56	166.69

Block Shear Rupture Check

Shear Yielding Component

	kips	kN
$\Phi 0.6 F_y A_{gv}$ =	128.42	571.26
Φ =	1.00	

Shear Rupture Component

	kips	kN
$\Phi 0.6 F_u A_{nv}$ =	118.02	524.98
Φ =	1.00	

Tension Rupture Component

	kips	kN
$\Phi F_u A_{nt}$ =	39.34	174.99
Φ =	1.00	

Block Shear Rupture = $\Phi F_u A_{nt} U_{bs}$ + min($\Phi 0.6 F_y A_{gv}$, $\Phi F_u A_{nv}$)

	kips	kN	U_{bs}
ΦR_n =	**137.69**	**612.48**	0.50

U_{bs} = 1.0 for uniform stress and 0.5 for non-uniform stress

Shear Yielding = $\Phi 0.6 F_y A_{gv}$

	kips	kN	Φ
ΦR_n =	**154.11**	**685.51**	1.00

Max t_p shear tab will yield prior to bolt shearing:

$M_{max} = (F_{nv}/0.9)*A_bC'$ $\quad t_{max} = 6M_{max}/F_yL^2$

	ksi	MPa
F_{nv} =	74.40	512.97
	kip-in	kNm
M_{max} =	1022.59	115.53
	in.	mm
t_{max} =	1.33	33.84

Yielding due to flexure

$(V_r/V_c)^2 + (M_r/M_c)^2 \le 1.0$

	kip-in	kNm
$M_r = V_r \times e$	272.00	30.73
$M_c = \phi_b \times F_y \times Z$	577.91	65.29
Φ_b =	1.00	
	kips	kN
V_r =	**136.00**	**604.96**
$V_c = \phi_v \times 0.6 \times F_y \times A_g$ =	154.11	685.51
Φ_v =	1.00	

$(V_r/V_c)^2 + (M_r/M_c)^2$ = 1.00 $\le$ 1.0

Local Plate Buckling Check = $\Phi F_{yp}Q = \Phi F_{cr}$

	in.	mm
h_o =	9.00	228.60
c =	2.00	50.80
λ =	0.17	
Q =	1.00	
	ksi	MPa
$\Phi F_{yp}Q$ =	56.85	391.97
(V x a)/Z =	56.86	392.03
Φ =	1.00	
	kips	kN
$V = R_n$ =	289.00	1285.54

Shear Rupture = $\Phi 0.6F_uA_n$

	kips	kN	Φ
ΦR_n =	**141.63**	**629.98**	1.00

Section Modulus

	in^3	mm^3
Z_{net} =	7.64	125122
Z =	10.17	166583

Flexural Rupture Check = $\Phi M_n = \Phi F_uZ_{net}$

	kip-in	kN-m
$\Phi F_{up}Z_{net}$ =	547.08	61.81
Φ =	1.00	
	kips	kN
$\Phi M/a = \Phi R_n$ =	**273.54**	**1216.76**

Summary of Limit States

	kips	kN	
Shear Resistance of Bolt Group OR Bearing Resistance of Web	143	635	
Block Shear Rupture	138	612	
Shear Yielding	154	686	
Shear Rupture	142	630	
Yielding due to Flexure	136	605	<== CONTROLS
Local Plate Buckling Check	289	1286	

* F_v based on 0.62 of tensile F_u from "Guide to Design Criteria for Bolted and Riveted Joints" by Kulak, Fisher, and Struik. F_v NOT taken from 14th edition of AISC steel construction manual.

TESTS 2 AND 8 - Modified Design Methode based on AISC Manual - 14th Edition - Extended Configuration

Bolt Parameters

Holes =	DRILLED	(Input PUNCHED or DRILLED)
Set Φ = 1.00?	YES	(Input YES or NO)
Bolt Type	A325	(Input A325 or A490)
Thread condition	EXCLUDED	(Input INCLUDED or EXCLUDED)
Shear planes	1	(Input 1 or 2)

Bolts / column =	6
# of col's =	3

	in.	mm	
d_b =	0.88	22.23	
d_h =	0.94	23.81	
Pitch =	3.00	76.20	
Gage =	3.00	76.20	
L_{ev} =	1.50	38.10	(Table J3.4 for $L_{ev\text{-}min}$)
L_{eh} =	1.50	38.10	(Table J3.4 for $L_{eh\text{-}min}$)

	ksi	MPa
F_{ub} =	120.00	827.37
*F_v =	74.40	512.97

Shear Resistance per Bolt

	kips	kN
$\Phi F_v A_b$ =	44.74	199.01
Φ =	1.00	

Bearing Strength of Bolt

	kips	kN
$\Phi 3.0 F_{up} d_b t_p$ =	123.64	549.97
$\Phi 3.0 F_u d_b t_w$ =	67.30	299.35
Φ =	1.00	

Governing Criterion

	kips	kN
Φr_n =	44.74	199.01
	BOLT SHEAR CONTROLS	

	in.	mm
Eccentricity, e_x =	5.00	127.00
Refer to AISC 14th edition:	Table 7-10	for C & C'
C =	12.10	
C' =	88.50	
Strength of the bolt group:	kips	kN
$\Phi R_n = C\Phi r_n$ =	**541.33**	**2407.97**

Beam Parameters

Material Parameters

	ksi	MPa
F_{yp} =	63.0	434.4
F_{up} =	82.7	570.2
E =	30023.0	207001.3

Web Thickness

	in	mm
t_w =	0.31	7.87

Plate Parameters

Material Parameters

	ksi	MPa
F_{yp} =	57.0	393.0
F_{up} =	75.0	517.1
E =	29440.0	202981.6

Plate Layout

	in.	mm
t_p =	0.628	15.95
L_{total} =	18.00	457.20
a =	2.00	50.80
L_{gv} =	16.50	419.10
L_{nv} =	11.34	288.13
L_{nt} =	1.03	26.19
L_n =	12.38	314.33

Block Shear Rupture Check

Shear Yielding Component

	kips	kN
$\Phi 0.6 F_y A_{gv}$ =	354.38	1576.36
Φ =	1.00	

Shear Rupture Component

	kips	kN
$\Phi 0.6 F_u A_{nv}$ =	320.57	1425.99
Φ =	1.00	

Tension Rupture Component

	kips	kN
$\Phi F_u A_{nt}$ =	48.57	216.06
Φ =	1.00	

Block Shear Rupture = $\Phi F_u A_{nt} U_{bs}$ + min($\Phi 0.6 F_y A_{gv}$, $\Phi F_u A_{nv}$)

	kips	kN	U_{bs}
ΦR_n =	**344.86**	**1534.02**	0.50

U_{bs} = 1.0 for uniform stress and 0.5 for non-uniform stress

Shear Yielding = $\Phi 0.6 F_y A_{gv}$

	kips	kN	Φ
ΦR_n =	**386.60**	**1719.67**	1.00

Max t_p shear tab will yield prior to bolt shearing:

$M_{max} = (F_{nv}/0.9)*A_bC'$ $\quad t_{max} = 6M_{max}/F_yL^2$

	ksi	MPa
F_{nv} =	74.40	512.97
	kip-in	kNm
M_{max} =	4399.26	497.03
	in.	mm
t_{max} =	1.43	36.30

Yielding due to flexure

$(V_r/V_c)^2 + (M_r/M_c)^2 \le 1.0$

	kip-in	kNm
$M_r = V_r \times e$	748.00	84.51
$M_c = \phi_b \times F_y \times Z$	2899.48	327.58
Φ_b =	1.00	
	kips	kN
V_r =	**374.00**	**1663.64**
$V_c = \phi_v \times 0.6 \times F_y \times A_g$ =	386.60	1719.67
Φ_v =	1.00	

$(V_r/V_c)^2 + (M_r/M_c)^2$ = 1.00 $\le$ 1.0

Local Plate Buckling Check = $\Phi F_{yp}Q = \Phi F_{cr}$

	in.	mm
h_o =	18.00	457.20
c =	2.00	50.80
λ =	0.14	
Q =	1.00	
	ksi	MPa
$\Phi F_{yp}Q$ =	57.00	393.00
(V x a)/Z =	56.97	392.80
Φ =	1.00	
	kips	kN
$V = R_n$ =	1449.00	6445.47

Shear Rupture = $\Phi 0.6F_uA_n$

	kips	kN	Φ
ΦR_n =	**349.72**	**1555.62**	1.00

Section Modulus

	in^3	mm^3
Z_{net} =	34.97	573084
Z =	50.87	833577

Flexural Rupture Check = $\Phi M_n = \Phi F_uZ_{net}$

	kip-in	kN-m
$\Phi F_{up}Z_{net}$ =	2622.88	296.33
Φ =	1.00	
	kips	kN
$\Phi M/a = \Phi R_n$ =	**1311.44**	**5833.58**

Summary of Limit States

	kips	kN	
Shear Resistance of Bolt Group OR Bearing Resistance of Web	541	2408	
Block Shear Rupture	345	1534	<== CONTROLS
Shear Yielding	387	1720	
Shear Rupture	350	1556	
Yielding due to Flexure	374	1664	
Local Plate Buckling Check	1449	6445	

* F_v based on 0.62 of tensile F_u from "Guide to Design Criteria for Bolted and Riveted Joints" by Kulak, Fisher, and Struik. F_v NOT taken from 14th edition of AISC steel construction manual.

TESTS 5 AND 7 - Modified Design Methode based on AISC Manual - 14th Edition - Extended Configuration

Bolt Parameters

Holes =	DRILLED	(Input PUNCHED or DRILLED)
Set Φ = 1.00?	YES	(Input YES or NO)
Bolt Type	A325	(Input A325 or A490)
Thread condition	EXCLUDED	(Input INCLUDED or EXCLUDED)
Shear planes	1	(Input 1 or 2)

Bolts / column =	3
# of col's =	2

	in.	mm	
d_b =	0.75	19.05	
d_h =	0.81	20.64	
Pitch =	3.00	76.20	
Gage =	3.00	76.20	
L_{ev} =	1.50	38.10	(Table J3.4 for $L_{ev\text{-}min}$)
L_{eh} =	1.50	38.10	(Table J3.4 for $L_{eh\text{-}min}$)

	ksi	MPa
F_{ub} =	120.00	827.37
*F_v =	74.40	512.97

Shear Resistance per Bolt

	kips	kN
$\Phi F_v A_b$ =	32.87	146.21
Φ =	1.00	

Bearing Strength of Bolt

	kips	kN
$\Phi 3.0 F_{up} d_b t_p$ =	64.56	287.17
$\Phi 3.0 F_u d_b t_w$ =	50.12	222.96
Φ =	1.00	

Governing Criterion

	kips	kN
Φr_n =	32.87	146.21
	BOLT SHEAR CONTROLS	

	in.	mm
Eccentricity, e_x =	3.50	88.90
Refer to AISC 14th edition:	Table 7-7	for C & C'
C =	3.37	
C' =	15.80	
Strength of the bolt group:	kips	kN
$\Phi R_n = C\Phi r_n$ =	**110.77**	**492.72**

Beam Parameters

Material Parameters

	ksi	MPa
F_{yp} =	57.9	398.9
F_{up} =	72.8	501.9
E =	30167.0	207994.1

Web Thickness

	in	mm
t_w =	0.31	7.77

Plate Parameters

Material Parameters

	ksi	MPa
F_{yp} =	69.3	477.8
F_{up} =	79.5	548.0
E =	29009.0	200010.0

Plate Layout

	in.	mm
t_p =	0.361	9.17
L_{total} =	9.00	228.60
a =	2.00	50.80
L_{gv} =	7.50	190.50
L_{nv} =	5.47	138.91
L_{nt} =	1.09	27.78
L_n =	6.56	166.69

Block Shear Rupture Check

Shear Yielding Component

	kips	kN
$\Phi 0.6 F_y A_{gv}$ =	112.58	500.77
Φ =	1.00	

Shear Rupture Component

	kips	kN
$\Phi 0.6 F_u A_{nv}$ =	94.15	418.78
Φ =	1.00	

Tension Rupture Component

	kips	kN
$\Phi F_u A_{nt}$ =	31.38	139.59
Φ =	1.00	

Block Shear Rupture = $\Phi F_u A_{nt} U_{bs} + \min(\Phi 0.6 F_y A_{gv}, \Phi F_u A_{nv})$

	kips	kN	U_{bs}
ΦR_n =	**109.84**	**488.58**	0.50

U_{bs} = 1.0 for uniform stress and 0.5 for non-uniform stress

Shear Yielding = $\Phi 0.6 F_y A_{gv}$

	kips	kN	Φ
ΦR_n =	**135.09**	**600.93**	1.00

Max t_p shear tab will yield prior to bolt shearing:

$M_{max} = (F_{nv}/0.9)*A_bC'$ $\quad t_{max} = 6M_{max}/F_yL^2$

	ksi	MPa
F_{nv} =	74.40	512.97
	kip-in	kNm
M_{max} =	577.03	65.19
	in.	mm
t_{max} =	0.62	15.67

Yielding due to flexure

$(V_r/V_c)^2 + (M_r/M_c)^2 \le 1.0$

	kip-in	kNm
$M_r = V_r \times e$	346.50	39.15
$M_c = \phi_b \times F_y \times Z$	506.60	57.24
Φ_b =	1.00	
	kips	kN
V_r =	**99.00**	**440.37**
$V_c = \phi_v \times 0.6 \times F_y \times A_g$ =	135.09	600.93
Φ_v =	1.00	

$(V_r/V_c)^2 + (M_r/M_c)^2$ = 1.00 $\le$ 1.0

Local Plate Buckling Check = $\Phi F_{yp}Q = \Phi F_{cr}$

	in.	mm
h_o =	9.00	228.60
c =	2.00	50.80
λ =	0.26	
Q =	1.00	
	ksi	MPa
$\Phi F_{yp}Q$ =	69.30	477.81
(V x a)/Z =	69.35	478.18
Φ =	1.00	
	kips	kN
$V = R_n$ =	253.50	1127.62

Shear Rupture = $\Phi 0.6F_uA_n$

	kips	kN	Φ
ΦR_n =	**112.98**	**502.54**	1.00

Section Modulus

	in^3	mm^3
Z_{net} =	5.49	89978
Z =	7.31	119794

Flexural Rupture Check = $\Phi M_n = \Phi F_uZ_{net}$

	kip-in	kN-m
$\Phi F_{up}Z_{net}$ =	436.41	49.31
Φ =	1.00	
	kips	kN
$\Phi M/a = \Phi R_n$ =	**218.20**	**970.62**

Summary of Limit States

	kips	kN	
Shear Resistance of Bolt Group OR Bearing Resistance of Web	111	493	
Block Shear Rupture	110	489	
Shear Yielding	135	601	
Shear Rupture	113	503	
Yielding due to Flexure	99	440	<== CONTROLS
Local Plate Buckling Check	254	1128	

* F_v based on 0.62 of tensile F_u from "Guide to Design Criteria for Bolted and Riveted Joints" by Kulak, Fisher, and Struik. F_v NOT taken from 14th edition of AISC steel construction manual.

TESTS 6 AND 9 - Modified Design Methode based on AISC Manual - 14th Edition - Extended Configuration

Bolt Parameters

Holes =	DRILLED	(Input PUNCHED or DRILLED)
Set Φ = 1.00?	YES	(Input YES or NO)
Bolt Type	A325	(Input A325 or A490)
Thread condition	EXCLUDED	(Input INCLUDED or EXCLUDED)
Shear planes	1	(Input 1 or 2)

Bolts / column =	6
# of col's =	2

	in.	mm	
d_b =	0.88	22.23	
d_h =	0.94	23.81	
Pitch =	3.00	76.20	
Gage =	3.00	76.20	
L_{ev} =	1.50	38.10	(Table J3.4 for $L_{ev\text{-}min}$)
L_{eh} =	1.50	38.10	(Table J3.4 for $L_{eh\text{-}min}$)

	ksi	MPa
F_{ub} =	120.00	827.37
*F_v =	74.40	512.97

Shear Resistance per Bolt

	kips	kN
$\Phi F_v A_b$ =	44.74	199.01
Φ =	1.00	

Bearing Strength of Bolt

	kips	kN
$\Phi 3.0 F_{up} d_b t_p$ =	135.05	600.74
$\Phi 3.0 F_u d_b t_w$ =	105.09	467.46
Φ =	1.00	

Governing Criterion

	kips	kN
Φr_n =	44.74	199.01
	BOLT SHEAR CONTROLS	

	in.	mm
Eccentricity, e_x =	3.50	88.90
Refer to AISC 14th edition:	Table 7-7	for C & C'
C =	9.42	
C' =	54.20	
Strength of the bolt group:	kips	kN
$\Phi R_n = C\Phi r_n$ =	**421.43**	**1874.63**

Beam Parameters

Material Parameters

	ksi	MPa
F_{yp} =	59.4	409.5
F_{up} =	74.0	510.2
E =	30312.0	208993.9

Web Thickness

	in	mm
t_w =	0.54	13.74

Plate Parameters

Material Parameters

	ksi	MPa
F_{yp} =	72.1	497.0
F_{up} =	83.3	574.0
E =	30167.0	207994.1

Plate Layout

	in.	mm
t_p =	0.618	15.70
L_{total} =	18.00	457.20
a =	2.00	50.80
L_{gv} =	16.50	419.10
L_{nv} =	11.34	288.13
L_{nt} =	1.03	26.19
L_n =	12.38	314.33

Block Shear Rupture Check

Shear Yielding Component

	kips	kN
$\Phi 0.6 F_y A_{gv}$ =	441.00	1961.67
Φ =	1.00	

Shear Rupture Component

	kips	kN
$\Phi 0.6 F_u A_{nv}$ =	350.17	1557.64
Φ =	1.00	

Tension Rupture Component

	kips	kN
$\Phi F_u A_{nt}$ =	53.06	236.01
Φ =	1.00	

Block Shear Rupture = $\Phi F_u A_{nt} U_{bs}$ + min($\Phi 0.6 F_y A_{gv}$, $\Phi F_u A_{nv}$)

	kips	kN	U_{bs}
ΦR_n =	**376.70**	**1675.64**	0.50

U_{bs} = 1.0 for uniform stress and 0.5 for non-uniform stress

Shear Yielding = $\Phi 0.6 F_y A_{gv}$

	kips	kN	Φ
ΦR_n =	**481.09**	**2140.00**	1.00

Max t_p shear tab will yield prior to bolt shearing:

$M_{max} = (F_{nv}/0.9)*A_bC'$ $\quad t_{max} = 6M_{max}/F_yL^2$

	ksi	MPa
F_{nv} =	74.40	512.97
	kip-in	kNm
M_{max} =	2694.24	304.39
	in.	mm
t_{max} =	0.69	17.58

Yielding due to flexure

$(V_r/V_c)^2 + (M_r/M_c)^2 \le 1.0$

	kip-in	kNm
$M_r = V_r \times e$	1522.15	171.97
$M_c = \phi_b \times F_y \times Z$	3608.18	407.65
Φ_b =	1.00	
	kips	kN
V_r =	**434.90**	**1934.53**
$V_c = \phi_v \times 0.6 \times F_y \times A_g$ =	481.09	2140.00
Φ_v =	1.00	
$(V_r/V_c)^2 + (M_r/M_c)^2$ =	1.00	≤ 1.0

Local Plate Buckling Check = $\Phi F_{yp}Q = \Phi F_{cr}$

	in.	mm
h_o =	18.00	457.20
c =	2.00	50.80
λ =	0.16	
Q =	1.00	
	ksi	MPa
$\Phi F_{yp}Q$ =	72.08	496.97
(V x a)/Z =	72.08	496.95
Φ =	1.00	
	kips	kN
$V = R_n$ =	1804.00	8024.59

Shear Rupture = $\Phi 0.6F_uA_n$

	kips	kN	Φ
ΦR_n =	**382.01**	**1699.24**	1.00

Section Modulus

	in^3	mm^3
Z_{net} =	34.41	563959
Z =	50.06	820304

Flexural Rupture Check = $\Phi M_n = \Phi F_uZ_{net}$

	kip-in	kN-m
$\Phi F_{up}Z_{net}$ =	2865.04	323.69
Φ =	1.00	
	kips	kN
$\Phi M/a = \Phi R_n$ =	**1432.52**	**6372.16**

Summary of Limit States

	kips	kN	
Shear Resistance of Bolt Group OR Bearing Resistance of Web	421	1875	
Block Shear Rupture	377	1676	<== CONTROLS
Shear Yielding	481	2140	
Shear Rupture	382	1699	
Yielding due to Flexure	435	1935	
Local Plate Buckling Check	1804	8025	

* F_v based on 0.62 of tensile F_u from "Guide to Design Criteria for Bolted and Riveted Joints" by Kulak, Fisher, and Struik. F_v NOT taken from 14th edition of AISC steel construction manual.

APPENDIX C: TEST RESULT PHOTOGRAPHS

TEST 1: Three Vertical Rows of Three Bolts

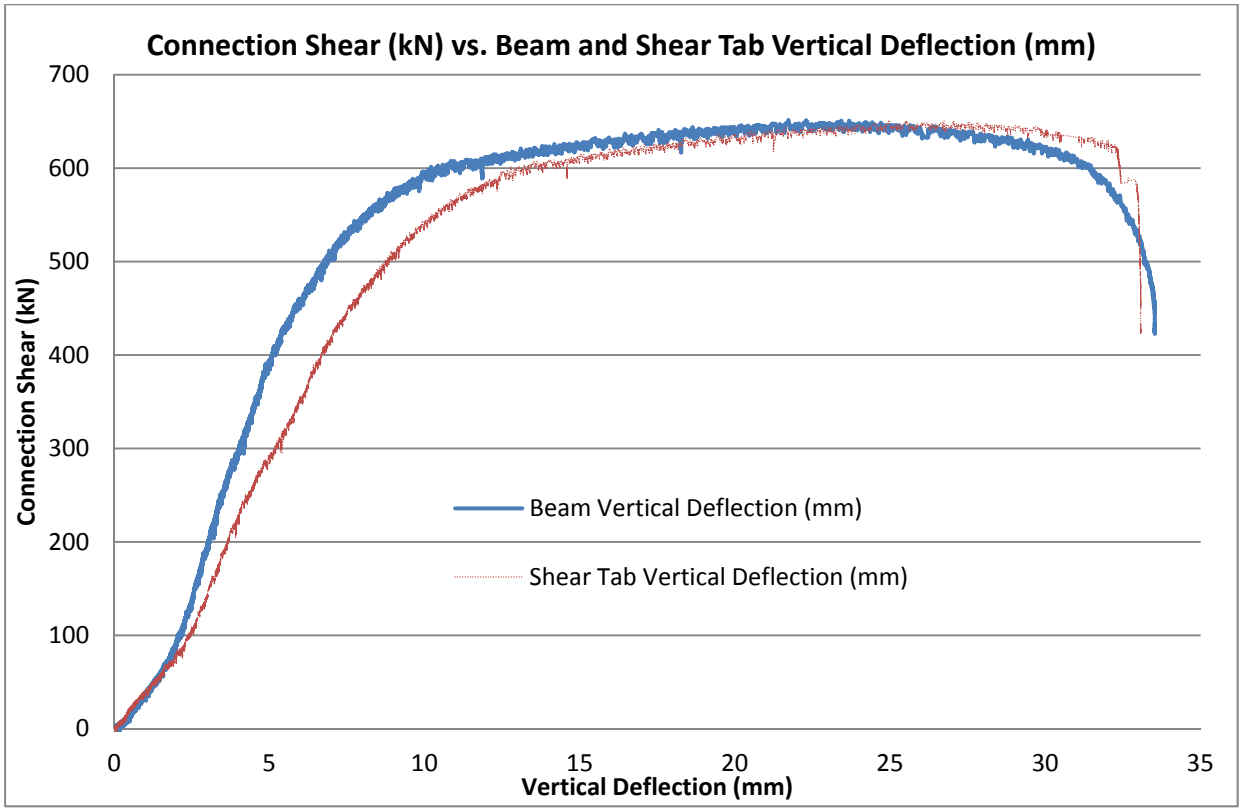

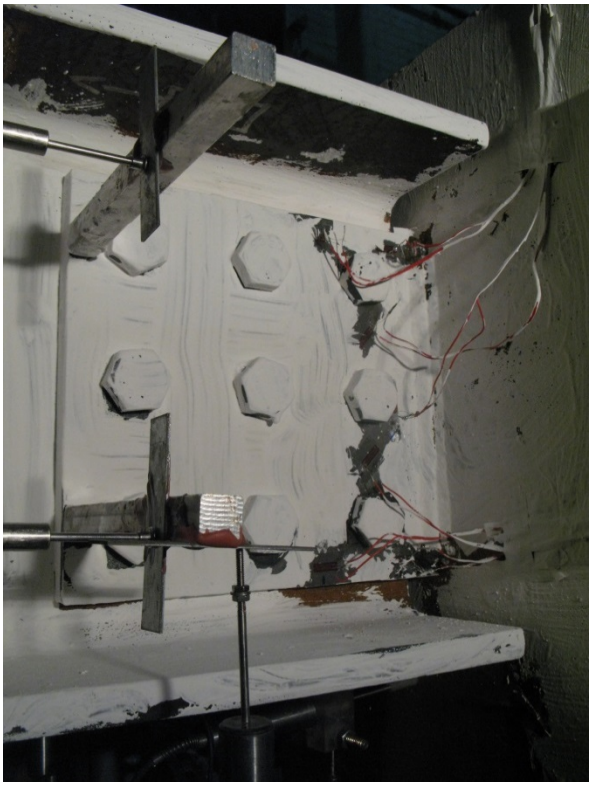

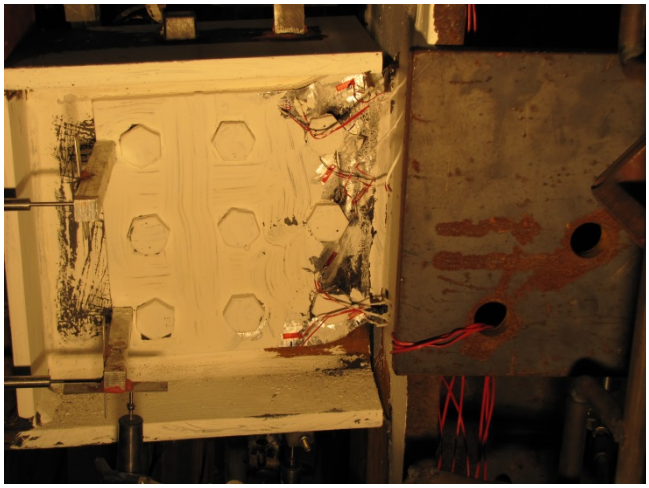

TEST 2: Three Vertical Rows of Six Bolts

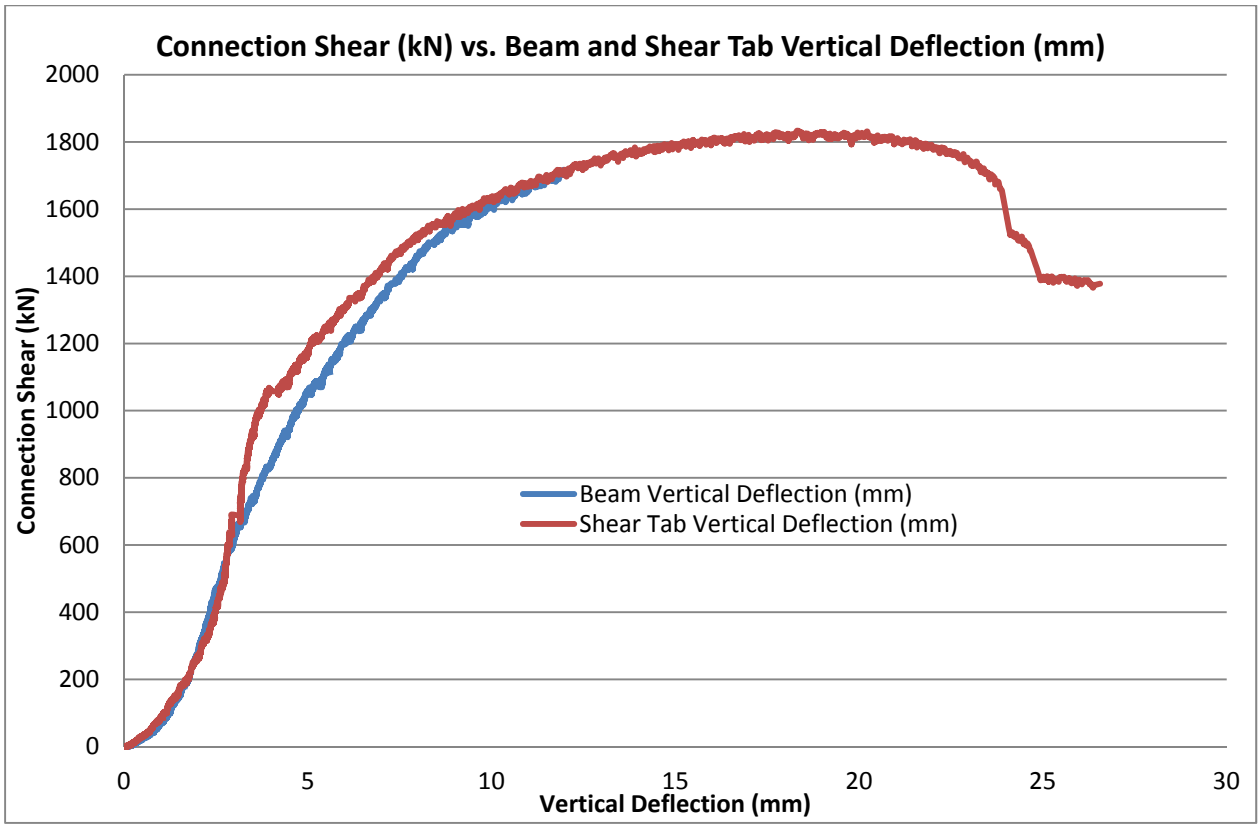

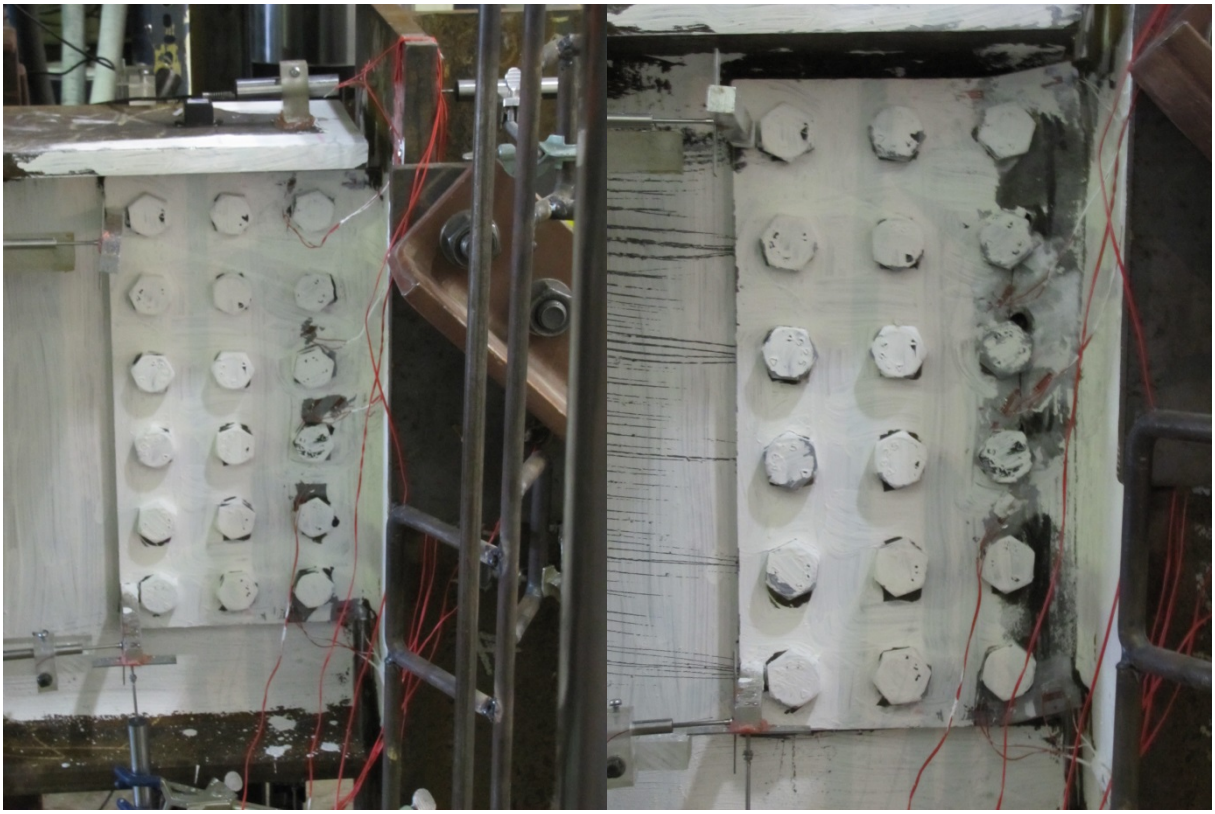

TEST 3: Single Vertical Row Partial C-Shape Weld Retrofit

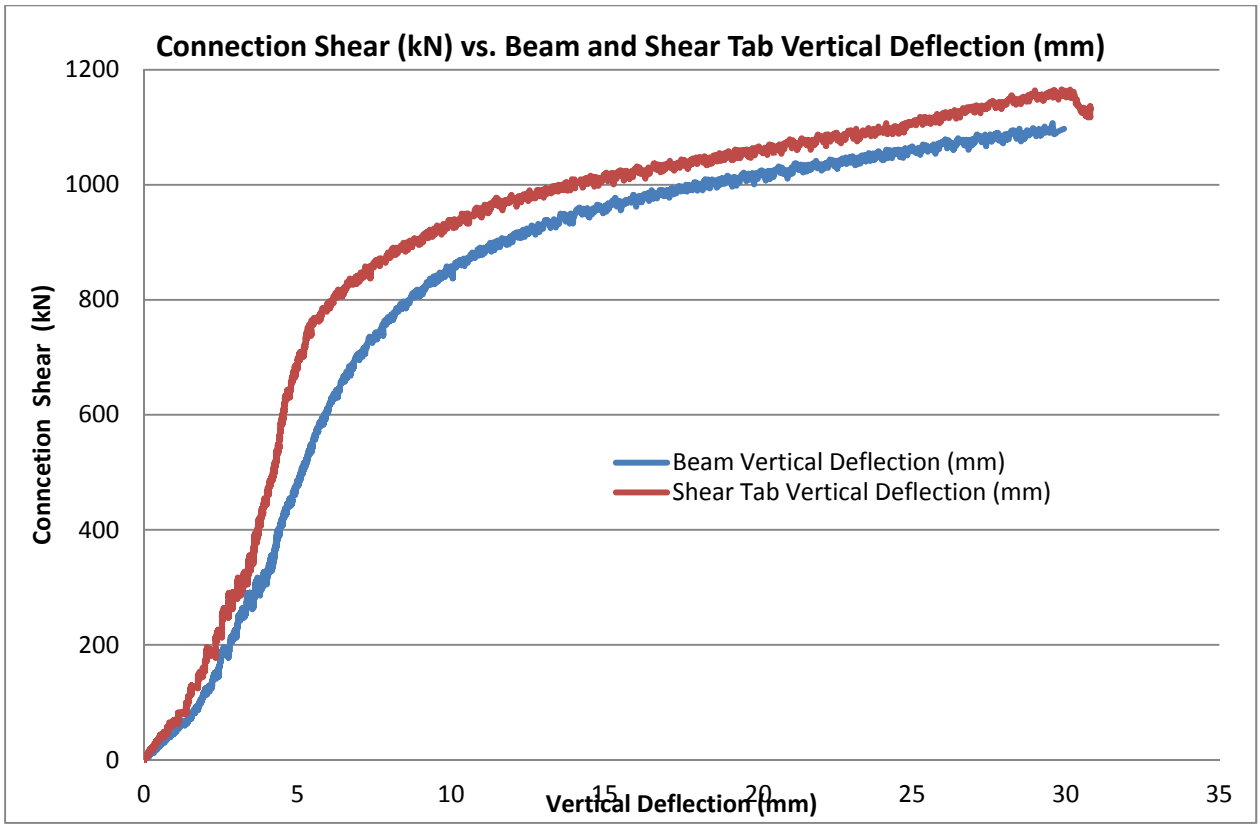

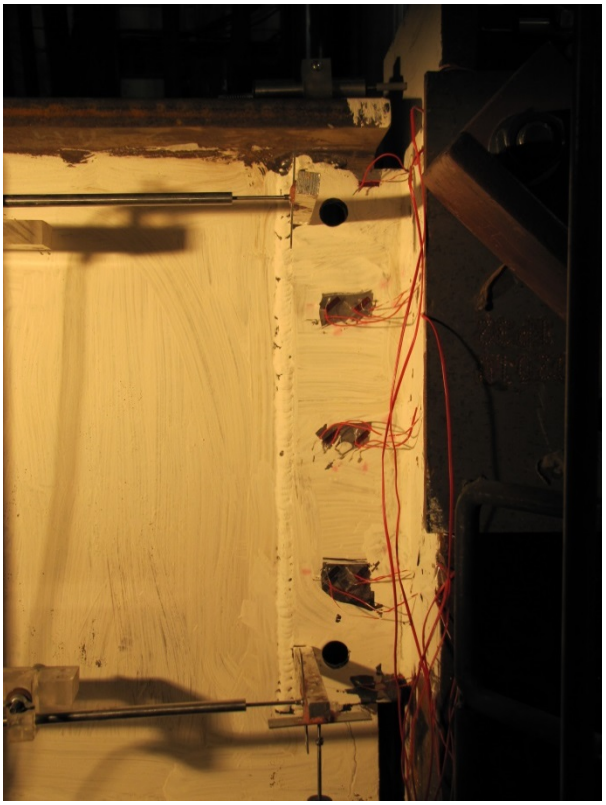

TEST 4: Double Vertical Row Partial C-Shape Weld Retrofit

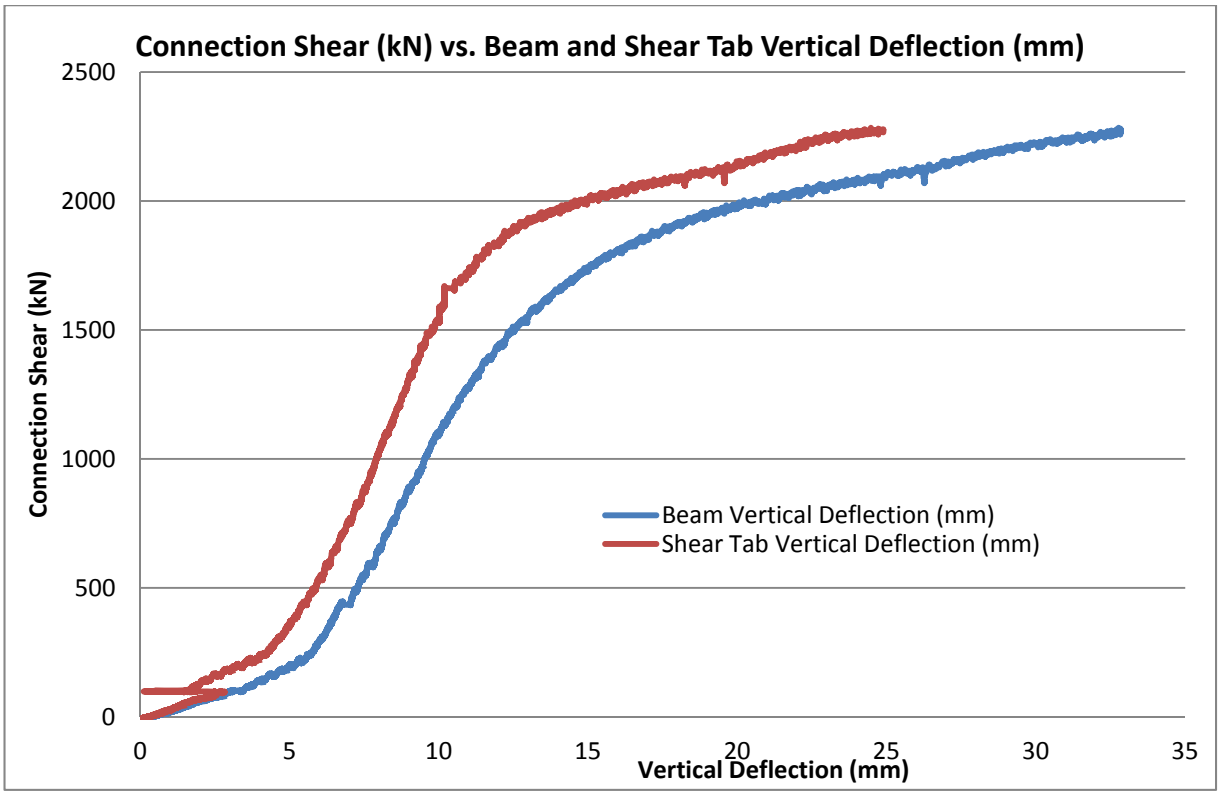

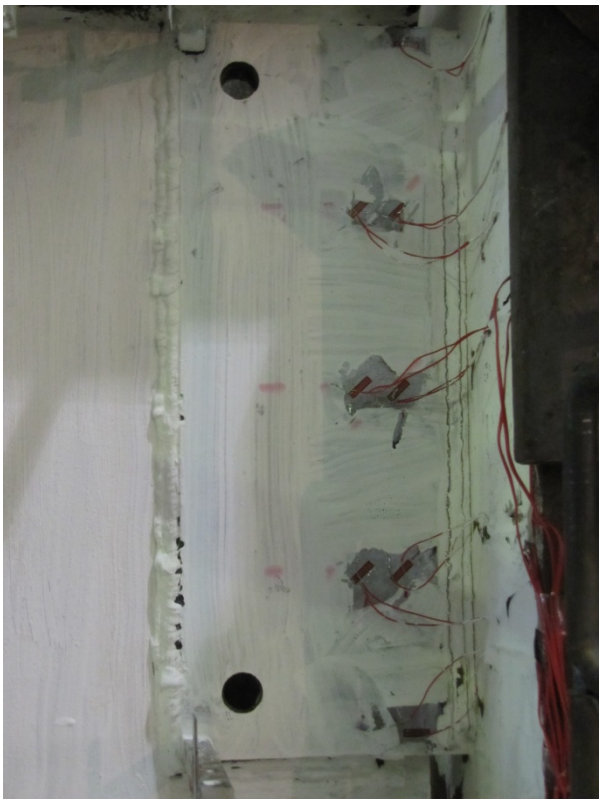

TEST 5: Two Vertical Rows of Three Bolts

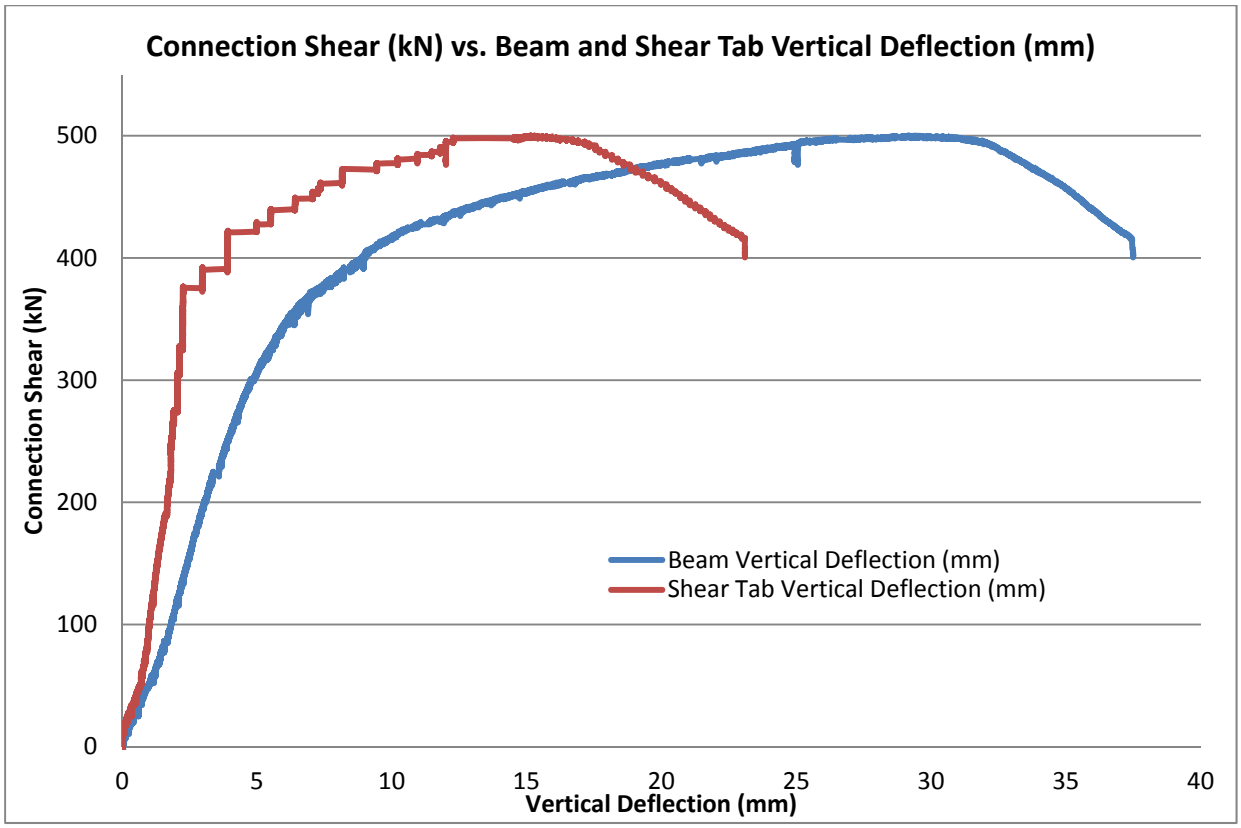

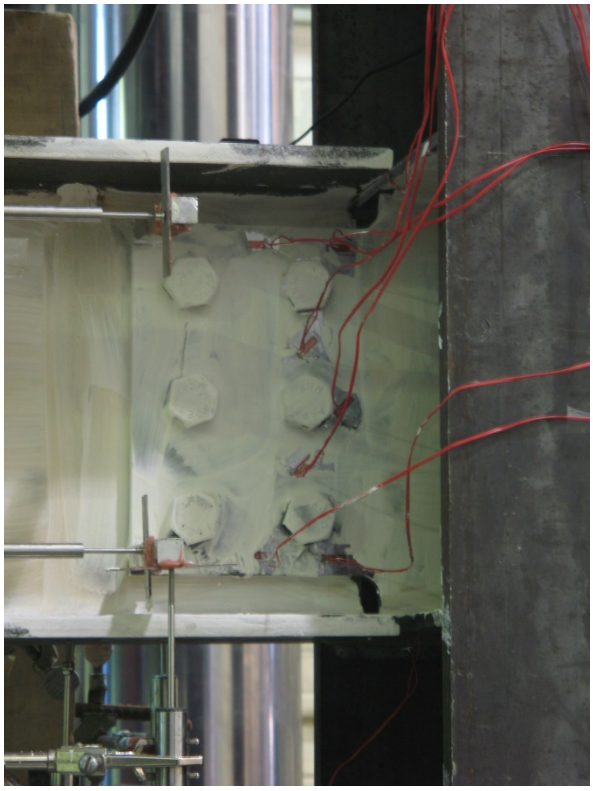

TEST 6: Two Vertical Rows of Six Bolts

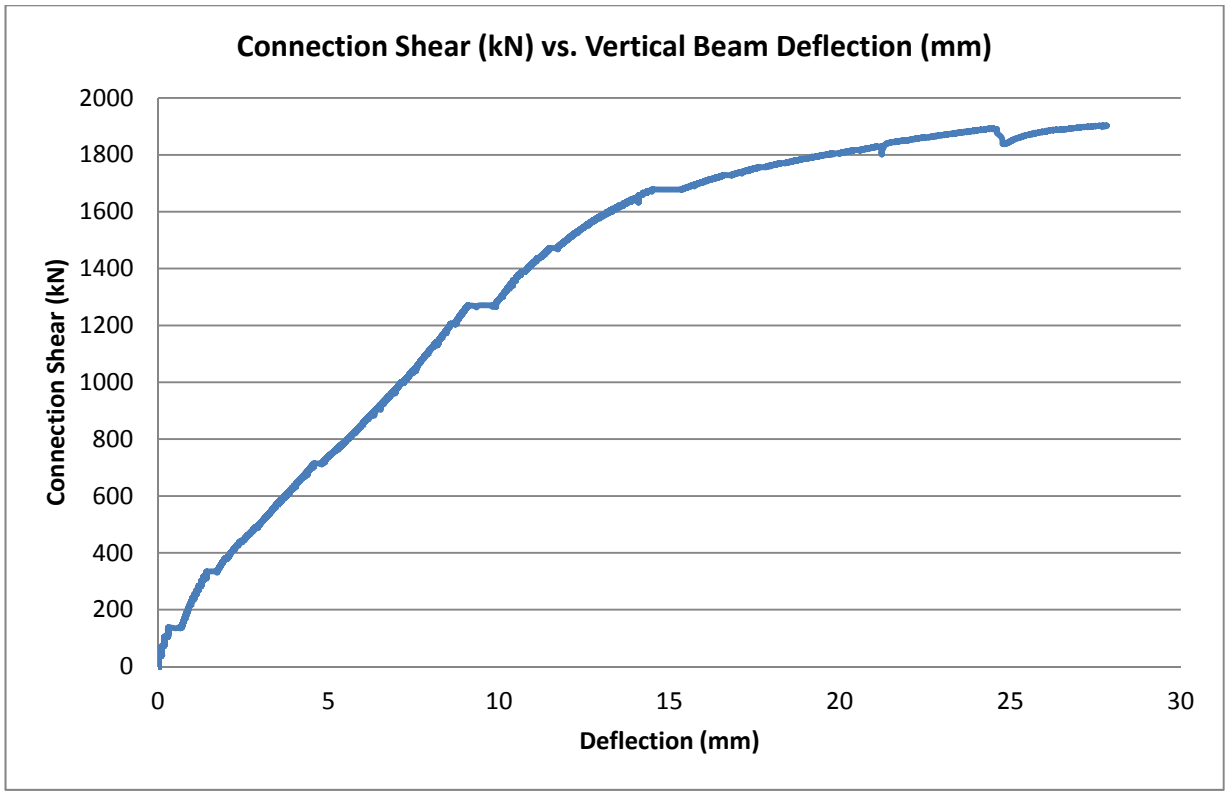

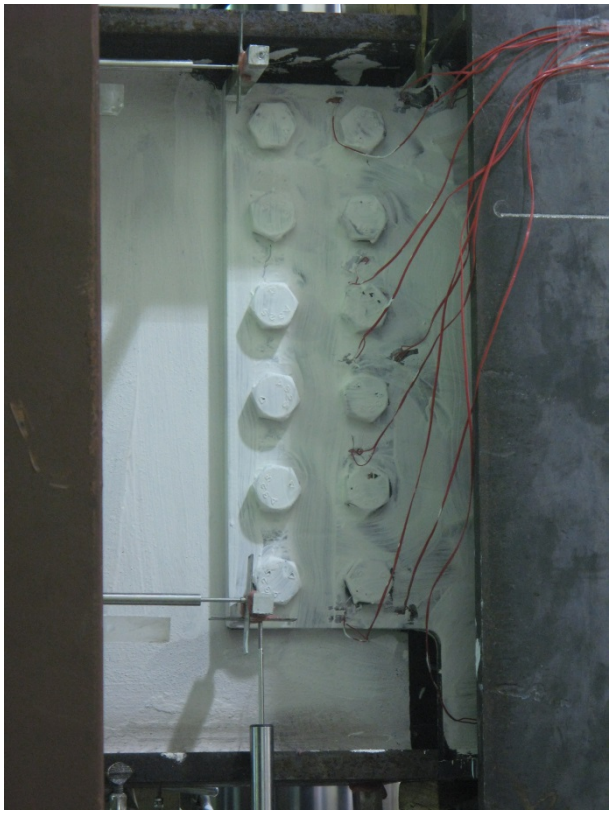

TEST 7: Two Vertical Rows of Three Bolts

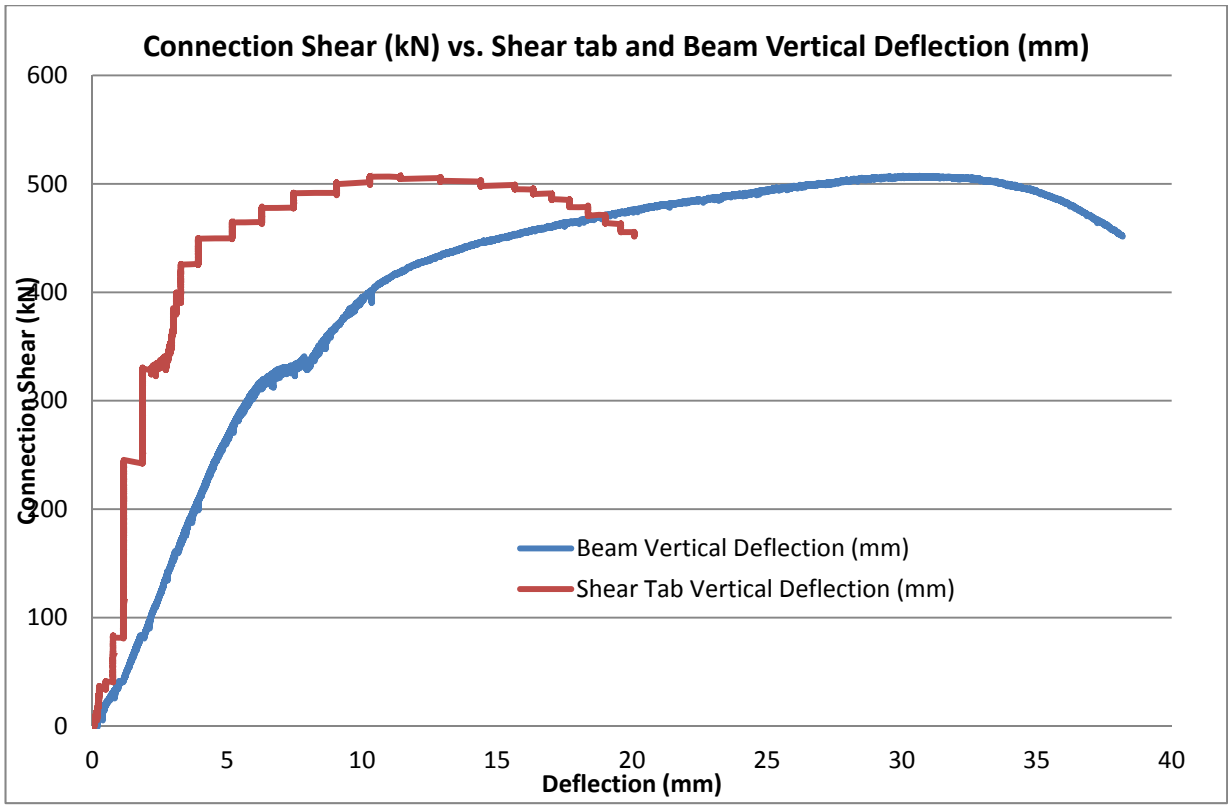

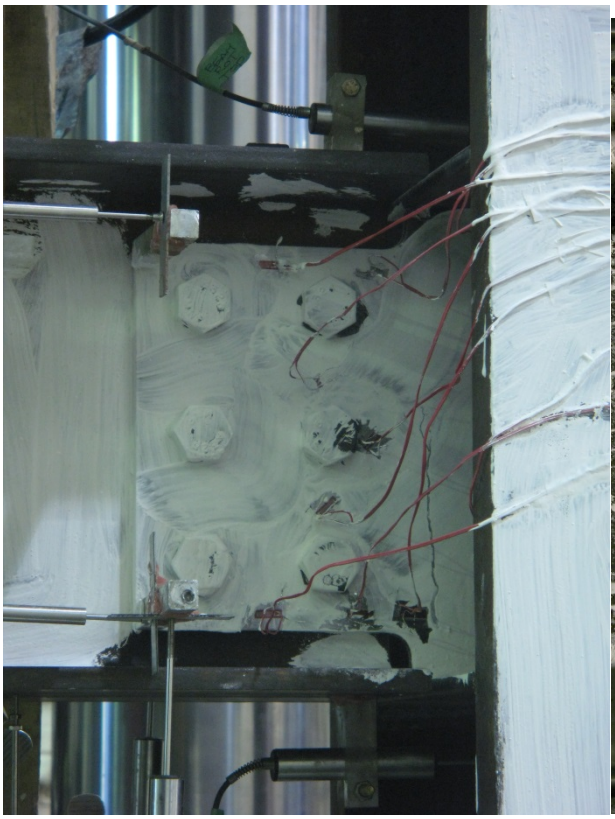

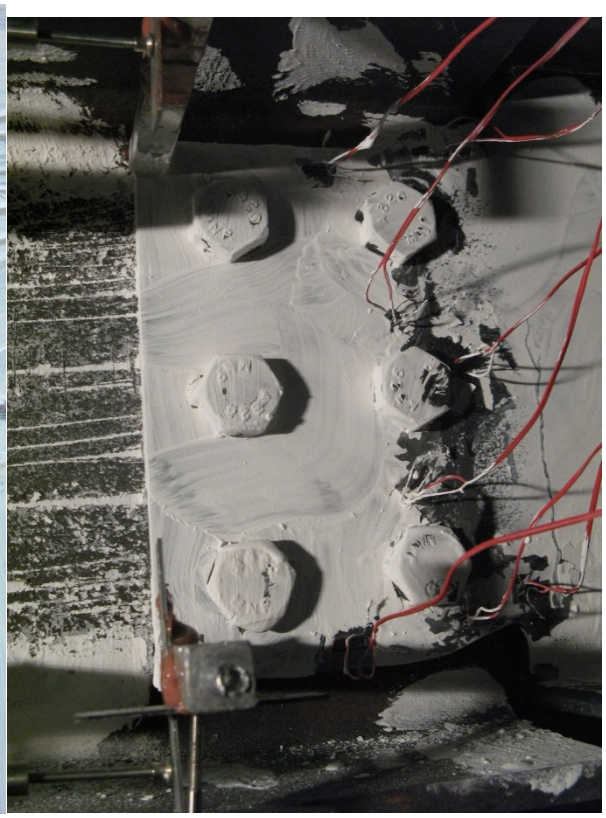

TEST 8: Three Vertical Rows of Three Bolts

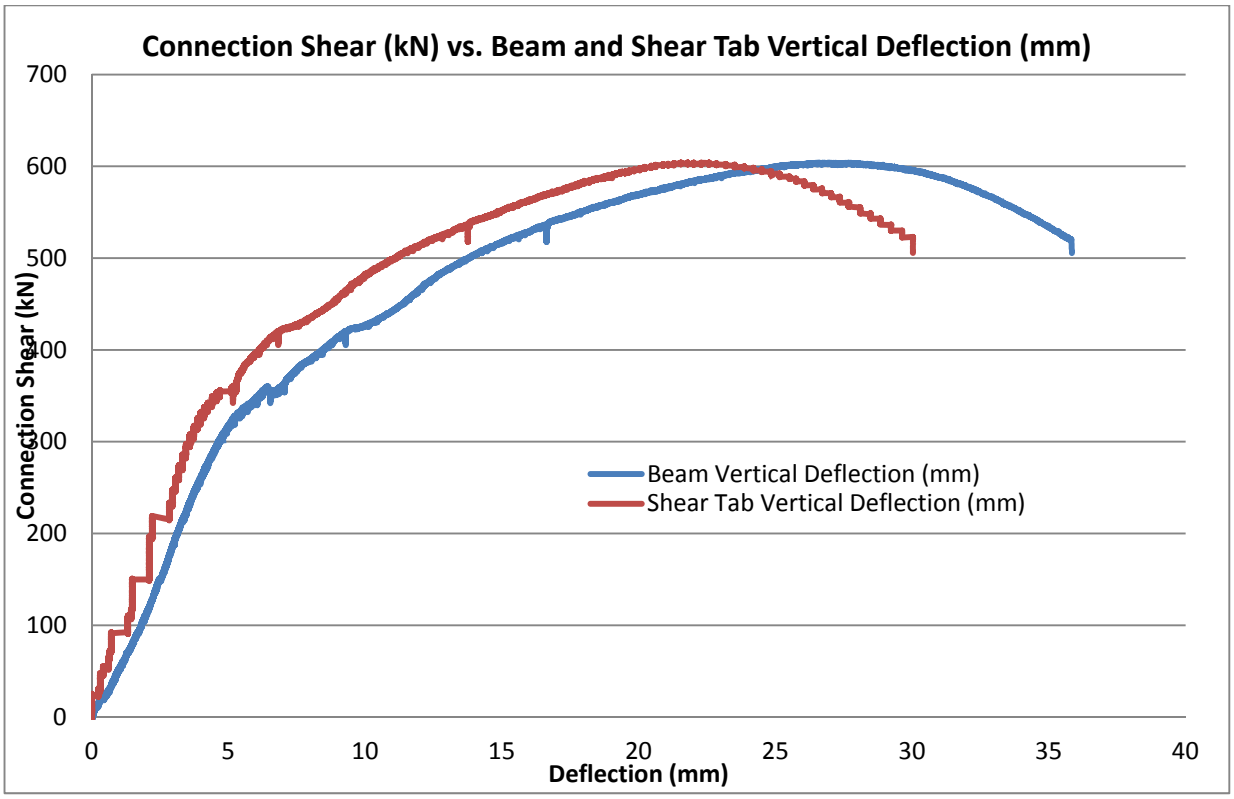

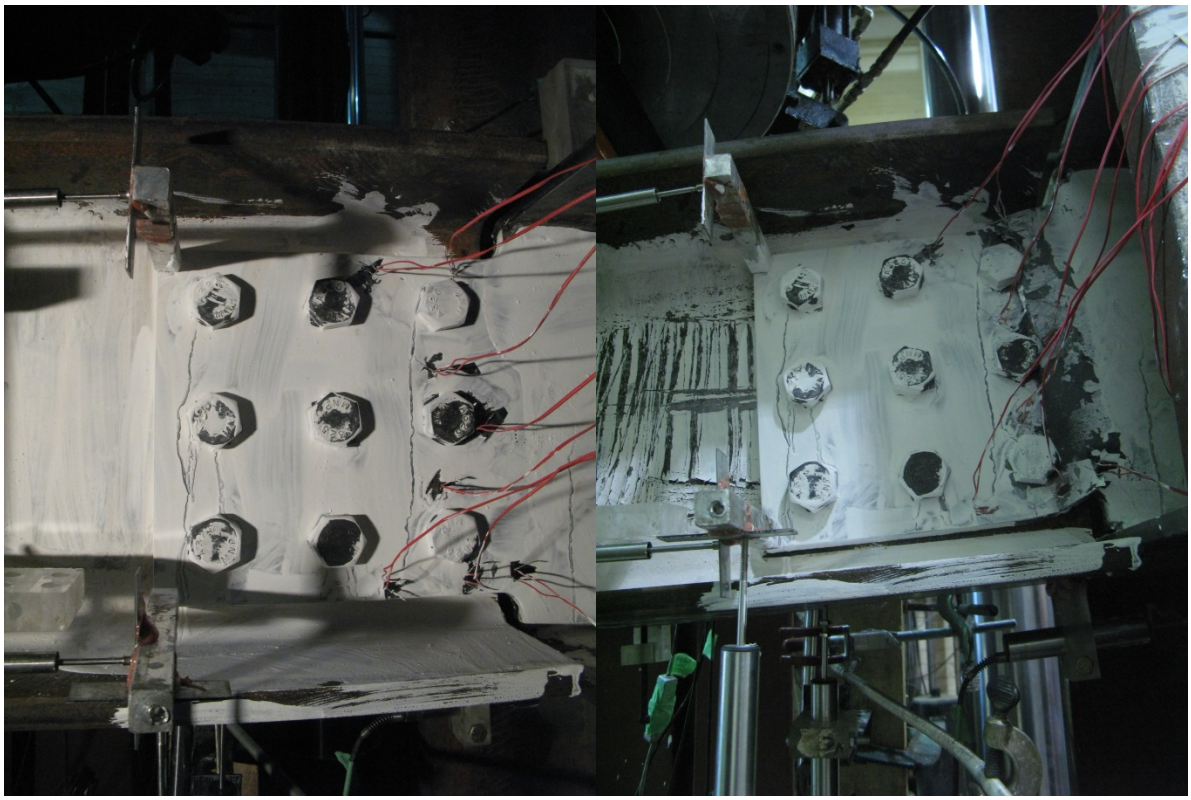

TEST 9: Two Vertical Rows of Six Bolts

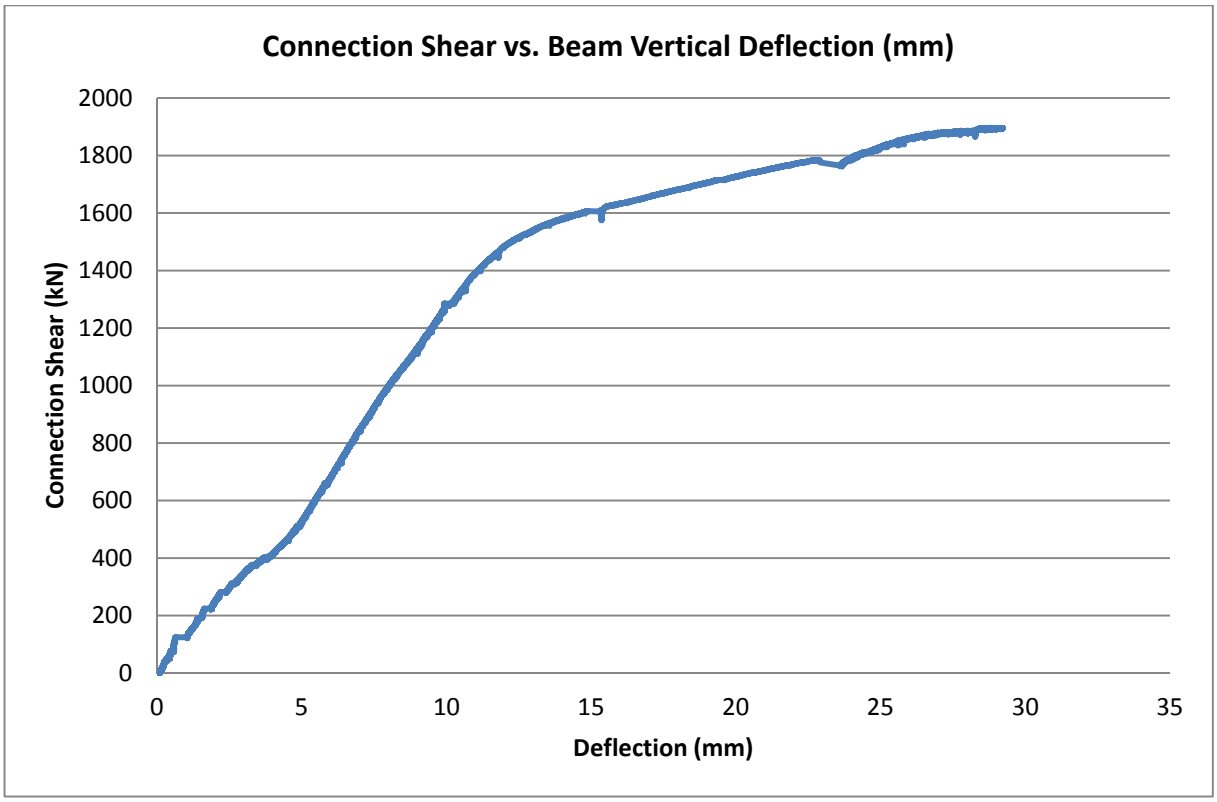

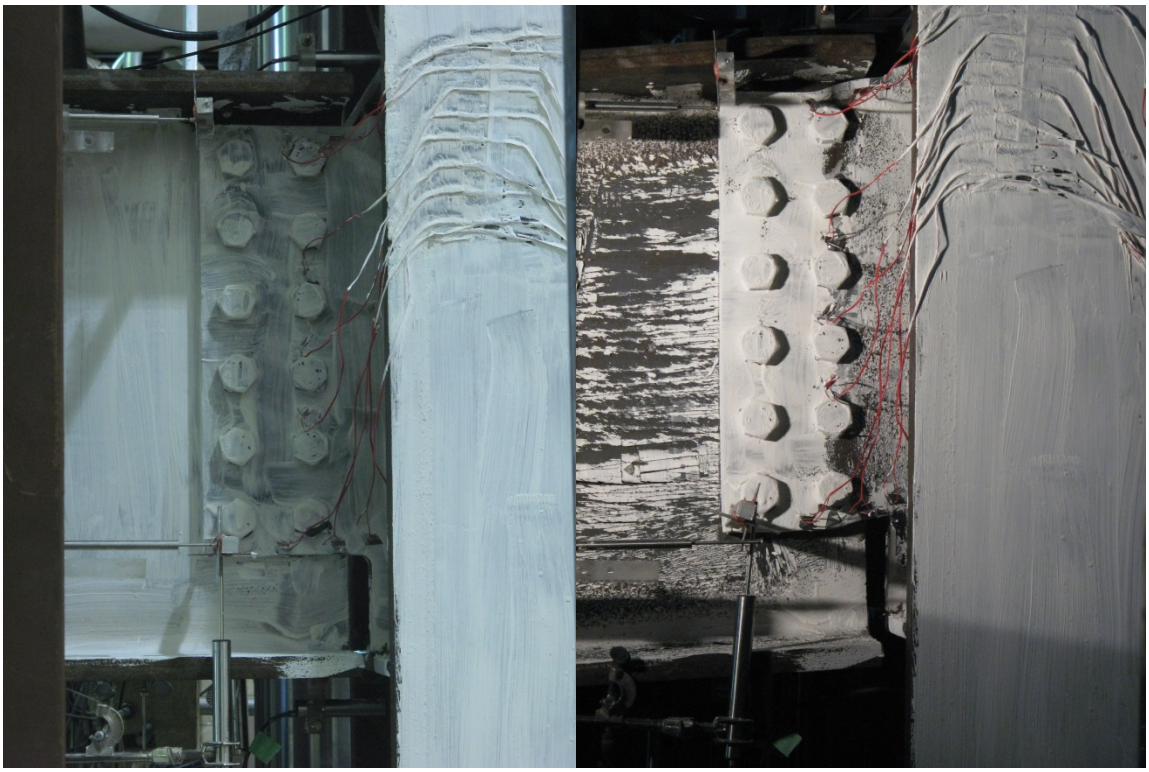

TEST 10: Three Vertical Rows of Six Bolts

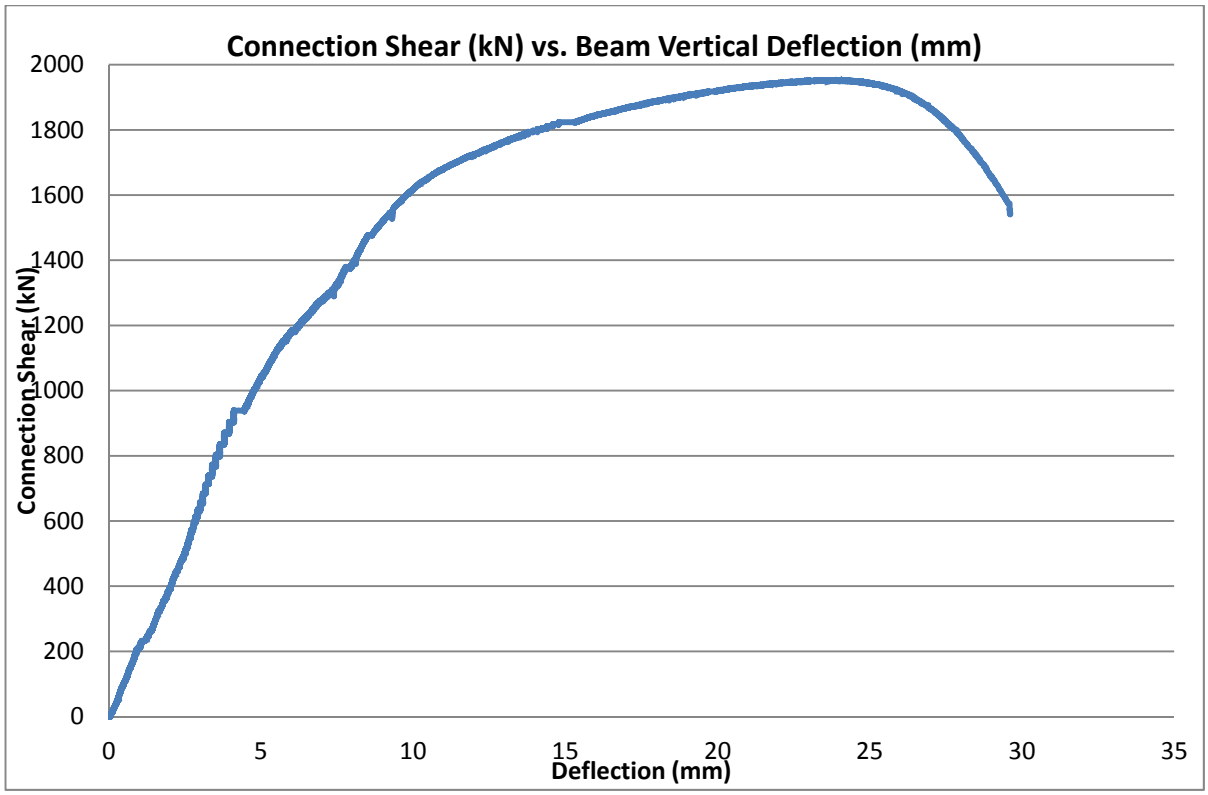

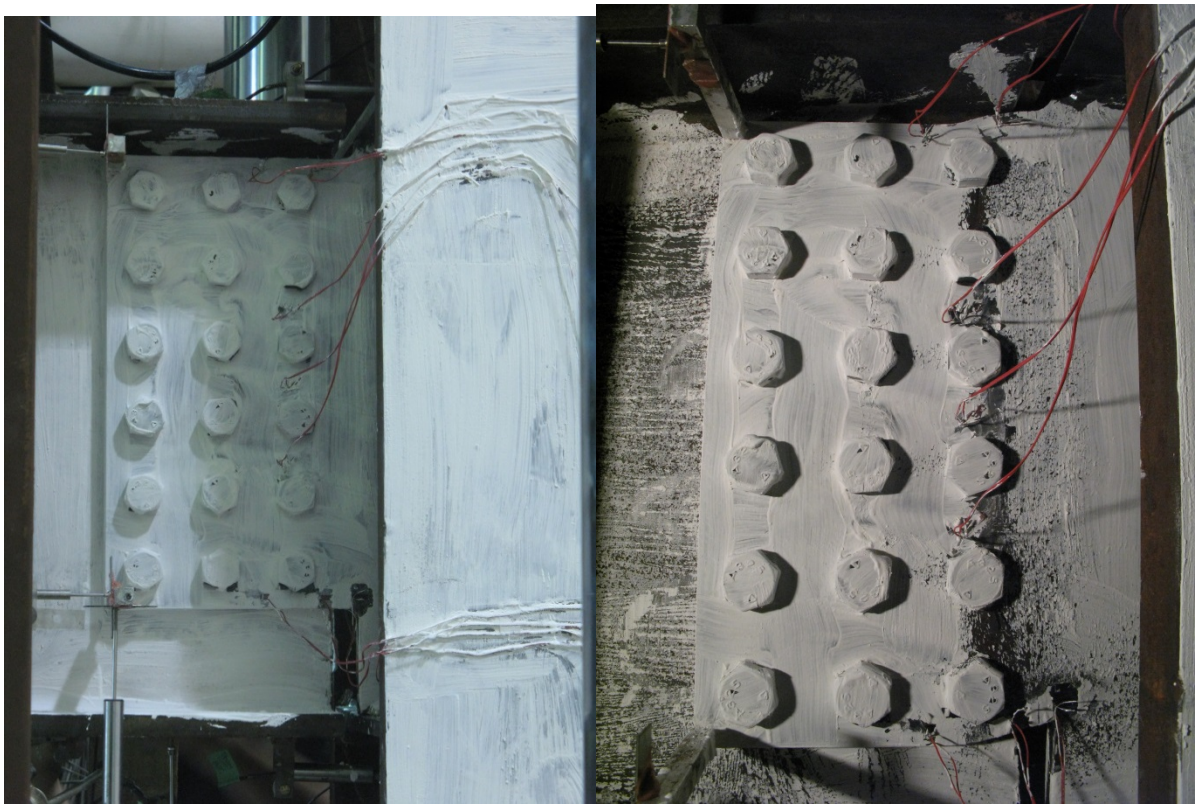

APPENDIX D: SHOP DRAWINGS

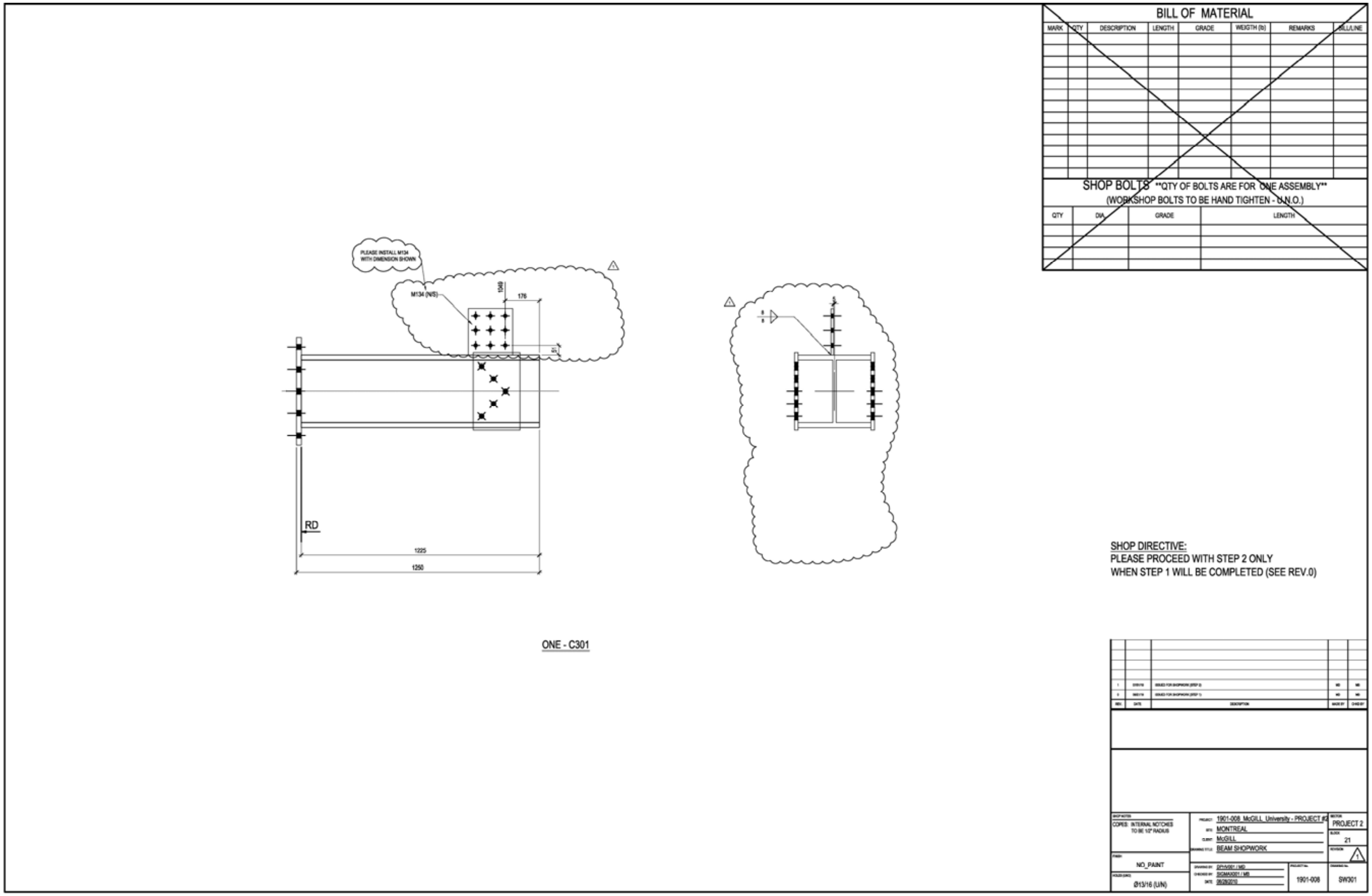
BILL OF MATERIAL
MARK
QTY
DESCRIPTION
LENGTH
GRADE
WEIGTH (lb)
REMARKS
BILL/LINE
SHOP BOLTS **QTY OF BOLTS ARE FOR ONE ASSEMBLY**
(WORKSHOP BOLTS TO BE HAND TIGHTEN - U.N.O.)
QTY
DIA.
GRADE
LENGTH
PLEASE INSTALL M134
WITH DIMENSION SHOWN
M134 (N/S)
176
RD
1225
1250
ONE - C301
SHOP DIRECTIVE:
PLEASE PROCEED WITH STEP 2 ONLY
WHEN STEP 1 WILL BE COMPLETED (SEE REV.0)
COPES: INTERNAL NOTCHES
TO BE 1/2" RADIUS
NO_PAINT
Ø13/16 (U/N)
1901-008, McGILL, University - PROJECT #2
MONTREAL
McGILL
BEAM SHOPWORK
PROJECT 2
21
1901-008
SW301

BILL OF MATERIAL

MARK	QTY	DESCRIPTION	LENGTH	GRADE	WEIGTH (lb)	REMARKS	BILL/UNE

SHOP BOLTS **QTY OF BOLTS ARE FOR ONE ASSEMBLY**
(WORKSHOP BOLTS TO BE HAND TIGHTEN - S.N.O.)

QTY	DIA	GRADE	LENGTH

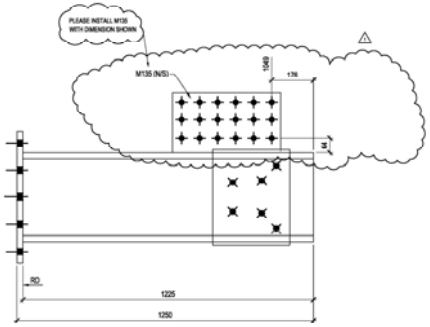

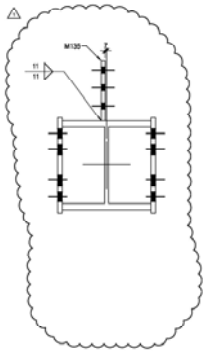

ONE - C302

SHOP DIRECTIVE:
PLEASE PROCEED WITH STEP 2 ONLY
WHEN STEP 1 WILL BE COMPLETED (SEE REV.0)

NO.	DATE	DESCRIPTION	MADE BY	CHECKED
1	01/6/2015	ISSUED FOR SHOPWORK (STEP 2)	MD	MB
0	09/01/2015	ISSUED FOR SHOPWORK (STEP 1)	MD	MB

SHOP NOTES: COPES INTERNAL NOTCHES TO BE 10" RADIUS	PROJECT: 1901-008 McGILL University - PROJECT #2
	AREA: MONTREAL
	CLIENT: McGILL
	DRAWING TITLE: COLUMN SHOPWORK
FINISH: NO_PAINT	DRAWING BY: DT1/2007 / MB
FOLDER (DWG): Ø13/16 (U/N)	CHECKED BY: SIGMA/DT1 / MB
	DATE: 06/28/2010
	PROJECT No.: 1901-008
SECTION: PROJECT 2	BLOCK: 21
REVISION: 1	DRAWING No.: SW302

BILL OF MATERIAL

MARK	QTY	DESCRIPTION	LENGTH	GRADE	WEIGTH (lb)	REMARKS	BILL/UNIT

SHOP BOLTS **QTY OF BOLTS ARE FOR ONE ASSEMBLY**
(WORKSHOP BOLTS TO BE HAND TIGHTEN - U.N.O.)

QTY	DIA	GRADE	LENGTH

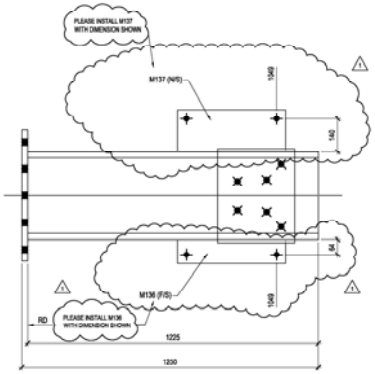

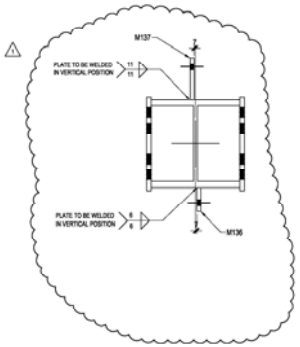

ONE - C306

SHOP DIRECTIVE:
PLEASE PROCEED WITH STEP 2 ONLY
WHEN STEP 1 WILL BE COMPLETED (SEE REV.0)

NO	DATE	DESCRIPTION	DRAWN BY	CHECKED
1	07/01/2010	ISSUED FOR SHOPWORK (STEP 2)	MD	MB
0	19/01/2010	ISSUED FOR SHOPWORK (STEP 1)	MD	MB

COPES: INTERNAL NOTCHES TO BE 1/2" RADIUS

PROJECT: 1901-008 McGILL University - PROJECT #2
SITE: MONTREAL
CLIENT: McGILL
DRAWING TITLE: COLUMN SHOPWORK

SECTION: PROJECT 2
BLOCK: 21
REVISION: 1

FINISH: NO PAINT
HOLES (DIAM.): Ø13/16 (U/N)

DRAWING NO.: SW306
JOB NO.: 1901-008
DRAWN BY: DT/1/2001 / MD
CHECKED BY: SCSM/2007 / MB
DATE: 06/28/2010

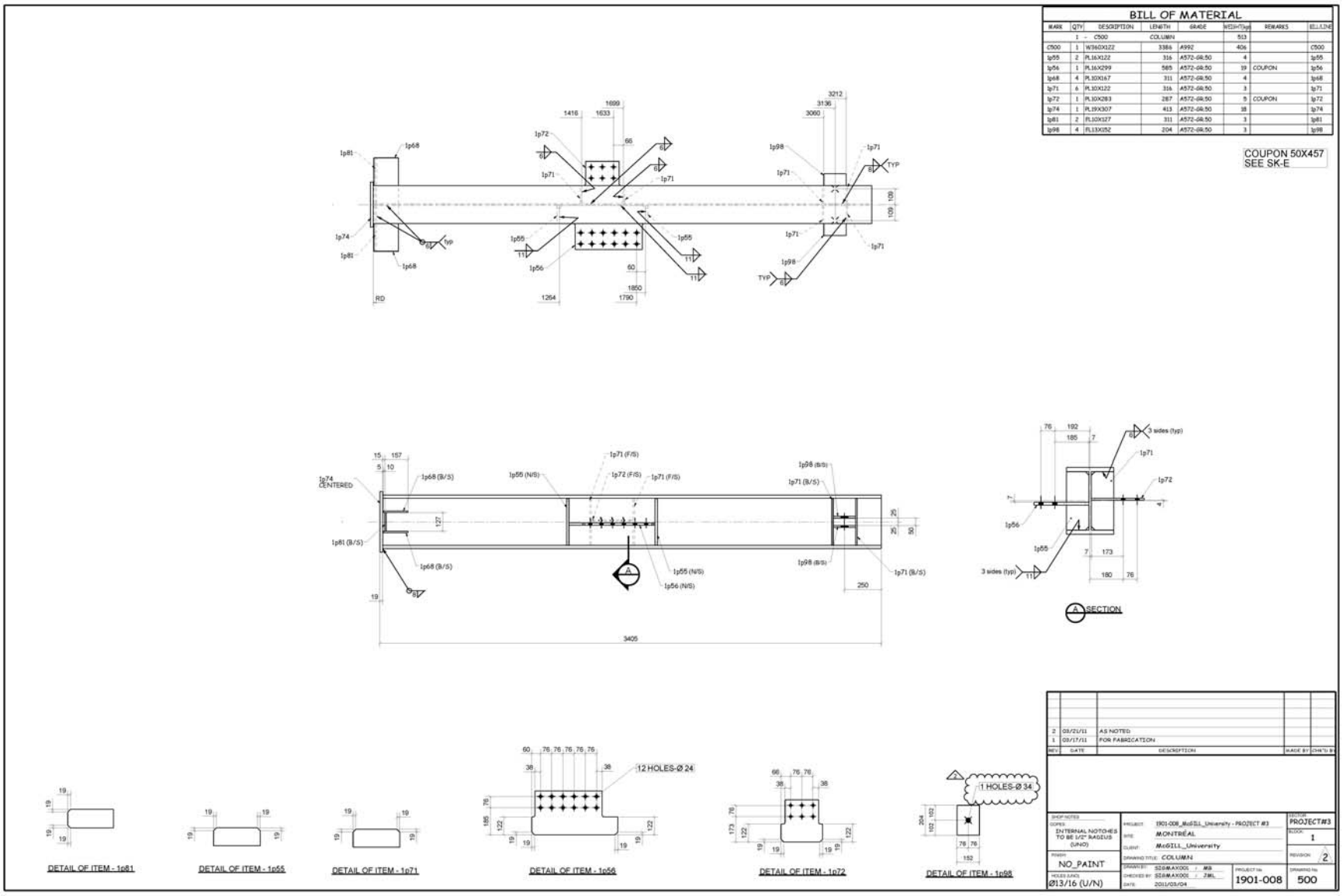

BILL OF MATERIAL

MARK	QTY	DESCRIPTION	LENGTH	GRADE	WEIGHT(kg)	REMARKS	ELEM
1	-	C500	COLUMN		513		
C500	1	W360X122	3386	A992	406		C500
1p55	2	PL16X122	316	A572-GR.50	4		1p55
1p56	1	PL16X299	585	A572-GR.50	19	COUPON	1p56
1p68	4	PL10X167	311	A572-GR.50	4		1p68
1p71	6	PL10X122	316	A572-GR.50	3		1p71
1p72	1	PL10X283	287	A572-GR.50	5	COUPON	1p72
1p74	1	PL19X307	413	A572-GR.50	18		1p74
1p81	2	PL10X127	311	A572-GR.50	3		1p81
1p98	4	PL13X152	204	A572-GR.50	3		1p98

COUPON 50X457
SEE SK-E

DETAIL OF ITEM - 1p81

DETAIL OF ITEM - 1p55

DETAIL OF ITEM - 1p71

DETAIL OF ITEM - 1p56

DETAIL OF ITEM - 1p72

DETAIL OF ITEM - 1p98

REV.	DATE	DESCRIPTION	MADE BY	CHK'D BY
2	03/21/11	AS NOTED		
1	03/17/11	FOR FABRICATION		

SHOP NOTES
COPES:
ENTERNAL NOTCHES TO BE 1/2" RADIUS (UNO)
FINISH:
NO_PAINT
HOLES (UNO):
Ø13/16 (U/N)

PROJECT: 1901-008_McGILL_University - PROJECT #3
SITE: MONTRÉAL
CLIENT: McGILL_University
DRAWING TITLE: COLUMN
DRAWN BY: SDAMAXOOL / MB
CHECKED BY: SDAMAXOOL / JML
DATE: 2011/03/04

SECTION: PROJECT#3
BLOCK: 1
REVISION: 2
PROJECT No: 1901-008
DRAWING No: 500

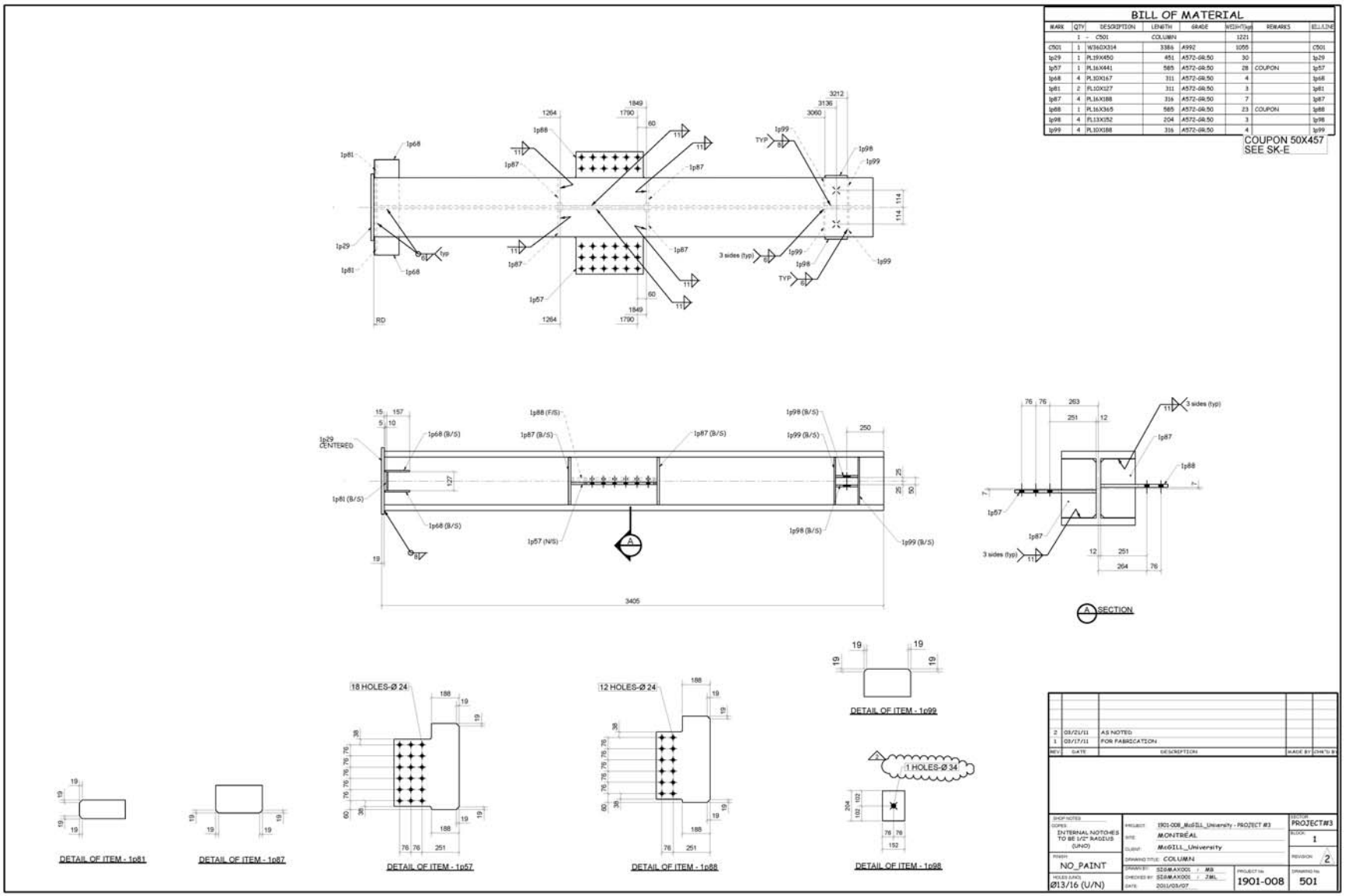

BILL OF MATERIAL

MARK	QTY	DESCRIPTION	LENGTH	GRADE	WEIGHT(kg)	REMARKS	ELLINE
	1	-	C501	COLUMN	1221		
C501	1		W360X314	3386	A992	1055	C501
lp29	1		PL19X450	451	A572-GR.50	30	lp29
lp57	1		PL16X441	585	A572-GR.50	28	COUPON lp57
lp68	4		PL10X167	311	A572-GR.50	4	lp68
lp81	2		PL10X127	311	A572-GR.50	3	lp81
lp87	4		PL16X188	316	A572-GR.50	7	lp87
lp88	1		PL16X365	585	A572-GR.50	23	COUPON lp88
lp98	4		PL13X152	204	A572-GR.50	3	lp98
lp99	4		PL10X188	316	A572-GR.50	4	lp99

COUPON 50X457
SEE SK-E

DETAIL OF ITEM - 1p81

DETAIL OF ITEM - 1p87

DETAIL OF ITEM - 1p57

DETAIL OF ITEM - 1p88

DETAIL OF ITEM - 1p99

DETAIL OF ITEM - 1p98

A SECTION

REV.	DATE	DESCRIPTION	MADE BY	CHK'D BY
2	03/21/11	AS NOTED		
1	03/17/11	FOR FABRICATION		

SHOP NOTES
COPES:
ENTERNAL NOTCHES TO BE 1/2" RADIUS (UNO)
FINISH:
NO_PAINT
HOLES (UNO):
Ø13/16 (U/N)

PROJECT: 1901-008_McGILL_University - PROJECT #3
SITE: MONTRÉAL
CLIENT: McGILL_University
DRAWING TITLE: COLUMN
DRAWING BY: SDAMAXOOL / MB
CHECKED BY: SDAMAXOOL / JML
DATE: 2011/03/07

SECTION: PROJECT#3
BLOCK: 1
REVISION: 2
PROJECT No.: 1901-008
DRAWING No.: 501

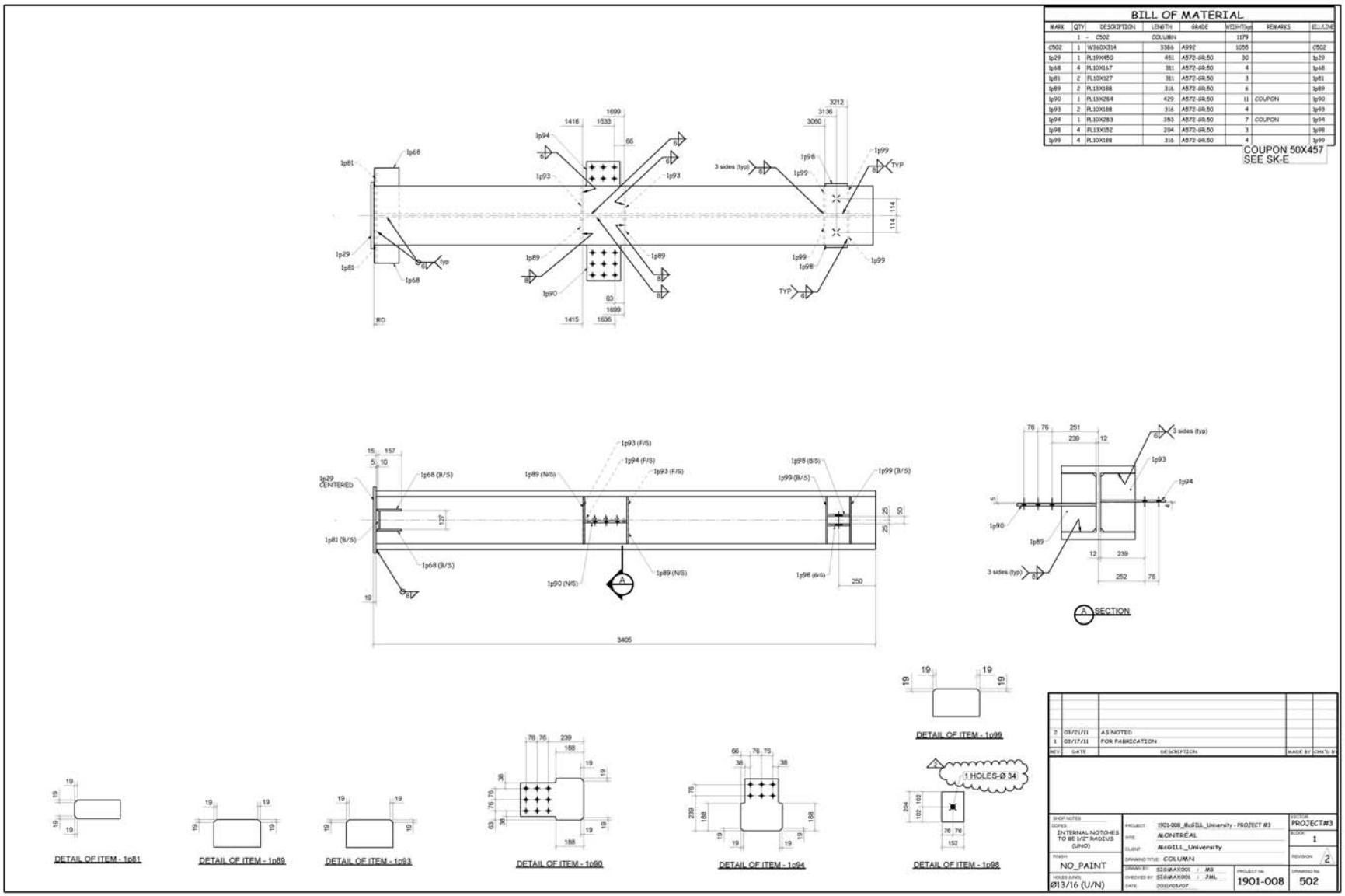

BILL OF MATERIAL

MARK	QTY	DESCRIPTION	LENGTH	GRADE	WEIGHT(kg)	REMARKS	ELEM
	1	-	C502 COLUMN		1179		
C502	1	W360X314	3386	A992	1055		C502
1p29	1	PL19X450	451	A572-GR.50	30		1p29
1p68	4	PL10X167	311	A572-GR.50	4		1p48
1p81	2	PL10X327	311	A572-GR.50	3		1p81
1p89	2	PL13X188	316	A572-GR.50	6		1p89
1p90	1	PL13X264	429	A572-GR.50	11	COUPON	1p90
1p93	2	PL10X188	316	A572-GR.50	4		1p93
1p94	1	PL10X283	353	A572-GR.50	7	COUPON	1p94
1p98	4	FL13X152	204	A572-GR.50	3		1p98
1p99	4	PL10X188	316	A572-GR.50	4		1p99

COUPON 50X457
SEE SK-E

REV.	DATE	DESCRIPTION	MADE BY	CHK'D BY
2	03/21/11	AS NOTED		
1	03/17/11	FOR FABRICATION		

SHOP NOTES
COPES:
ENTERNAL NOTCHES TO BE 1/2" RADIUS (UNO)
FINISH:
NO_PAINT
HOLES (UNO):
Ø13/16 (U/N)

PROJECT: 1901-008_McGILL_University - PROJECT #3
SITE: MONTRÉAL
CLIENT: McGILL_University
DRAWING TITLE: COLUMN
DRAWN BY: SD@MAXOS / MB
CHECKED BY: SD@MAXOS / JML
DATE: 2011/03/07
PROJECT No: 1901-008
SECTION: PROJECT#3
BLOCK: 1
REVISION: 2
DRAWING No: 502

BILL OF MATERIAL

MARK	QTY	DESCRIPTION	LENGTH	GRADE	WEIGHT(kg)	REMARKS	KILL/LINE
	1	B203	BEAM		1152		
B203	1	W610X140	8167	A992	1098	COUPON(+457)	B203
lp9	8	FL16X95	572	A572-GR.50	6		lp9

COUPON 50X457
SEE SK-A

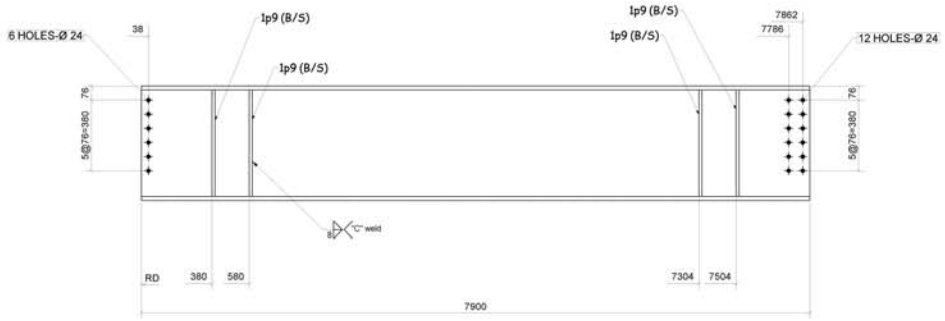

DETAIL - lp9

REV	DATE	DESCRIPTION	MADE BY	CHK'D BY
2	09/05/09	FOR FABRICATION		
1	09/07/28	FOR APPROVAL		

SHOP NOTES
COPES: INTERNAL NOTCHES TO BE 1/2" RADIUS (UNO)
FINISH: NO_PAINT
HOLES (UNO): Ø13/16 (U/N)

PROJECT: 1901-008_McGILL_University - PROJECT #1
SITE: MONTRÉAL
CLIENT: McGILL_University
DRAWING TITLE: BEAM
DRAWN BY: SSIMAKOO1 / MB
CHECKED BY: SSIMAKOO1 / ALB
DATE: 2009/07/22

PROJECT No: 1901-008

DETAIL: PROJECT#1
BLOCK: 2
REVISION: 2
DRAWING No: 203

BILL OF MATERIAL

MARK	QTY	DESCRIPTION	LENGTH	GRADE	WEIGTH (lb)	REMARKS	BILL/LINE
B214	1	W310X74	4638	A992			B214
pa	4	FL13X90	276	A572-GR50			pa

SHOP BOLTS **QTY OF BOLTS ARE FOR ONE ASSEMBLY**
(WORKSHOP BOLTS TO BE HAND TIGHTEN - U.N.O.)

QTY	DIA.	GRADE	LENGTH

B214 COUPON 50x457 SEE SK-D

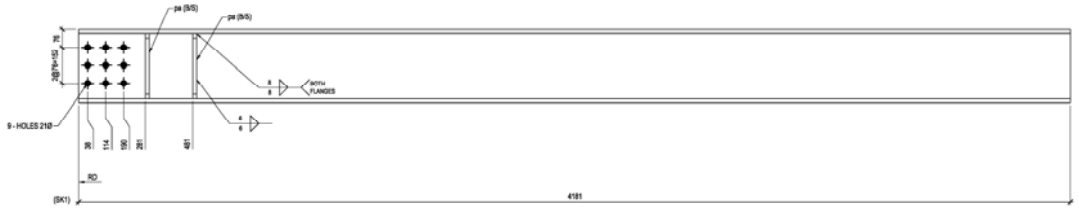

ONE - B214

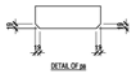

REV.	DATE	DESCRIPTION	MADE BY	CHKD BY
1	02/01/16	FOR FABRICATION	MD	MK

INSPECTED: COPES INTERNAL NOTCHES TO BE 10" RADIUS	PROJECT: 1901-008 McGILL University - PROJECT #2
	SITE: MONTREAL
	CLIENT: McGILL
	DRAWING TITLE: BEAM
FINISH: NO_PAINT	DRAWING BY: 2013-0301 / MB
HOLES (DIA): Ø13/16 (U/N)	CHECKED BY: SCMA-0001 / MB
	DATE: 06/28/2016
	PROJECT No.: 1901-008
	SECTION: PROJECT 2
	BLOCK: 21
	REVISION: 1
	DRAWING No.: 214

BILL OF MATERIAL

MARK	QTY	DESCRIPTION	LENGTH	GRADE	WEIGHT(kg)	REMARKS	ELEMENT
	1	B400	BEAM		892		
B400	1	W610X140	5978	A992	831	COUPON (-457)	B400
lp54	8	PL16X107	570	A572-GR.50	7		lp54

COUPON 50X457
SEE SK-E

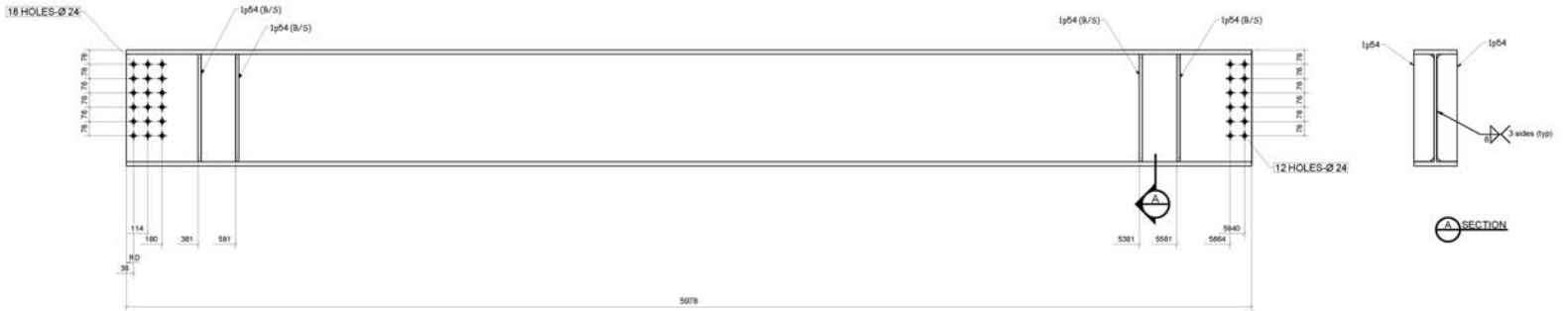

DETAIL OF ITEM - lp54

REV.	DATE	DESCRIPTION	MADE BY	CHK'D BY
1	03/17/11	FOR FABRICATION		

SHOP NOTES
COPES: ENTERNAL NOTCHES TO BE 1/2" RADIUS (UNO)
FINISH: NO_PAINT
HOLES (UNO): Ø13/16 (U/N)

PROJECT: 1901-008_McGILL_University - PROJECT #3
SITE: MONTRÉAL
CLIENT: McGILL_University
DRAWING TITLE: BEAM
DRAWN BY: SDAMAKOS / MB
CHECKED BY: SDAMAKOS / JML
DATE: 2011/03/07

SECTION: PROJECT#3
BLOCK: 1
REVISION: 1
PROJECT No: 1901-008
DRAWING No: 400

BILL OF MATERIAL

MARK	QTY	DESCRIPTION	LENGTH	GRADE	WEIGHT(kg)	REMARKS	ELEMENT
	1	B401	BEAM		253		
B401	1	W310X60	4002	A992	232	COUPON (-457)	B401
lp61	8	PL13X95	276	A572-GR.50	2		lp61

COUPON 50X457
SEE SK-E

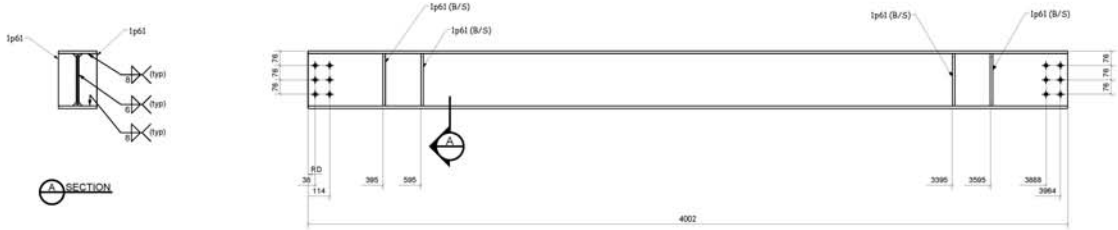

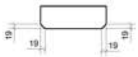

DETAIL OF ITEM - lp61

REV.	DATE	DESCRIPTION	MADE BY	CHK'D BY
1	03/17/11	FOR FABRICATION		

SHOP NOTES
COPES:
ENTERNAL NOTCHES TO BE 1/2" RADIUS (UNO)

FINISH:
NO_PAINT

HOLES (UNO):
Ø13/16 (U/N)

PROJECT: 1901-008_McGILL_University - PROJECT #3
SITE: MONTRÉAL
CLIENT: McGILL_University
DRAWING TITLE: BEAM
DRAWN BY: S2@MAXOS / MB
CHECKED BY: S2@MAXOS / JML
DATE: 2011/03/07

SECTION: PROJECT#3
BLOCK: 1
REVISION: 1
PROJECT No: 1901-008
DRAWING No: 401

BILL OF MATERIAL

MARK	QTY	DESCRIPTION	LENGTH	GRADE	WEIGHT(kg)	REMARKS	ELEMENT
	1	B402	BEAM		286		
B402	1	W310X74	3783	A992	275	COUPON (-457)	B402
1p97	4	PL13X95	276	A572-GR.50	2		1p97

COUPON 50X457
SEE SK-E

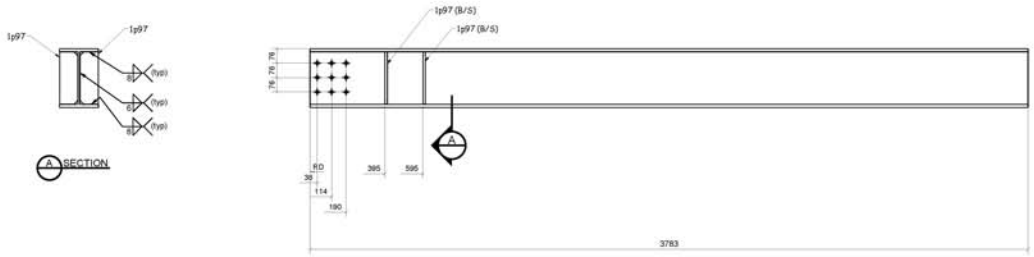

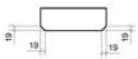

DETAIL OF ITEM - 1p97

REV.	DATE	DESCRIPTION	MADE BY	CHK'D BY
1	03/17/11	FOR FABRICATION		

SHOP NOTES
COPES:
ENTERNAL NOTCHES TO BE 1/2" RADIUS (UNO)

FINISH:
NO_PAINT

HOLES (UNO):
Ø13/16 (U/N)

PROJECT: 1901-008_McGILL_University - PROJECT #3
SITE: MONTRÉAL
CLIENT: McGILL_University
DRAWING TITLE: BEAM
DRAWN BY: SIDAKKOOL : MB
CHECKED BY: SIDAKKOOL : JML
DATE: 2011/03/04

SECTION: PROJECT#3
BLOCK: 1
REVISION: 1
PROJECT No: 1901-008
DRAWING No: 402

BILL OF MATERIAL

MARK	QTY	DESCRIPTION	LENGTH	GRADE	WEIGHT(kg)	REMARKS	ELEMENT
	1	B403	BEAM		832		
B403	1	W610X140	5771	A992	802	COUPON (-457)	B403
1p96	4	PL16X107	570	A572-GR.50	7		1p96

COUPON 50X457
SEE SK-E

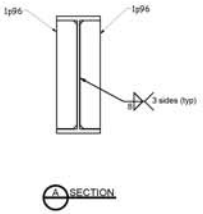

DETAIL OF ITEM - 1p96

REV.	DATE	DESCRIPTION	MADE BY	CHK'D BY
1	03/17/11	FOR FABRICATION		

SHOP NOTES COPES:	ENTERNAL NOTCHES TO BE 1/2" RADIUS (UNO)
FINISH:	NO_PAINT
HOLES (UNO):	Ø13/16 (U/N)
PROJECT:	1901-008_McGILL_University - PROJECT #3
SITE:	MONTRÉAL
CLIENT:	McGILL_University
DRAWING TITLE:	BEAM
DRAWN BY:	SIDAKKOOL / MB
CHECKED BY:	SIDAKKOOL / JML
DATE:	2011/03/04
SECTOR:	PROJECT#3
BLOCK:	1
REVISION:	1
PROJECT No:	1901-008
DRAWING No:	403